SSSU 52
ISSN 0140 3818

UNIVERSITY OF SOUTHAMPTON

DEPARTMENT OF SHIP SCIENCE

FACULTY OF ENGINEERING AND APPLIED SCIENCE

FURTHER WIND TUNNEL TESTS ON THE INFLUENCE OF PROPELLER LOADING ON SHIP RUDDER PERFORMANCE

by A.F. Molland and S.R. Turnock

Ship Science Report No. 52

February 1992

SSSU 52
ISSN 0140 3818

UNIVERSITY OF SOUTHAMPTON

DEPARTMENT OF SHIP SCIENCE

FACULTY OF ENGINEERING AND APPLIED SCIENCE

FURTHER WIND TUNNEL TESTS ON THE INFLUENCE OF PROPELLER LOADING ON SHIP RUDDER PERFORMANCE

by A.F. Molland and S.R. Turnock

Ship Science Report No. 52

February 1992

FURTHER WIND TUNNEL TESTS ON THE INFLUENCE OF PROPELLER LOADING ON SHIP RUDDER PERFORMANCE

by

A.F.Molland and S.R.Turnock

Ship Science Report No 52

University of Southampton

January 1992

SUMMARY

An experimental investigation has been carried out into the geometrical and flow parameters which control the interaction between a ship rudder and propeller. The tests used the 3.5m x 2.5m low speed wind tunnel at the University of Southampton. This report presents further results for a series of rectangular all-movable rudders of varying span and chord but with a constant NACA0020 profile. A four-bladed, 800mm diameter, adjustable pitch propeller was used. This propeller is a modified version of the Wageningen B4.40 series. Open-water results for the modified design were validated against published data.

The test consisted of a series of studies into the effect of propeller pitch ratio, rudder aspect ratio, position of the rudder stock, coverage of the rudder by the propeller race, lateral and vertical separation of rudder and propeller. A five-component strain-gauge dynamometer was used to measure lift, drag and three moments on the rudder and a rotating strain gauge dynamometer the developed thrust and torque of the propeller. In addition, both spanwise and chordwise pressure distributions were measured on the rudder surface. Propeller revolutions were varied between 0 and 3,000 rpm and tunnel wind speeds up to 20m/s were used.

Results are presented in the form of non-dimensional coefficients of lift(C_L), drag(C_D), spanwise(CP_s) and chordwise(CP_c) position of the centre of pressure variation with incidence for the rudder. The influence of rudder on propeller performance is given in terms of non-dimensional thrust(K_T) and torque(K_Q) coefficient variation with advance ratio (J). The surface pressure measurements on the rudder are presented as both a spanwise distribution of the local lift coefficient (C_L) and as a surface pressure distribution.

The results offer an insight into the physics of rudder-propeller interaction. The data presented are suitable for design purposes and will also be of considerable use in numerically modelling the flow interaction and in the development of more advanced ship manoeuvring simulations.

TABLE OF CONTENTS

LIST OF FIGURES

Figure 34 Variation with rudder incidence of the spanwise distribution of local section C_N of all-movable Rudder No. 2 with a propeller ratio setting P/D=0.69 at an advance ratio J=0.42.

Figure 35 Variation with rudder incidence of the spanwise distribution of local section C_N of all-movable Rudder No. 2 with a propeller ratio setting P/D=1.34 at an advance ratio J=0.61.

Figure 36 Variation with rudder incidence of the spanwise distribution of local section C_N of all-movable Rudder No. 5 for an advance ratio J=0.51.

Figure 37 Variation with rudder incidence of the spanwise distribution of local section C_N of all-movable Rudder No. 6 for an advance ratio J=0.51.

Figure 38 Variation with rudder incidence of the spanwise distribution of local section C_N of all-movable Rudder No. 2 with a rudder stock position at 54% chord at an advance ratio J=0.51.

Figure 39 Variation with rudder incidence of the spanwise distribution of local section C_N of all-movable Rudder No. 2 at a lateral separation Y/D = -0.25 at an advance ratio J=0.94.

Figure 40 Variation with rudder incidence of the spanwise distribution of local section C_N of all-movable Rudder No. 2 at a lateral separation Y/D = -0.25 at an advance ratio J=0.51.

Figure 41 Variation with rudder incidence of the spanwise distribution of local section C_N of all-movable Rudder No. 2 at a lateral separation Y/D = -0.25 at an advance ratio J=0.35.

Figure 42 Variation with rudder incidence of the spanwise distribution of local section C_N of all-movable Rudder No. 2 at a lateral separation Y/D = +0.25 at an advance ratio J=0.94.

Figure 43 Variation with rudder incidence of the spanwise distribution of local section C_N of all-movable Rudder No. 2 at a lateral separation Y/D = +0.25 at an advance ratio J=0.51.

Figure 44 Variation with rudder incidence of the spanwise distribution of local section C_N of all-movable Rudder No. 2 at a lateral separation Y/D = +0.25 at an advance ratio J=0.35.

Figure 45 Variation with rudder incidence of the spanwise distribution of local section C_N of all-movable Rudder No. 2 with the propeller axis height of 900mm for an advance ratio J=0.51.

Figure 46 Variation with rudder incidence of the spanwise distribution of local section C_N of all-movable Rudder No. 4 with the propeller axis height of 900mm for an advance ratio J=0.51.

Figure 47 Comparison of propeller thrust and thrust increment against advance ratio for all-movable Rudder No's 2, 5 and 6.

Figure 48 Comparison of propeller thrust and thrust increment against advance ratio for a lateral separation of rudder and propeller of Y/D = -0.25, 0.0, +0.25.

Figure 49 Comparison of propeller thrust and thrust increment against advance ratio for propeller axis heights of 600mm and 900mm.

Figure 50 Comparison of propeller thrust and thrust increment against advance ratio for all-movable Rudder No's 2, 3 and 4.

Figure 51 Chordwise pressure distributions at 8 spanwise positions for all-movable Rudder No. 2 at J=0.42 and P/D=0.69 for rudder incidences of -30.4°, -20.4°, -10.4°, -0.4°, 9.6°, 19.6°, and 29.6°.

Figure 52 Chordwise pressure distributions at 8 spanwise positions for all-movable Rudder No. 2 at J=0.61 and P/D=1.34 for rudder incidences of -30.4°, -20.4°, -10.4°, -0.4°, 9.6°, 19.6°, and 29.6°.

Figure 53 Chordwise pressure distributions at 8 spanwise positions for all-movable Rudder No. 5 at J=0.51 for rudder incidences of -30.4°, -20.4°, -10.4°, -0.4°, 9.6°, 19.6°, and 29.6°.

Figure 54 Chordwise pressure distributions at 8 spanwise positions for all-movable Rudder No. 6 at J=0.51 for rudder incidences of -30.4°, -20.4°, -10.4°, -0.4°, 9.6°, 19.6°, and 29.6°.

Figure 55 Chordwise pressure distributions at 8 spanwise positions for all-movable Rudder No. 2 with the rudder stock at 54% chord and at J=0.51 for rudder incidences of -30.4°, -20.4°, -10.4°, -0.4°, 9.6°, 19.6°, and 29.6°.

Figure 56 Chordwise pressure distributions at 8 spanwise positions for all-movable Rudder No. 2 with a lateral separation Y/D=-0.25 and at J=0.94 for rudder incidences of -30.4°, -20.4°, -10.4°, -0.4°, 9.6°, 19.6°, and 29.6°.

Figure 57 Chordwise pressure distributions at 8 spanwise positions for all-movable Rudder No. 2 with a lateral separation Y/D=-0.25 and at J=0.51 for rudder incidences of -30.4°, -20.4°, -10.4°, -0.4°, 9.6°, 19.6°, and 29.6°.

Figure 58 Chordwise pressure distributions at 8 spanwise positions for all-movable Rudder No. 2 with a lateral separation Y/D=-0.25 and at J=0.35 for rudder incidences of -30.4°, -20.4°, -10.4°, -0.4°, 9.6°, 19.6°, and 29.6°.

LIST OF TABLES

NOMENCLATURE

A	-	Rudder Area (m^2)
AR	-	Rudder Geometric Aspect Ratio
c	-	Mean Rudder Chord (m)
S	-	Rudder Span (m)
C_T	-	Rudder Tip Chord (m)
C_R	-	Rudder Root Chord (m)
D	-	Propeller Diameter (m)
n	-	revolutions per second
Uo	-	Freestream Wind speed (m/s)
d	-	Aerodynamic Drag (N)
L	-	Aerodynamic Lift (N)
Mx	-	Aerodynamic Moment about x-axis (Nm)
My	-	Aerodynamic Moment about y-axis (Nm)
Mz	-	Aerodynamic Moment about z-axis (Nm)
N	-	Normal Force (N)
Q	-	Torque (Nm)
T	-	Thrust (N)
V	-	Vertical Distance of Dynamometer Measurement Centre to Rudder Root (m)

W	-	Horizontal Distance of Dynamometer Rudder Stock From Rudder Leading Edge (m)
X	-	Longitudinal Separation of Rudder Leading Edge and propeller plane of rotation (m)
Y	-	Lateral Separation of Rudder Stock and propeller axis
Z	-	Vertical separation of rudder root and propeller axis (m)
V_{Dp}	-	Scanivalve Dynamic Pressure Voltage (v)
V_P	-	Scanivalve Port Voltage (v)
V_{Po}	-	Scanivalve Zero Wind Voltage (v)
C_l	-	Lift coefficient per unit span
C_L	-	Non-dimensional Lift (sideforce)
C_n	-	Normal force per unit span
C_d	-	Drag coefficient per unit span
C_D	-	Non-Dimensional drag
CP_c	-	Chordwise centre of pressure, %c, measured from leading edge
CP_s	-	Spanwise centre of pressure, %S, measured from root
C_{Mz}	-	Non-dimensional Moment about rudder stock
C_{Mx}	-	Non-dimensional moment about rudder root chord
C_{My}	-	Non-dimensional moment about y axis
C_p	-	Non-Dimensional Pressure Coefficient
K_T	-	Thrust Coefficient ($T/\rho\ n^2D^4$)
K_Q	-	Torque Coefficient ($Q/\rho\ n^2D^5$)
α	-	Rudder incidence
η	-	Efficiency ($J\ K_T/2\pi\ K_Q$)
J	-	Advance Ratio (V/nD)
λ	-	Fraction of propeller diameter in way of propeller race.
ξ	-	Coverage of rudder span by propeller race λ D/S
ρ	-	Air Density (Kg/m3)

1. INTRODUCTION

A propeller upstream of a ship rudder accelerates and rotates the inflow onto the rudder. Additionally the ship rudder both blocks and diverts the flow arriving at the propeller. The physical modelling of these interactions is, at present, limited by the availability of good experimental data for a wide range of representative ship rudder and propeller combinations.

This report presents further results from a detailed wind tunnel investigation into the performance of a series of rudders downstream from a propeller. Details of previous test results are reported in Molland and Turnock [1]. The experiments were carried out in the University of Southampton's 3.5m x 2.5m low-speed wind tunnel. The use of air as a working fluid rather than water significantly eases the measurement of data and the test procedures. Propeller cavitation cannot be studied, but this is not considered a significant factor in the context of the current investigation.

The aim of this report is to provide a comprehensive presentation of the results obtained in two weeks of tunnel testing carried out in September 1991. Section 2 details the rudder and propeller models used. The test rig design and the tests carried out are described in Section 3. Sections 4 and 5 respectively detail the data reduction and its presentation. Section 6 discusses the results obtained. Conclusions and recommendations drawn from the test results are presented as Section 7.

2. DESCRIPTION OF MODELS

2.1 Rudders

For these tests an additional two rectangular all-movable rudders were manufactured and designated Rudder No. 5 and Rudder No. 6. These rudders have a span of 1m, a NACA 0020 section, and a chord of 800mm and 556mm respectively. An additional 100m span extension piece was produced to allow a 1.3m span rudder to be assembled (Rudder No. 4). This consists of the base rectangular rudder (No.2: span = 1m, chord = 667mm) with a 100mm and 200mm extension piece attached to the tip. A detailed description of the

method of manufacture of the rudder models is given in Turnock [2]. Table I presents the particulars for each of the rudders used in the wind tunnel investigation and Figure 1 their overall dimensions. All rudder models had pressure tappings to give complete coverage of the rudder surface, as detailed in Figure 1. The pressure tappings were manufactured using the technique developed by Molland [3]. This consists of mounting small-bore plastic tubing in routed grooves running from rudder root to tip. The rudder surface is made smooth by filling over the tube/groove and 1mm diameter holes are drilled through into the tube at the desired span-wise locations. One end of each tube is sealed and the other attached to a port of a rotary pressure transducer (scanivalve). Only one hole on a tube is exposed at a time the others being sealed with clear adhesive tape.

For the tests carried out all rudders had a roughness strip with its leading edge attached at a distance of 5.7% chord from the leading edge of the chord on both sides of the rudder. The roughness strips were manufactured from 12mm wide double-sided tape densely covered with 100 Grade carborundum grit(0.15mm diameter).

2.2 Propeller

A representative propeller design, based on the Wageningen B4.40 series, was chosen. A four-bladed propeller with a diameter of 800mm and a blade area ratio of 0.4 was manufactured. Modifications were made to the basic Wageningen design. These modifications are detailed in Turnock [4] and consisted of altering the blade root shape to allow an adjustable pitch design with four separate blades and a split hub, removing rake and decreasing blade sweep to reduce centripetal loading moments at the root, and increasing the hub/diameter ratio from 0.167 to 0.25. Overall propeller details are summarised in Table II. Figure 2 shows a comparison of the modified blade shape and the basis Wageningen B4.40.

The split hub was manufactured from aluminium alloy and a positive clamping action allows the four blades to be rotated to the desired pitch ratio setting. The four blades

were manufactured using hybrid carbon/glass fibre composite laid up in the same split female mould to produce identical blades. The production of the composite blades is detailed in Molland and Turnock [5] and the machining of the split female mould in Turnock [4]. Figure 3 shows views of the four blades, split hub and the final assembly. The hub nose cone was made from glass fibre and its dimensions and those of the hub are given in Turnock [2]. In appearance the hub/blade root region is very similar to that of a typical controllable pitch propeller.

For these tests, four identical spherical hub caps were manufactured. These allowed the hub to be used with four, two or no blades. The spherical hub cap clamps into the hub in the same way as the blade to give a smooth surface over the hub. The use of different numbers of blades requires different combinations of balancing weights.

3. APPARATUS AND TESTS

3.1 General

The tests were carried out in the 3.5m x 2.5m low-speed wind tunnel at the University of Southampton. The overall rig for testing the interaction of ship rudder and propellers is shown in Figure 4. The rig consists of two independent units which allow free-stream(open-water) tests to be carried out independently on rudders and propellers as well the investigation of their interaction.

3.2 Rudder Rig/Dynamometer

A rig originally developed for determining the free stream performance of semi-balanced skeg rudders (Molland [6]) was used to support the rudder models. This rig consists of a cast steel pedestal attached to the floor and a welded steel extension which supports a five-component strain gauge dynamometer below the working section. The dynamometer, the design and calibration of which is given in Molland [7], allows the forces and moments on both all-movable and semi-balanced skeg rudders to be measured. The rudder and/or skeg stems are bolted directly to the dynamometer. The

dynamometer is levelled and adjusted vertically so that there is a small gap of approximately 2.5mm (0.004c) between the rudder root and the working section floor.

3.3 Propeller Rig

Figure 5 shows a side view of the propeller rig installed in the 3.5m x 2.5m wind tunnel. The installation process is described in Turnock[2]. The tests detailed in this report were carried out with the propeller's axis of rotation either at 600mm or 900mm above the wind tunnel floor and oriented in the flow direction. The propeller rotates anti-clockwise when viewed from aft (locking upstream). The aerofoil fairing around the propeller drive shaft support tubes and drive belt has a NACA63040 profile with a chord of 550mm and 25% maximum thickness. The trailing edge of the fairing is located 0.5 of the propeller diameter (400mm) upstream of the propeller's plane of rotation. The fairing around the propeller drive shaft has a diameter equal to the minimum hub diameter (180mm). The hub cone and nose cone have an identical profile, the dimensions of which are given in Turnock[2].

An in-line strain gauge dynamometer mounted close to the propeller was used to measure the delivered thrust and torque. The design and static calibration of this dynamometer is detailed in Molland and Turnock[8]. The two measurement components of the dynamometer are connected via a slip-ring assembly to Fylde Bridge balance units with a built in stabilised power supply. The bridge balance output voltage is measured directly (without amplification) using a Schlumberger Minate Digital Voltmeter. Data acquisition is controlled by a Research Machines personal computer and results stored on a 3.5" floppy disk for subsequent analysis.

A Fuji Variable Frequency Inverter is used to control the 30kw electric motor. The propeller rpm can be continuously varied in small discrete steps between 0 and 3000 rpm. The controller has a voltage output proportional to its output supply frequency and hence propeller rpm. This voltage is recorded to give the propeller rpm for a given measurement of thrust and torque.

Tests were carried out at four windspeeds of 5m/s, 10m/s, 15m/s, and 20m/s. This speed was set using the wind tunnel speed controller and measured using a Betz manometer. For given propeller revolutions the wind speed controller was varied as necessary to compensate for the wind speed imparted by the propeller.

3.4 Data Acquisition System

The large number of individual data readings required the use of an automated system for data acquisition. The system used is based on that developed for measuring the performance of 2-D aerofoil sections (Turnock[9]).

Data is recorded from the six-component strain-gauge dynamometer which measures the forces and moments acting on the rudder. The propeller's torque and thrust are measured using the in-line strain gauge dynamometer.

An optical shaft encoder was used to measure propeller revolutions and gives a voltage proportional to shaft rpm. The encoder is also used to generate a reference pulse once per revolution for use by the wind tunnel's LDA equipment. Pressure measurements over the surface of the rudder are obtained using a compressed air stepping Scanivalve which for each step exposes each of four differential pressure transducers to one of 36 input ports. This allows pressure data to be measured from a maximum of 144 individual pressure tubes.

The measurement component of the system is an accurate digital voltmeter connected to one of 18 input channels. The voltmeter and input channels are controlled by software running on a Research Machines Nimbus via an IEEE connection. The stepping of the scanivalve is also controlled via an RS232c system connected to the PC. The computer provides data storage and backup through the use of twin floppy disk drives. In September 1991 all four pressure transducers were used.

The software used for acquiring data and controlling the devices connected to the Nimbus PC is based on that developed for the 2-D aerofoil tests (Turnock[9]).

Executable programs were developed using the PROPASCAL dialect of Pascal as a wide variety of procedures were available for driving the devices connected to the PC.

To ease subsequent data analysis a flexible menu driven system was used to allow the operator to define which particular subset of data was to be recorded. A graphical screen display was used to allow monitoring of the data acquired and to produce pressure plots on the screen. A single data file was created for each data recording session which contained all the information necessary to analyse the data. This data was stored in ASCII format and allowed a readable hardcopy to be made immediately after each test.

3.5 Tests in September 1991

Results are reported from a 10 working day session of testing in the 3.5m x 2.5m low-speed wind tunnel. Running of the tunnel was restricted to between 9 am and 5 pm. Figure 6 shows a dimensioned view of the various test arrangements for the rudder and propeller combination.

The basic propeller-rudder tests were carried out at a nominal Reynolds number of 0.4×10^6, based on a free stream velocity of 10m/s. Velocities induced by the propeller at the higher thrust loadings led to effective Reynolds numbers of up to 1.0×10^6 over much of the rudder based on rudder chord. English[10] indicated that a satisfactory Reynolds number, based on propeller diameter and rpm, to avoid scaling problems would be greater than 1.4×10^6. The lowest rpm used in these tests was 800 rpm which for an 800mm diameter propeller gives a Reynolds number, based on propeller diameter and rpm, of 1.53×10^6.

A series of open-water propeller tests were carried out with four blades at pitch ratio settings of 0.69, 0.95, and 1.34 and two blades at a pitch ratio setting of 0.95. Free-stream rudder tests were carried out with the propeller removed to measure the flow mis-alignment to the tunnel axis. The flow alignment was found to be $+0.4°$ for all rudders tested.

Rudder no. 2 was tested in the base position with the propeller axis 600mm above the wind tunnel floor, zero lateral separation, and a longitudinal separation X/D=0.39. A four-bladed propeller configuration with a pitch ratio setting, P/D=0.95, was used This arrangement corresponded to the mid-longitudinal position used in the previous test in March and August 1990 and reported in Molland and Turnock[1]. Correspondence of results between test sessions was good and demonstrated the repeatability of the test methodology.

Table III tabulates the various flow and geometrical parameters varied during the two week session. The base flow parameters were taken to be an advance ratio J=0.51 which corresponds at a freestream velocity of 10m/s to a rate of revolution of the propeller of 1470 rpm. For most cases, a more limited set of measurements were also carried out at advance ratios of 0.94 and 0.35. These correspond to respective propeller rotation rates of 800 rpm and 2150 rpm. Measurements of the propeller and rudder force dynamometers were made at incidence increments of 5° between -35.4° and 39.6°. Surface pressure surveys were carried out at 10° increments between -30.4° and 29.6°.

The change of rudder stock position was achieved by attaching the rudder onto the skeg fitting on the rudder dynamometer. The effect of this is to move the centre of rotation of the rudder aft by 159mm (6.25").

To investigate the effect of propeller pitch ratio setting the propeller rate of revolution was adjusted so that the open-water thrust loading (K_T/J^2) was comparable between the pitch ratio settings of 0.69 and 1.34 with a base setting of 0.95.

4. DATA REDUCTION AND CORRECTIONS

The software controlling the data acquisition generated a data file for each individual test. Data was stored as ASCII text which allowed a direct transcription of all data recorded to be obtained. The data recorded were the unprocessed voltages read from the voltmeter. The hard copy allowed 'by hand' verification checks to be made of the

software used to analyse the test data files. The format of the test data file is described in the appendix of Molland and Turnock[1]. The data file format was designed to ease the subsequent analysis.

Data reduction was divided into the three distinct tasks of rudder dynamometer forces, rudder surface pressures, and propeller thrust and torque. The data reduction of the three categories is detailed in Molland and Turnock[1].

The non-dimensional coefficient form of the rudder forces are obtained as shown:

$$C_L = \frac{L}{\frac{1}{2}\rho Uo^2 A}$$

$$C_D = \frac{d}{\frac{1}{2}\rho Uo^2 A}$$

$$C_{Mz} = \frac{M_z}{\frac{1}{2}\rho Uo^2 A\ c}$$

$$C_{Mx} = \frac{M_x}{\frac{1}{2}\rho Uo^2 A\ S}$$

$$C_{My} = \frac{M_y}{\frac{1}{2}\rho Uo^2 A\ S}$$

where ρ is the tunnel air density (kg/m^3), Uo the free stream velocity (m/s), S the rudder span, c the mean rudder chord, and A the total rudder area (A = S .c). The position of the centre of pressure on the rudder in the spanwise and chordwise directions are obtained as follows:

$$CP_c = \left(\frac{M_z}{N} + W \right) \times \frac{100}{c}$$

$$CP_s = \left(\frac{M_N}{L} - V \right) \times \frac{100}{S}$$

where W is the distance of the dynamometer rudder stock from the leading edge and V the distance from the dynamometer measurement centre to the rudder root.

No corrections were made to the values of non-dimensional coefficients thus determined as effects such as tunnel blockage for the 3.5m x 2.5m working section were found to have a negligible effect for the rudder size and propeller diameter tested.

The four differential pressure transducers used in conjunction with the rotary scanivalve give a maximum of 144 individual pressure measurements for any test. The no-wind pressure transducer output voltage V_{Po} was measured at the beginning of each test. The reference pressure connected to all four transducers was the static line of the main wind tunnel pitot-static probe. This line was also connected to one input port for each transducer to give a 'real' zero pressure difference value V_{Po}. The pitot line was connected to another input port to give a voltage V_{Dp} proportional to the total tunnel dynamic pressure.

For each pressure port measurement V_P, the non-dimensional pressure coefficient C_p is obtained directly as:

This expression does not require an explicit value for the calibration constant of the

$$C_p = \frac{V_P - V_{Po}}{V_{Dp}}$$

particular pressure transducer, since the transducer has a linear response.

As the location of each pressure measurement on the rudder surface is known, integration of C_p around the chord of the rudder for a constant span allows the local non-dimensional Normal Force coefficient C_n to be calculated. This integration was carried out using a quadratic numerical procedure similar to Simpson's rule but with variable spacing.

The static calibration carried out on the Torque-Thrust dynamometer gave a linear response to loading of both thrust and torque with negligible interactions (Molland and Turnock[8]).

Using the relevant wind speed V (m/s) and n (revs/sec) the advance ratio J is calculated as:

$$J = \frac{V}{n\,D}$$

where D is propeller diameter. The non-dimensional thrust coefficient(K_T) and torque coefficient(K_Q) are given by

$$K_T = \frac{T}{\rho\, n^2\, D^4}$$

$$K_Q = \frac{Q}{\rho\, n^2\, D^5}$$

where ρ is the air density. The propeller efficiency η is:

$$\eta = \left(\frac{J}{2\pi}\right) \times \left(\frac{K_T}{K_Q}\right)$$

5. PRESENTATION OF DATA

The notation of rudder incidence and coefficients used in the presentation is given in Figure 7. The propeller rotates in an anti-clockwise direction when viewed from aft as shown in the diagram. Care must be taken to relate this correctly to the direction of positive rudder sideforce and rudder incidence.

The results of the tests are presented graphically. Figures 8 to 33 show force coefficients, centre of pressure chordwise(as a percentage of mean chord from its leading edge) and centre of pressure spanwise(percentage of span from rudder root) versus rudder angle of attack. The data are presented in terms of J values rather than directly as thrust loadings (K_T/J^2). This is to eliminate ambiguity between the use of the nominal free-stream (open water) thrust loading and the actual thrust loading in the presence of the rudder. The latter is larger than that in the freestream for the same free stream J value. Figures 47 to 50 quantify the influence of the parameters tested on the experimentally measured propeller thrust coefficient K_T, which includes spinner loading effects.

In Figures 34 to 46 the distribution of local chordwise two-dimensional normal force coefficients over the complete rudder span are shown for the range of rudder incidence tested. The C_n presented is for unit chord, not actual chord (0.667). It is assumed that the local C_n at the root is equal to that at the next inboard section and that at the rudder tip C_n is zero.

The corresponding rudder surface pressure distributions are given as Figures 51 to 63

and are for the three Advance Ratios of 0.35, 0.51 and 0.94 tested. Each Figure presents the pressure distribution at each spanwise station for the range of rudder incidences tested. The spanwise stations are numbered as shown in Figure 1 which includes the actual spanwise location. The section nearest to the rudder root is at the bottom of the figure and that near the tip at the top. The columns of pressure plots are presented in order from left to right of increasing rudder incidence from -30° to +30°. The x-axis of the individual pressure plots is given as a percentage of the local chord between 0 and 100%. The y-axis is in terms of C_p, with the convention of negative pressure in the positive (upward) direction. The y-scale increment is held constant at 5 for all plots. The dotted line represents , as per the axis convention of Figure 7, the pressures on the positive y side of the rudder and the solid line those on the negative y side.

The appendix to this report tabulates all the rudder dynamometer data obtained, averaged and used in the presentation of results.

6. DISCUSSION OF RESULTS

6.1 Parameters which control rudder-propeller interaction

In addressing the rudder-propeller interaction problem it is necessary to identify the various independent parameters on which the rudder forces depend. In the work to date the influence of the flow over the ship hull has not been considered. This allows the underlying physics of the flow for an isolated rudder and propeller to be investigated. Once this is understood the interaction between a hull and rudder-propeller combination becomes a more tractable problem. Free-surface effects and cavitation are not included as they are not considered fundamental in determining the operating conditions of the rudder and propeller.

In discussing the parameters which govern the interaction it is convenient to group them into four categories. These are:

i) Flow variables which control the magnitude of the forces developed. These include the time dependent quantities V (free-stream velocity) and n (propeller rate of

revolution) and the properties of the fluid, density (ρ) and dynamic viscosity (μ). Also included is the yaw angle γ between the rudder-propeller combination and the free-stream.

ii) Rudder geometric variables which determine how the flow passes over the rudder and hence the force developed. This is controlled by the rudder incidence α, span S, mean chord c, stock position X_1, thickness t, section shape, sweep and twist.

iii) Propeller geometric variables which control how the propeller imparts energy into the flow and generates thrust. This is determined by its diameter D, pitch P, boss diameter, sweep, pitch and thickness distributions, number of blades and blade area ratio.

iv) Relative position and size of the rudder and propeller. The two units can be separated longitudinally (X), laterally (Y) and vertically (Z). The relative size is defined as the coverage ξ and is equal to the proportion of the rudder span in way of the propeller race. This can be expresses as $\xi = \lambda D/S$ where λ is the fraction of propeller diameter impinging on the rudder.

The flow parameters in non-dimensional form become Reynolds number Rn and Advance Ratio J. The remaining three categories consist of solely geometric parameters. Figure 7 illustrates the geometry of a rudder-propeller combination and corresponds to the wind tunnel arrangements used. To achieve geometrical similarity between wind tunnel test and full-scale, representative rudder shapes and propeller design were used for the experimental investigation. A propeller design for a given pitch ratio setting will operate at the same condition of thrust K_T and torque K_Q if the advance ratio is kept the same between model test and full-scale. For complete flow similarity the propeller Reynolds number should be held constant between model and full-scale. However, it is normally acceptable for the model Reynolds number to be less than full-scale as long as turbulent flow has been established. This was confirmed in earlier tests using the rudder-propeller rig, Ref. [1], where the effect of Reynolds number was found to be small.

The dependent variables influenced by the non-dimensional parameters are the overall forces and moments acting on both the rudder and propeller. For ship manoeuvring, of principal interest is the rudder side force C_L and the position of the centre of action of the side force (CP_c and CP_s). The effect on ship resistance of the rudder drag and propeller thrust is of interest in the overall force balance used in determining the speed loss/gain of the vessel in a manoeuvre. The stall angle of the rudder for a given propeller advance ratio will be important for determining the optimum helm to execute a particular manoeuvre.

The information obtained from the parametric study carried out may be used for both the detailed design of ship manoeuvring equipment and for the assessment of the manoeuvring behaviour of existing ships. Once a rudder-propeller geometry has been fixed the side force production will be solely controlled by rudder incidence and advance ratio, (neglecting Reynolds number effects and assuming the propeller is operating at a fixed pitch ratio setting).

6.2 Performance of all-movable rudders

Figures 8 to 16 show the effect of different thrust loadings on rudder performance for the different rudder-propeller geometries tested. The overall shape of the rudder lift and drag curves varied little for the parameters tested. The effect of increasing thrust loading, as reported in Molland and Turnock[1], is to:

i) increase the lift-curve slope above that of free-stream;
ii) significantly delay stall, even for low thurst loading (high J);
iii) stall is no longer the same for positive and negative incidence;
iv) drag component due to lift increases;
v) CP_c moves forward from free-stream position;
vi) CP_s increases for positive incidence and decreases for negative incidence.

6.3 Effect of propeller pitch ratio

Figures 17 to 19 compare, for three different propeller open-water thrust loadings, the

effect of altering the propeller pitch ratio setting. At the low thrust loading ($K_T/J^2=0.05$), which corresponds to an advance ratio $J=0.94$ for $P/D=0.95$, there is little difference in lift-curve slope. Drag coefficient, CP_c, and CP_s are also not influenced to any great extent. However, there are some differences in C_{Lmax} for both positive and negative incidence, although this does not follow a trend with pitch ratio setting and may be due to running the propeller away from its design point.

For the mid-thrust loading ($K_T/J^2=0.88$), corresponding to an advance ratio $J=0.51$ for $P/D=0.95$, differences in rudder characteristic are more pronounced. The increase in pitch ratio setting slightly increasing the rudder lift-curve slope but decreasing drag for low rudder incidence.

At high thrust loading ($K_T/J^2=2.30$), corresponding to an advance ratio $J=0.35$ at $P/D=0.95$, the trend is broadly similar. The greater the pitch ratio setting the larger the lift-curve slope and the less the drag. For the pitch ratio setting of 1.34 the rudder generates a net thrust. The changes in chordwise centre of pressure are still small. For positive incidence the spanwise centre of pressure moves outboard for increasing pitch setting and in-board for negative incidence.

The variation of local normal force distribution for $P/D=0.69$ and 1.34 at $K_T/J^2=0.88$ is shown in Figures 34 and 35. It can be seen that the location of the peak values of C_n in way of the propeller race move outward from the propeller axis. This suggests an outward shift of the position of the maximum thrust and hence velocity on the blade.

6.4 Effect of rudder aspect ratio

The effect of varying aspect ratio for a constant coverage is shown for three advance ratios in Figures 20, 21 and 22. For the three rudders tested (No.'s 5, AR=2.5; 2, AR=3.0; and 6, AR=3.6), all with constant coverage ξ = 0.80, and at the same longitudinal separation showed for all three advance ratios an increase of lift-curve slope with increase in aspect ratio. This reproduces the effect of aspect ratio observed in the free-stream. The drag and centre of pressure follow the trends with change in aspect

ratio. Again, at low rudder incidence the drag appears sensitive to the structure of the propeller race and decreases with increasing aspect ratio, and at low J gives a thrust force. Also with decrease in J, the effect of aspect ratio is greater than that for a free-stream rudder.

Figures 36 and 37, which give the local spanwise load distribution show the same overall shape for a given incidence, although some of the pressure data (see Figs. 53 and 54) was unreliable.

In Figure 47 the influence of rudder aspect ratio on propeller thrust is shown. Only at high J, does there appear to be a significant difference in behaviour. The thrust increment increasing with aspect ratio.

6.5 Effect of rudder stock position

For two advance ratios of 0.94 and 0.51 Rudder No. 2 was attached to the skeg fixture on the rudder dynamometer. This effectively mounted the rudder stock at 54% chord from the leading edge as opposed to the standard 30% chord. The effect on rudder characteristics is shown in Figures 23 and 24. The change in pivot position had negligible effect on CPc, as would be expected. The lift and drag curves are almost identical, although for J=0.51 there was a slight decrease in C_L for a given incidence. The local lift distribution, Figure 38, is also very similar to that for 30%chord (see Ref. [1]).

6.6 Effect of lateral separation

The main effect of lateral movement of the rudder relative to the propeller, as seen in Figures 25, 26 and 27, is a shift so that zero lift no longer occurs at zero incidence. This angle offset increases with thrust loading. Corresponding to this is an increase in maximum lift in one direction and a decrease for the other. Likewise for the point of action of the sideforce as the rudder is moved from Y/D=-0.25 to Y/D=+0.25 the chordwise position moves forward. The spanwise position moves towards the root for

negative incidence and towards the tip for positive incidence.

The lift-curve slope is no longer symmetric about the origin and for positive incidence its value decreases as Y/D changes from - 0.25 to +0.25 and with the opposite shift for negative incidence.

The lateral movement alters the shape of the local spanwise load distribution (Figures 39 to 44). At low J there is a consdierable redistribution of load compared to the case of no lateral separation. It is interesting to note the similarity in shape between the negative incidence for Y/D=-0.25 and positive incidence for Y/D=+0.25. The lateral movement also reduces the thrust increment (Figure 48).

6.7 Effect of vertical separation

For Rudder No. 2, moving the propeller axis height from 600mm to 900mm changed Z/D from 0.75 to 1.125 and reduced the fraction of the propeller race in way of the rudder span (λ) from 1.0 to 0.625 leading to a coverage factor (ξ) of 0.50. The effect on the rudder characteristics, as shown in Figures 28, 29 and 20, is similar to that of a lateral movement except that there is now a significant shift aft in CP_c with increase in thrust loading. The lift characteristic is shifted so that a positive rudder incidence is required for zero lift. The positive stall angle is decreased as is the negative stall angle. The lift-curve slope decreases which is to be expected as the coverage decreased (see next section).

As the amount of rudder in way of the propeller decreases the amount of the rudder span having a free-stream lift distribution increases (Figure 45). It is noticeable how the load distribution only shows half of the distribution observed when all of the propeller race arrives at the rudder. Also, the effect of the tip vortex appears to be accentuated which may account for the observed drag characteristic at J=0.51. Again, like for a lateral separation, the propeller thrust increment is reduced (Figure 49).

6.8 Effect of coverage

Two rudders with constant chord but spans of 1000mm and 1300mm (Rudders 2 and 4, Figures 31, 32 and 33), were used to investigate the effect of coverage. For these tests the rudder was in way of all the propeller race so λ = 1.0. The effect of tip flow was the same for both rudders. From the results for aspect ratio it would be expected that with increase in span the lift-curve slope would increase. This is indeed observed at high J, but as J is decreased the lift-curve slope for the high aspect ratio rudder becomes progressively less than the other rudder. Also, the stall angle is slightly reduced. Chordwise centre of pressure is the same for both rudders for all J values. However, there is a significant shift outboard of the spanwise centre of pressure for Rudder No.4, especially at low J.

In a manner similar to the vertical movement, the effect of decreasing the coverage is to increase the fraction of the rudder span exhibiting a free-stream behaviour (Figure 46). This time as all of the propeller race arrives at the rudder the behaviour within the race is the same for Rudders 2 and 4. The effect on propeller thrust increment, Figure 50, is simialr for Rudders 2 and 4, whereas the values also shown for Rudder 3 are less. One reason for this may be that for Rudders 2 and 4 the maximum height of the propeller race coincides with the rudder tip.

7. CONCLUSION AND RECOMMENDATIONS

7.1 The overall shape of the rudder lift and drag curves varied little for the parameters tested.

7.2 Variation of rudder stock position gave very little change in rudder characteristics.

7.3 Rudder sideforce is controlled by thrust loading only and is not influenced to any great extent by the propeller pitch ratio setting.

7.4 The effect of aspect ratio on the rudder lift-curve slope is similar to that for free-

stream flow where the slope increases with aspect ratio.

7.5 Lateral separation of the rudder stock from the propeller axis causes a shift in rudder incidence for zero lift. This shift in incidence for zero lift increases with thrust loading.

7.6 The effect of reducing the amount of the propeller race arriving at the rudder is similar to that of a lateral movement. There is a shift in incidence for zero lift, the sign of which will be dependent on the propeller's direction of rotation.

7.7 Decreasing the percentage of the rudder span covered by the propeller race decreases the rudder lift-curve slope by increasing the amount of rudder behaving in a free-stream manner.

7.8 The work reported on forms part of an overall approach which entails identifying the influence of the propeller on the rudder, the rudder on the propeller, and the rudder-propeller combination on the hull. The work to date has only considered the isolated rudder-propeller combination in straight flow. However, a programme of research is currently underway to help identify the effect of a hull form and obliquity on the performance of the rudder-propeller combination.

ACKNOWLEDGEMENTS

The work described in this report covers part of a research project funded by the S.E.R.C./M.O.D. through the Marine Technology Directorate Ltd. under research grant Ref No GR/E/65289.

REFERENCES

1. Molland, A.F., and Turnock, S.R., "Wind Tunnel Investigation of the Influence of Propeller Loading on Ship Rudder Performance", Ship Science Report No. 46, University of Southampton, March 1991.

2. Turnock, S.R., "A Test Rig For The Investigation of Ship Propeller/Rudder Interactions", Ship Science Report No. 45, University of Southampton, November 1990.

3. Molland, A.F., "Pressure Distribution Investigation of a Semi-Balanced Ship Skeg-Rudder", Ship Science Report No. 5/81, University of Southampton, October 1980.

4. Turnock, S.R.," Computer aided Design and Numerically Controlled Manufacture of a Split mould for a Composite Model Ship Propeller", University of Southampton, Ship Science Report 42, December 1990.

5. Molland, A.F.,& Turnock, S.R.," The Design and Construction of Propeller Blades in Composite Materials for a Wind Tunnel Model". University of Southampton, Ship Science Report 41, October 1990.

6. Molland, A.F.,"The Free-Stream Characteristics of a Semi-Balanced Ship Skeg-Rudder", University of Southampton, Ship Science Report 3/77, May 1977.

7. Molland, A.F." The Design, Construction and Calibration of a five-component strain gauge wind tunnel dynamometer " , University of Southampton, Ship Science Report 1/77, Nov. 1976.

8. Molland, A.F., & Turnock, S.R.," The Design, Construction and Calibration of a Thrust and Torque Dynamometer for a Wind Tunnel Propeller Model", University of Southampton, Ship Science Report 44, October 1990.

9. Turnock, S.R., " Two-Dimensional Wind Tunnel Tests of SSS Series 1 Structurally Efficient Aerofoils for Wind Turbines", University of Southampton, Ship Science Report 38, June 1989.

10. English, J.W.; & Bain, D.C., "Some manoeuvring devices for use at zero and low ship speed." Trans. N.E.C.E.I.S., Vol. 88, 1971/72.

11. Molland, A.F., & Turnock, S.R.," Wind Tunnel Test Results for a Model Ship Propeller Based on a Modified Wageningen B4.40 ", University of Southampton, Ship Science Report 43, December 1990.

APPENDIX

Angle	V	RPM	Cl	Cn	Cd	Cmz	Cmx	Cmy	Cpc	Cps
-35.40	10.00	783.63	-1.0880	-1.217	0.570	-0.084	-0.7560	0.2950	36.870	47.177
-30.40	10.00	782.09	-1.0740	-1.149	0.440	-0.039	-0.7633	0.2410	33.390	50.449
-25.40	10.00	783.63	-1.1940	-1.217	0.322	0.015	-0.8120	0.1650	28.773	48.574
-20.40	10.00	782.09	-1.0167	-1.026	0.211	0.029	-0.6770	0.1080	27.185	48.025
-15.40	10.00	783.63	-0.8510	-0.856	0.133	0.040	-0.5400	0.0610	25.292	45.253
-10.40	10.00	782.09	-0.5663	-0.569	0.068	0.029	-0.3543	0.0287	24.903	44.601
-5.40	10.00	783.63	-0.2890	-0.291	0.038	0.016	-0.1760	0.0140	24.660	43.225
-0.40	10.00	782.48	-0.0060	-0.006	0.035	-0.002	-0.0005	0.0215	91.894	13.989
4.60	10.00	783.63	0.2520	0.255	0.048	-0.027	0.1700	0.0250	19.286	49.654
9.60	10.00	782.09	0.5170	0.521	0.068	-0.044	0.3373	0.0360	21.486	47.535
14.60	10.00	783.63	0.8080	0.815	0.131	-0.054	0.5360	0.0620	23.389	48.047
19.60	10.00	782.09	1.0553	1.059	0.192	-0.055	0.7027	0.1000	24.762	48.186
24.60	10.00	783.63	1.3090	1.315	0.300	-0.047	0.8810	0.1580	26.375	48.431
29.60	10.00	782.09	1.4823	1.496	0.419	-0.017	1.0170	0.2257	28.861	49.103
34.60	10.00	783.63	1.2450	1.369	0.606	0.065	0.8890	0.3250	34.751	49.403

RUDDER DYNAMOMETER e2lp.pd J=0.51

Angle	V	RPM	Cl	Cn	Cd	Cmz	Cmx	Cmy	Cpc	Cps
-35.40	10.00	1490.13	-3.0960	-3.195	1.159	-0.022	-2.0880	0.7190	30.660	48.796
-30.40	10.00	1487.79	-2.5790	-2.640	0.822	0.026	-1.7097	0.5080	28.983	48.075
-25.40	10.00	1490.13	-2.0950	-2.145	0.589	0.063	-1.3770	0.3560	27.069	47.585
-20.40	10.00	1487.79	-1.6113	-1.639	0.368	0.090	-1.0243	0.2213	24.455	45.800
-15.40	10.00	1490.13	-1.1280	-1.149	0.232	0.105	-0.6960	0.1370	20.870	44.069
-10.40	10.00	1487.79	-0.6307	-0.644	0.128	0.096	-0.3637	0.0747	15.092	40.138
-5.40	10.00	1490.13	-0.1620	-0.170	0.096	0.073	-0.0630	0.0550	-12.897	22.195
-0.40	10.00	1488.37	0.2485	0.248	0.087	0.041	0.2052	0.0580	46.594	65.127
4.60	10.00	1490.13	0.6250	0.632	0.116	-0.001	0.4630	0.0750	29.767	56.501
9.60	10.00	1487.79	1.0133	1.027	0.170	-0.040	0.7250	0.1017	26.118	53.736
14.60	10.00	1490.13	1.4230	1.444	0.266	-0.072	1.0200	0.1580	25.006	53.652
19.60	10.00	1487.79	1.7690	1.793	0.377	-0.097	1.2667	0.2263	24.568	53.302
24.60	10.00	1490.13	2.1970	2.227	0.550	-0.114	1.5610	0.3360	24.881	52.501

29.60	10.00	1487.79	2.3647	2.408	0.713	-0.108	1.7170	0.4297	25.515	53.293
34.60	10.00	1490.13	2.3950	2.537	0.996	-0.051	1.7650	0.6300	27.960	53.867
39.60	10.00	1490.13	2.3330	2.669	1.367	0.020	1.7430	0.9130	30.747	54.639

RUDDER DYNAMOMETER e3lp.pd J=0.35

Angle	V	RPM	Cl	Cn	Cd	Cmz	Cmx	Cmy	Cpc	Cps
-35.40	10.00	2151.64	-4.3210	-4.599	1.859	-0.052	-2.8800	1.1420	31.112	47.919
-30.40	10.00	2159.14	-3.7003	-3.875	1.350	0.064	-2.4220	0.8303	28.338	47.258
-25.40	10.00	2151.64	-3.0110	-3.123	0.940	0.133	-1.9030	0.5690	25.712	45.347
-20.40	10.00	2159.14	-2.2013	-2.269	0.591	0.182	-1.3453	0.3527	21.940	43.490
-15.40	10.00	2151.64	-1.4360	-1.482	0.366	0.202	-0.8260	0.2180	16.326	40.131
-10.40	10.00	2159.14	-0.6763	-0.705	0.220	0.194	-0.3340	0.1253	2.394	32.373
-5.40	10.00	2151.64	0.0010	-0.014	0.164	0.174	0.1130	0.1000	-1174.639	-735.257
-0.40	10.00	2157.27	0.6440	0.643	0.168	0.126	0.5395	0.1160	49.628	66.368
4.60	10.00	2151.64	1.2040	1.218	0.229	0.064	0.9350	0.1530	35.231	59.978
9.60	10.00	2159.14	1.7260	1.754	0.311	-0.012	1.2987	0.2053	29.340	57.476
14.60	10.00	2151.64	2.2770	2.319	0.459	-0.084	1.6940	0.2940	26.363	56.410
19.60	10.00	2159.14	2.7700	2.825	0.643	-0.146	2.0803	0.4170	24.817	56.830
24.60	10.00	2151.64	3.1980	3.278	0.889	-0.197	2.4170	0.5730	23.983	56.810
29.60	10.00	2159.14	3.5697	3.682	1.172	-0.224	2.6983	0.7427	23.918	56.182
34.60	10.00	2151.64	3.8880	4.072	1.534	-0.227	2.9500	0.9930	24.415	55.985
39.60	10.00	2151.64	4.1010	4.439	2.007	-0.180	3.0610	1.3510	25.927	55.028

RUDDER DYNAMOMETER e1lm.pd Y/D=-0.25 J=0.91

Angle	V	RPM	Cl	Cn	Cd	Cmz	Cmx	Cmy	Cpc	Cps
-35.40	10.00	781.75	-1.0690	-1.207	0.580	-0.094	-0.7930	0.3210	37.745	51.412
-30.40	10.00	782.64	-1.0343	-1.123	0.457	-0.053	-0.7490	0.2617	34.723	51.809
-25.40	10.00	781.75	-0.9210	-0.982	0.349	-0.037	-0.6960	0.1940	33.760	55.024
-20.40	10.00	782.64	-1.0980	-1.092	0.179	0.039	-0.7310	0.1020	26.430	48.546
-15.40	10.00	781.75	-0.8640	-0.860	0.101	0.040	-0.5640	0.0540	25.342	47.328
-10.40	10.00	782.64	-0.5790	-0.579	0.049	0.031	-0.3673	0.0213	24.585	45.603
-5.40	10.00	781.75	-0.3200	-0.321	0.019	0.008	-0.1930	0.0020	27.468	42.555
-0.40	10.00	782.42	-0.0267	-0.027	0.024	0.000	-0.0135	0.0232	30.410	38.199
4.60	10.00	781.75	0.2430	0.246	0.035	-0.024	0.1620	0.0290	20.055	49.236
9.60	10.00	782.64	0.5187	0.523	0.070	-0.039	0.3423	0.0463	22.562	48.526

14.60	10.00	781.75	0.8050	0.810	0.125	-0.051	0.5430	0.0760	23.739	49.768
19.60	10.00	782.64	1.0810	1.087	0.203	-0.051	0.7370	0.1233	25.237	50.220
24.60	10.00	781.75	1.3360	1.340	0.299	-0.043	0.9140	0.1870	26.800	50.338
29.60	10.00	782.64	1.1620	1.231	0.446	0.047	0.7480	0.2477	33.798	45.316
34.60	10.00	781.75	1.2640	1.377	0.592	0.070	0.9420	0.3640	35.075	53.800
39.60	10.00	781.75	1.0210	1.270	0.758	0.095	0.7170	0.4520	37.498	48.709

RUDDER DYNAMOMETER e2lm.pd J=0.51

Angle	V	RPM	Cl	Cn	Cd	Cmz	Cmx	Cmy	Cpc	Cps
-35.40	10.00	1483.73	-2.5380	-2.706	1.099	-0.037	-1.8740	0.7490	31.356	54.982
-30.40	10.00	1475.44	-2.4113	-2.493	0.818	-0.002	-1.6993	0.5710	30.050	52.875
-25.40	10.00	1483.73	-2.1330	-2.176	0.583	0.029	-1.4970	0.4170	28.637	52.855
-20.40	10.00	1475.44	-1.7983	-1.807	0.350	0.069	-1.2173	0.2643	26.183	50.733
-15.40	10.00	1483.73	-1.4780	-1.483	0.217	0.065	-0.9820	0.1740	25.590	49.460
-10.40	10.00	1475.44	-1.0660	-1.072	0.130	0.033	-0.6947	0.1087	26.903	48.074
-5.40	10.00	1483.73	-0.7020	-0.705	0.074	-0.011	-0.4400	0.0710	31.475	45.512
-0.40	10.00	1477.51	-0.2618	-0.262	0.071	-0.043	-0.1578	0.0745	46.251	42.968
4.60	10.00	1483.73	0.1250	0.131	0.083	-0.080	0.1280	0.0790	-31.417	84.680
9.60	10.00	1475.44	0.5517	0.565	0.128	-0.102	0.4340	0.1050	11.878	61.308
14.60	10.00	1483.73	1.0420	1.065	0.223	-0.114	0.7910	0.1660	19.250	58.274
19.60	10.00	1475.44	1.4950	1.528	0.356	-0.103	1.1230	0.2603	23.252	57.443
24.60	10.00	1483.73	2.0220	2.071	0.558	-0.082	1.5080	0.4060	26.009	56.854
29.60	10.00	1475.44	2.4813	2.561	0.817	-0.038	1.8543	0.5740	28.483	56.528
34.60	10.00	1483.73	2.9970	3.120	1.151	0.008	2.2380	0.8120	30.254	56.320
39.60	10.00	1483.73	3.4680	3.644	1.525	0.063	2.5770	1.0770	31.718	55.834

RUDDER DYNAMOMETER e3lm.pd j=0.35

Angle	V	RPM	Cl	Cn	Cd	Cmz	Cmx	Cmy	Cpc	Cps
-35.40	10.00	2161.11	-3.9430	-4.165	1.641	0.104	-2.8610	1.2260	27.493	55.551
-30.40	10.00	2154.82	-3.7510	-3.881	1.276	0.098	-2.6710	0.9620	27.469	54.403
-25.40	10.00	2161.11	-3.3780	-3.463	0.959	0.074	-2.3750	0.7350	27.842	53.558
-20.40	10.00	2154.82	-2.8683	-2.904	0.617	0.110	-1.9833	0.5057	26.200	52.591
-15.40	10.00	2161.11	-2.3950	-2.418	0.410	0.071	-1.6390	0.3570	27.045	51.766
-10.40	10.00	2154.82	-1.8397	-1.858	0.268	0.002	-1.2337	0.2450	29.858	50.179
-5.40	10.00	2161.11	-1.3100	-1.320	0.177	-0.076	-0.8490	0.1730	35.755	47.770

-0.40	10.00	2156.32	-0.6685	-0.669	0.140	-0.138	-0.3955	0.1508	50.564	41.741
4.60	10.00	2161.11	-0.0730	-0.061	0.147	-0.189	0.0620	0.1440	341.915	-138.226
9.60	10.00	2154.82	0.5460	0.569	0.188	-0.226	0.5370	0.1823	-9.695	80.795
14.60	10.00	2161.11	1.2410	1.284	0.332	-0.231	1.0680	0.2810	12.028	68.486
19.60	10.00	2154.82	1.9637	2.033	0.547	-0.209	1.6027	0.4400	19.698	64.016
24.60	10.00	2161.11	2.7240	2.835	0.860	-0.163	2.1730	0.6680	24.247	62.018
29.60	10.00	2154.82	3.4357	3.614	1.269	-0.095	2.7043	0.9480	27.352	60.514
34.60	10.00	2161.11	4.1630	4.440	1.784	-0.010	3.2430	1.3140	29.755	59.426
39.60	10.00	2161.11	4.7780	5.199	2.381	0.084	3.7160	1.7190	31.607	58.637

RUDDER DYNAMOMETER e1cp.pd change of pivot j=0.94

Angle	V	RPM	Cl	Cn	Cd	Cmz	Cmx	Cmy	Cpc	Cps
-25.40	10.00	783.63	-1.2560	-1.273	0.323	0.344	-0.8400	0.2450	26.809	50.361
-20.40	10.00	783.63	-1.0410	-1.047	0.207	0.300	-0.6820	0.1680	25.198	49.083
-15.40	10.00	783.63	-0.7830	-0.788	0.122	0.242	-0.5150	0.1050	23.030	49.027
-10.40	10.00	783.63	-0.5410	-0.544	0.063	0.176	-0.3410	0.0630	21.381	46.308
-5.40	10.00	783.63	-0.2800	-0.282	0.033	0.098	-0.1700	0.0380	18.913	43.628
-0.40	10.00	783.63	-0.0355	-0.036	0.030	0.013	-0.0045	0.0300	17.821	-3.675
4.60	10.00	783.63	0.2500	0.253	0.043	-0.074	0.1720	0.0390	24.589	51.436
9.60	10.00	783.63	0.5120	0.518	0.078	-0.155	0.3450	0.0600	23.831	50.153
14.60	10.00	783.63	0.7650	0.775	0.140	-0.231	0.5240	0.0990	24.026	51.136
19.60	10.00	783.63	1.0280	1.042	0.220	-0.295	0.7040	0.1590	25.484	51.249
24.60	10.00	783.63	1.1980	1.234	0.348	-0.327	0.8420	0.2380	27.277	52.560

RUDDER DYNAMOMETER e2cp.pd j=0.51

Angle	V	RPM	Cl	Cn	Cd	Cmz	Cmx	Cmy	Cpc	Cps
-25.40	10.00	1462.66	-2.3400	-2.378	0.617	0.699	-1.4840	0.4390	24.422	46.792
-20.40	10.00	1460.62	-1.8885	-1.906	0.390	0.590	-1.1895	0.3015	22.857	46.487
-15.40	10.00	1462.66	-1.4060	-1.414	0.218	0.454	-0.8500	0.1840	21.704	43.934
-10.40	10.00	1460.62	-0.9385	-0.946	0.126	0.315	-0.5410	0.1125	20.524	40.889
-5.40	10.00	1462.66	-0.4800	-0.482	0.049	0.165	-0.2360	0.0580	19.497	32.360
-0.40	10.00	1460.62	-0.0540	-0.055	0.044	0.020	0.0425	0.0430	15.579	-98.896
4.60	10.00	1462.66	0.3540	0.358	0.057	-0.129	0.3330	0.0540	17.840	76.483
9.60	10.00	1460.62	0.7990	0.810	0.130	-0.267	0.6415	0.1075	20.796	62.865
14.60	10.00	1462.66	1.2260	1.244	0.229	-0.400	0.9450	0.1840	21.618	59.757

19.60	10.00	1460.62	1.6760	1.711	0.396	-0.516	1.2810	0.3100	23.617	59.097
24.60	10.00	1462.66	2.0940	2.152	0.595	-0.615	1.5880	0.4590	25.230	58.469

RUDDER DYNAMOMETER e1vo.pd vertical offset j=0.94

Angle	V	RPM	Cl	Cn	Cd	Cmz	Cmx	Cmy	Cpc	Cps
-35.40	10.00	783.59	-0.9400	-1.091	0.561	-0.085	-0.6800	0.2800	37.813	48.130
-30.40	10.00	783.59	-0.9840	-1.086	0.468	-0.059	-0.7330	0.2160	35.390	50.830
-25.40	10.00	783.59	-1.1510	-1.157	0.274	0.011	-0.8220	0.1240	29.008	51.321
-20.40	10.00	783.59	-0.9670	-0.973	0.192	0.027	-0.6760	0.0710	27.213	50.166
-15.40	10.00	783.59	-0.7670	-0.769	0.109	0.036	-0.5240	0.0350	25.365	49.443
-10.40	10.00	783.59	-0.5850	-0.585	0.051	0.043	-0.3870	0.0060	22.678	47.711
-5.40	10.00	783.59	-0.3370	-0.338	0.025	0.028	-0.2220	-0.0080	21.617	47.781
-0.40	10.00	783.59	-0.0735	-0.073	0.026	0.008	-0.0620	-0.0095	20.091	67.564
4.60	10.00	783.59	0.1560	0.158	0.034	-0.010	0.1020	-0.0020	23.451	46.633
9.60	10.00	783.59	0.4260	0.431	0.063	-0.030	0.2740	0.0150	22.979	45.874
14.60	10.00	783.59	0.6950	0.702	0.117	-0.040	0.4590	0.0490	24.346	47.478
19.60	10.00	783.59	0.9380	0.951	0.201	-0.034	0.6300	0.0980	26.383	48.351
24.60	10.00	783.59	1.1120	1.138	0.303	-0.014	0.7810	0.1650	28.741	50.975
29.60	10.00	783.59	1.2950	1.345	0.442	0.003	0.9090	0.2420	30.217	50.214
34.60	10.00	783.59	0.9880	1.110	0.522	0.060	0.7190	0.2770	35.393	49.965
39.60	10.00	783.59	0.9990	1.185	0.651	0.086	0.7300	0.3530	37.226	48.956

RUDDER DYNAMOMETER e2vo.pd j=0.51

Angle	V	RPM	Cl	Cn	Cd	Cmz	Cmx	Cmy	Cpc	Cps
-35.40	10.00	1458.76	-2.0590	-2.133	0.785	-0.046	-1.6780	0.4930	32.136	60.013
-30.40	10.00	1462.57	-1.9397	-1.982	0.611	-0.014	-1.5013	0.3913	30.675	57.829
-25.40	10.00	1458.76	-2.0200	-1.989	0.383	0.068	-1.5080	0.2380	26.569	56.117
-20.40	10.00	1462.57	-1.7347	-1.702	0.218	0.107	-1.3003	0.1363	23.659	56.922
-15.40	10.00	1458.76	-1.3260	-1.314	0.133	0.095	-1.0060	0.0670	22.792	57.653
-10.40	10.00	1462.57	-0.9960	-0.990	0.059	0.109	-0.7600	0.0337	18.984	58.594
-5.40	10.00	1458.76	-0.6820	-0.681	0.023	0.090	-0.5170	-0.0030	16.721	58.116
-0.40	10.00	1462.57	-0.3013	-0.302	0.030	0.076	-0.2467	0.0137	4.806	64.313
4.60	10.00	1458.76	0.0710	0.075	0.056	0.045	0.0430	0.0320	90.131	42.454
9.60	10.00	1462.57	0.4650	0.480	0.129	0.030	0.3280	0.0907	36.217	53.075
14.60	10.00	1458.76	0.8340	0.862	0.218	0.010	0.6180	0.1520	31.151	56.363

19.60	10.00	1462.57	1.2017	1.255	0.366	0.020	0.9203	0.2703	31.567	58.855
24.60	10.00	1458.76	1.6010	1.686	0.552	0.038	1.2370	0.4110	32.226	59.378
29.60	10.00	1462.57	1.7093	1.864	0.765	0.082	1.3743	0.5763	34.391	61.908
34.60	10.00	1458.76	1.6670	1.932	0.985	0.110	1.4170	0.7000	35.696	63.491
39.60	10.00	1458.76	1.8020	2.155	1.202	0.126	1.5210	0.8730	35.818	62.715

RUDDER DYNAMOMETER e3vo.pd j=0.34

Angle	V	RPM	Cl	Cn	Cd	Cmz	Cmx	Cmy	Cpc	Cps
-35.40	10.00	2164.59	-3.6780	-3.703	1.218	0.015	-3.0270	0.8610	29.593	62.591
-30.40	10.00	2164.59	-3.4000	-3.381	0.887	0.066	-2.7650	0.6260	28.029	62.400
-25.40	10.00	2164.59	-3.1540	-3.067	0.507	0.179	-2.4940	0.3660	24.161	61.098
-20.40	10.00	2164.59	-2.6910	-2.617	0.271	0.221	-2.1260	0.1910	21.542	61.167
-15.40	10.00	2164.59	-2.1670	-2.121	0.122	0.223	-1.7230	0.0780	19.456	61.778
-10.40	10.00	2164.59	-1.5880	-1.568	0.036	0.212	-1.2770	0.0080	16.478	62.701
-5.40	10.00	2164.59	-1.0850	-1.079	-0.015	0.198	-0.8830	-0.0290	11.665	63.699
-0.40	10.00	2164.59	-0.4847	-0.485	0.002	0.134	-0.3980	-0.0180	3.281	64.523
4.60	10.00	2164.59	-0.0650	-0.060	0.057	0.140	-0.0370	0.0200	-204.035	41.076
9.60	10.00	2164.59	0.5020	0.524	0.173	0.112	0.4230	0.1090	51.324	65.541
14.60	10.00	2164.59	1.0330	1.082	0.325	0.088	0.8720	0.2430	38.138	66.140
19.60	10.00	2164.59	1.5370	1.623	0.520	0.069	1.3030	0.4070	34.254	66.598
24.60	10.00	2164.59	2.0210	2.160	0.775	0.064	1.7170	0.6240	32.948	66.813
29.60	10.00	2164.59	2.2770	2.527	1.107	0.100	2.0400	0.9030	33.949	70.355
34.60	10.00	2164.59	2.5660	2.970	1.511	0.145	2.2650	1.2110	34.871	68.427
39.60	10.00	2164.59	2.8910	3.449	1.917	0.157	2.6250	1.5630	34.549	70.022

RUDDER DYNAMOMETER e1pp.pd P/D=1.4 j=0.94

Angle	V	RPM	Cl	Cn	Cd	Cmz	Cmx	Cmy	Cpc	Cps
-35.40	10.00	573.86	-0.7830	-0.982	0.594	-0.094	-0.5790	0.2900	39.517	47.691
-30.40	10.00	573.86	-0.8430	-0.924	0.389	-0.041	-0.6180	0.2070	34.432	51.475
-25.40	10.00	573.86	-0.9470	-0.987	0.307	-0.013	-0.6850	0.1680	31.268	52.497
-20.40	10.00	573.86	-0.9930	-0.997	0.191	0.035	-0.6620	0.1060	26.515	48.436
-15.40	10.00	573.86	-0.7270	-0.734	0.122	0.036	-0.4840	0.0620	25.097	48.303
-10.40	10.00	573.86	-0.4710	-0.476	0.071	0.029	-0.3120	0.0290	23.990	48.171
-5.40	10.00	573.86	-0.2320	-0.234	0.039	0.020	-0.1560	0.0170	21.474	49.672
-0.40	10.00	573.86	0.0167	0.017	0.035	0.004	0.0023	0.0320	55.412	0.420

4.60	10.00	573.86	0.2520	0.255	0.047	-0.016	0.1550	0.0360	23.853	44.408
9.60	10.00	573.86	0.5140	0.520	0.082	-0.030	0.3180	0.0490	24.281	44.316
14.60	10.00	573.86	0.7500	0.758	0.129	-0.038	0.4840	0.0740	25.007	46.663
19.60	10.00	573.86	0.9430	0.958	0.207	-0.034	0.6280	0.1170	26.437	48.378
24.60	10.00	573.86	1.0940	1.120	0.302	-0.011	0.7560	0.1740	28.987	50.309
29.60	10.00	573.86	1.2860	1.329	0.428	0.019	0.8940	0.2360	31.414	49.786
34.60	10.00	573.86	1.3140	1.398	0.556	0.053	0.8930	0.3030	33.797	47.388
39.60	10.00	573.86	1.0860	1.305	0.735	0.099	0.6910	0.4040	37.586	43.026

RUDDER DYNAMOMETER e2pp.pd j=0.51

Angle	V	RPM	Cl	Cn	Cd	Cmz	Cmx	Cmy	Cpc	Cps
-35.40	10.00	1220.52	-1.9850	-2.382	1.318	-0.172	-1.2510	0.7600	37.199	43.822
-30.40	10.00	1219.06	-2.3210	-2.457	0.899	-0.062	-1.4810	0.5555	32.552	45.928
-25.40	10.00	1220.52	-2.2840	-2.277	0.500	0.074	-1.4580	0.3420	26.745	46.785
-20.40	10.00	1219.06	-1.8750	-1.867	0.314	0.096	-1.1620	0.2085	24.851	44.747
-15.40	10.00	1220.52	-1.4060	-1.400	0.167	0.084	-0.8470	0.1150	23.997	42.973
-10.40	10.00	1219.06	-0.9540	-0.952	0.074	0.069	-0.5345	0.0505	22.733	38.756
-5.40	10.00	1220.52	-0.5130	-0.512	0.018	0.031	-0.2480	0.0150	23.844	30.953
-0.40	10.00	1219.55	-0.0443	-0.045	0.013	0.005	0.0617	0.0150	17.913	-155.480
4.60	10.00	1220.52	0.3980	0.399	0.034	-0.028	0.3720	0.0270	22.905	76.059
9.60	10.00	1219.06	0.8540	0.856	0.089	-0.055	0.6975	0.0590	23.592	63.911
14.60	10.00	1220.52	1.2760	1.283	0.192	-0.072	0.9980	0.1240	24.352	60.206
19.60	10.00	1219.06	1.6985	1.710	0.329	-0.073	1.3040	0.2135	25.690	58.522
24.60	10.00	1220.52	2.0550	2.084	0.519	-0.058	1.5650	0.3450	27.191	57.670
29.60	10.00	1219.06	2.3725	2.461	0.806	0.003	1.8340	0.5450	30.106	58.239
34.60	10.00	1220.52	2.5040	2.717	1.156	0.106	1.8990	0.7970	33.901	56.663
39.60	10.00	1220.52	2.5670	2.993	1.593	0.190	1.8250	1.0920	36.323	52.718

RUDDER DYNAMOMETER e3pp.pd j=0.34

Angle	V	RPM	Cl	Cn	Cd	Cmz	Cmx	Cmy	Cpc	Cps
-35.40	10.00	1718.85	-3.9030	-4.239	1.825	-0.117	-2.3960	1.1350	32.745	44.083
-30.40	10.00	1718.85	-3.7600	-3.848	1.195	0.060	-2.3040	0.7330	28.429	43.782
-25.40	10.00	1718.85	-3.2790	-3.251	0.674	0.157	-2.0200	0.4410	25.158	44.434
-20.40	10.00	1718.85	-2.6910	-2.657	0.385	0.160	-1.6060	0.2540	23.970	42.510
-15.40	10.00	1718.85	-2.0660	-2.037	0.170	0.134	-1.1840	0.1190	23.395	40.068

-10.40	10.00	1718.85	-1.4100	-1.393	0.034	0.096	-0.7560	0.0250	23.088	36.223
-5.40	10.00	1718.85	-0.7490	-0.742	-0.045	0.044	-0.3140	-0.0310	24.061	24.306
-0.40	10.00	1718.85	-0.0755	-0.075	-0.067	-0.009	0.1405	-0.0405	43.618	-216.536
4.60	10.00	1718.85	0.5550	0.550	-0.033	-0.062	0.6010	-0.0280	18.767	90.996
9.60	10.00	1718.85	1.1740	1.165	0.047	-0.107	1.0570	0.0240	20.831	72.294
14.60	10.00	1718.85	1.7740	1.763	0.181	-0.148	1.4890	0.1160	21.572	65.879
19.60	10.00	1718.85	2.3940	2.388	0.396	-0.179	1.9680	0.2660	22.494	63.855
24.60	10.00	1718.85	2.9930	3.003	0.676	-0.184	2.4220	0.4690	23.852	62.334
29.60	10.00	1718.85	3.5490	3.588	1.018	-0.161	2.8610	0.7090	25.487	61.586
34.60	10.00	1718.85	3.9560	4.122	1.526	-0.044	3.1500	1.0790	28.908	60.273
39.60	10.00	1718.85	3.9810	4.447	2.165	0.157	3.1820	1.6160	33.511	60.780

RUDDER DYNAMOMETER e1pm.pd P/D=0.75 j=0.94

Angle	V	RPM	Cl	Cn	Cd	Cmz	Cmx	Cmy	Cpc	Cps
-35.40	10.00	1072.32	-1.0630	-1.196	0.569	-0.085	-0.7840	0.3050	37.110	50.729
-30.40	10.00	1072.32	-1.1750	-1.248	0.463	-0.047	-0.8310	0.2630	33.721	50.556
-25.40	10.00	1072.32	-1.3270	-1.336	0.319	0.028	-0.8970	0.1870	27.898	49.134
-20.40	10.00	1072.32	-1.0680	-1.076	0.214	0.041	-0.7120	0.1200	26.219	48.486
-15.40	10.00	1072.32	-0.7940	-0.803	0.140	0.039	-0.5100	0.0740	25.141	46.238
-10.40	10.00	1072.32	-0.5210	-0.526	0.077	0.031	-0.3270	0.0360	23.997	44.795
-5.40	10.00	1072.32	-0.2650	-0.267	0.038	0.023	-0.1640	0.0210	21.430	44.433
-0.40	10.00	1072.32	-0.0150	-0.015	0.036	0.003	-0.0010	0.0280	5.481	-6.379
4.60	10.00	1072.32	0.2440	0.247	0.047	-0.019	0.1630	0.0340	22.473	49.616
9.60	10.00	1072.32	0.4970	0.504	0.082	-0.035	0.3340	0.0500	22.953	49.520
14.60	10.00	1072.32	0.7650	0.776	0.142	-0.042	0.5120	0.0810	24.585	48.913
19.60	10.00	1072.32	0.9750	0.994	0.226	-0.035	0.6700	0.1280	26.446	50.332
24.60	10.00	1072.32	1.1580	1.194	0.340	-0.012	0.8080	0.1930	28.958	50.692
29.60	10.00	1072.32	1.2980	1.374	0.496	0.038	0.9290	0.2760	32.786	51.215
34.60	10.00	1072.32	1.4900	1.573	0.610	0.047	1.0720	0.3480	32.971	51.173
39.60	10.00	1072.32	1.2170	1.467	0.830	0.112	0.8340	0.4960	37.636	47.869

RUDDER DYNAMOMETER e2pm.pd j=0.51

Angle	V	RPM	Cl	Cn	Cd	Cmz	Cmx	Cmy	Cpc	Cps
-30.40	10.00	1789.91	-2.6070	-2.642	0.776	0.078	-1.7425	0.5015	27.032	49.015
-20.40	10.00	1789.91	-1.7680	-1.779	0.349	0.112	-1.1450	0.2225	23.644	47.203

-10.40	10.00	1789.91	-0.8645	-0.873	0.126	0.077	-0.5305	0.0845	21.120	43.969
-0.40	10.00	1789.97	-0.0263	-0.027	0.058	0.006	0.0357	0.0393	0.358	-177.993
9.60	10.00	1789.90	1.0660	1.085	0.205	-0.076	0.7867	0.1257	22.425	57.220
14.60	10.00	1790.11	1.2030	1.220	0.221	-0.086	0.9120	0.1330	22.973	57.556
19.60	10.00	1789.97	1.6080	1.632	0.349	-0.091	1.2010	0.2197	24.377	56.373
24.60	10.00	1790.11	2.0240	2.059	0.524	-0.085	1.5120	0.3440	25.874	56.238
29.60	10.00	1789.97	2.3880	2.469	0.795	-0.037	1.7717	0.5227	28.478	55.353
34.60	10.00	1790.11	2.6150	2.811	1.158	0.092	1.9350	0.7700	33.248	54.724
39.60	10.00	1790.11	2.5320	2.951	1.569	0.204	1.7650	1.0370	36.887	50.974

RUDDER DYNAMOMETER e3pm.pd j=0.35

Angle	V	RPM	Cl	Cn	Cd	Cmz	Cmx	Cmy	Cpc	Cps
-35.40	10.00	2556.50	-4.3300	-4.462	1.609	0.119	-2.7780	1.1190	27.312	47.787
-30.40	10.00	2556.50	-3.8080	-3.847	1.112	0.217	-2.5420	0.7410	24.346	49.238
-25.40	10.00	2556.50	-3.2340	-3.256	0.780	0.221	-2.1280	0.5220	23.200	48.411
-20.40	10.00	2556.50	-2.6220	-2.633	0.503	0.208	-1.6830	0.3440	22.087	46.941
-15.40	10.00	2556.50	-1.9630	-1.971	0.294	0.180	-1.2280	0.2120	20.877	45.424
-10.40	10.00	2556.50	-1.3230	-1.329	0.153	0.121	-0.7850	0.1110	20.888	42.048
-5.40	10.00	2556.50	-0.6950	-0.700	0.085	0.060	-0.3670	0.0610	21.415	35.518
-0.40	10.00	2556.50	-0.0570	-0.058	0.067	-0.007	0.0805	0.0515	41.014	-157.081
4.60	10.00	2556.50	0.5450	0.551	0.097	-0.069	0.5170	0.0640	17.422	76.974
9.60	10.00	2556.50	1.1660	1.179	0.178	-0.127	0.9760	0.1130	19.176	65.712
14.60	10.00	2556.50	1.7750	1.796	0.312	-0.172	1.4060	0.2060	20.408	61.122
19.60	10.00	2556.50	2.3800	2.414	0.514	-0.206	1.8710	0.3490	21.464	60.353
24.60	10.00	2556.50	3.0210	3.079	0.796	-0.217	2.3430	0.5500	22.941	59.137
29.60	10.00	2556.50	3.6480	3.736	1.142	-0.207	2.8200	0.7875	24.460	58.543
34.60	10.00	2556.50	4.2190	4.369	1.579	-0.159	3.2780	1.1000	26.354	58.546
39.60	10.00	2556.50	4.3920	4.845	2.291	0.074	3.4200	1.6180	31.506	58.174

RUDDER DYNAMOMETER e14r.pd Rudder No. 4 j=0.91

Angle	V	RPM	Cl	Cn	Cd	Cmz	Cmx	Cmy	Cpc	Cps
-35.40	10.00	779.61	-1.0230	-1.159	0.561	-0.075	-0.6870	0.3260	36.499	51.115
-30.40	10.00	779.61	-0.9660	-1.065	0.459	-0.047	-0.6490	0.2450	34.444	50.700
-25.40	10.00	779.61	-1.1070	-1.147	0.343	-0.009	-0.7110	0.1990	30.792	49.939
-20.40	10.00	779.61	-1.0180	-1.024	0.199	0.029	-0.6400	0.1160	27.169	49.107

-15.40	10.00	779.61	-0.7880	-0.793	0.124	0.034	-0.4830	0.0730	25.670	47.668
-10.40	10.00	779.61	-0.5590	-0.562	0.064	0.039	-0.3260	0.0430	23.099	45.105
-5.40	10.00	779.61	-0.3000	-0.302	0.036	0.024	-0.1670	0.0290	21.919	42.414
-0.40	10.00	779.61	-0.0180	-0.019	0.028	0.000	-0.0055	0.0245	27.915	19.525
4.60	10.00	779.61	0.2490	0.251	0.038	-0.023	0.1560	0.0310	20.874	49.442
9.60	10.00	779.61	0.5380	0.541	0.068	-0.040	0.3250	0.0460	22.579	47.242
14.60	10.00	779.61	0.8310	0.833	0.116	-0.049	0.5020	0.0750	24.079	47.082
19.60	10.00	779.61	1.0980	1.097	0.188	-0.050	0.6710	0.1160	25.397	47.686
24.60	10.00	779.61	1.1540	1.169	0.288	-0.012	0.7350	0.1800	28.941	50.161
29.60	10.00	779.61	1.1780	1.232	0.421	0.025	0.7700	0.2440	31.996	50.636
34.60	10.00	779.61	1.2000	1.326	0.595	0.060	0.7840	0.3430	34.506	49.897
39.60	10.00	779.61	1.1140	1.356	0.781	0.105	0.7300	0.4540	37.741	49.361

RUDDER DYNAMOMETER e24r.pd Rudder No.4 j=0.51

Angle	V	RPM	Cl	Cn	Cd	Cmz	Cmx	Cmy	Cpc	Cps
-35.40	10.00	1462.43	-2.1990	-2.342	0.948	-0.033	-1.5580	0.6310	31.406	56.370
-30.40	10.00	1459.95	-2.1140	-2.191	0.726	0.009	-1.4630	0.4790	29.569	55.222
-25.40	10.00	1462.43	-2.0400	-2.055	0.496	0.038	-1.2840	0.3400	28.125	50.070
-20.40	10.00	1459.95	-1.7683	-1.759	0.292	0.090	-1.1240	0.2063	24.860	50.493
-15.40	10.00	1462.43	-1.2460	-1.248	0.174	0.071	-0.7800	0.1280	24.289	49.506
-10.40	10.00	1459.95	-0.8613	-0.863	0.089	0.068	-0.5157	0.0650	22.085	46.675
-5.40	10.00	1462.43	-0.4650	-0.467	0.042	0.037	-0.2540	0.0410	22.149	41.481
-0.40	10.00	1460.57	-0.0500	-0.050	0.036	0.004	0.0163	0.0302	21.467	-45.516
4.60	10.00	1462.43	0.3650	0.368	0.052	-0.032	0.2940	0.0450	21.222	66.999
9.60	10.00	1459.95	0.8193	0.826	0.109	-0.061	0.5937	0.0757	22.631	58.950
14.60	10.00	1462.43	1.1940	1.202	0.184	-0.079	0.8520	0.1320	23.446	57.890
19.60	10.00	1459.95	1.6193	1.630	0.310	-0.082	1.1437	0.2123	24.910	57.012
24.60	10.00	1462.43	1.8660	1.891	0.468	-0.061	1.3430	0.3290	26.777	58.341
29.60	10.00	1459.95	2.0003	2.093	0.715	-0.003	1.5047	0.4850	29.868	60.526
34.60	10.00	1462.43	2.0640	2.304	1.065	0.096	1.5520	0.7330	34.159	60.067

RUDDER DYNAMOMETER e34r.pd j=0.35

Angle	V	RPM	Cl	Cn	Cd	Cmz	Cmx	Cmy	Cpc	Cps
-35.40	10.00	2163.13	-3.7900	-3.929	1.450	0.071	-2.6780	1.0180	28.190	57.109
-30.40	10.00	2163.13	-3.4470	-3.507	1.056	0.118	-2.3950	0.7550	26.628	56.314

-25.40	10.00	2163.13	-3.1000	-3.096	0.689	0.171	-2.1020	0.5120	24.465	54.976
-20.40	10.00	2163.13	-2.5250	-2.509	0.409	0.192	-1.6560	0.3190	22.344	52.829
-15.40	10.00	2163.13	-1.8770	-1.868	0.218	0.160	-1.1980	0.1800	21.440	50.931
-10.40	10.00	2163.13	-1.2020	-1.199	0.094	0.112	-0.7360	0.0800	20.605	48.093
-5.40	10.00	2163.13	-0.6250	-0.624	0.019	0.065	-0.3250	0.0270	19.610	38.740
-0.40	10.00	2163.13	-0.0327	-0.033	0.003	0.003	0.0940	0.0100	22.419	-308.515
4.60	10.00	2163.13	0.5250	0.526	0.029	-0.057	0.4980	0.0250	19.132	81.339
9.60	10.00	2163.13	1.1100	1.112	0.105	-0.113	0.9220	0.0810	19.814	69.464
14.60	10.00	2163.13	1.6730	1.678	0.232	-0.154	1.3280	0.1720	20.795	65.742
19.60	10.00	2163.13	2.2320	2.240	0.410	-0.183	1.7470	0.3080	21.801	64.606
24.60	10.00	2163.13	2.6530	2.695	0.680	-0.172	2.1080	0.4910	23.619	65.239
29.60	10.00	2163.13	3.0920	3.213	1.062	-0.122	2.4640	0.7500	26.196	64.739
34.60	10.00	2163.13	3.5090	3.711	1.448	-0.064	2.8020	1.0460	28.269	64.707
39.60	10.00	2163.13	3.4670	4.015	2.108	0.123	2.7390	1.5720	33.049	64.069

RUDDER DYNAMOMETER e15r.pd Rudder No. 5 J=0.94

Angle	V	RPM	Cl	Cn	Cd	Cmz	Cmx	Cmy	Cpc	Cps
-35.40	10.00	785.34	-1.1630	-1.304	0.614	-0.061	-0.7940	0.3010	34.662	45.524
-30.40	10.00	785.34	-1.1630	-1.259	0.506	-0.020	-0.7600	0.2910	31.552	46.214
-25.40	10.00	785.34	-1.0820	-1.140	0.379	0.011	-0.7370	0.2270	29.032	49.467
-20.40	10.00	785.34	-0.9630	-0.997	0.269	0.045	-0.6160	0.1680	25.490	46.282
-15.40	10.00	785.34	-0.7420	-0.765	0.186	0.053	-0.4610	0.1270	23.090	45.034
-10.40	10.00	785.34	-0.5070	-0.522	0.129	0.050	-0.3010	0.0940	20.478	42.497
-5.40	10.00	785.34	-0.2590	-0.267	0.097	0.034	-0.1520	0.0770	17.430	41.914
-0.40	10.00	785.34	-0.0190	-0.020	0.086	0.011	-0.0050	0.0725	-25.520	12.077
4.60	10.00	785.34	0.2270	0.234	0.100	-0.009	0.1440	0.0790	26.018	46.520
9.60	10.00	785.34	0.5400	0.556	0.141	-0.028	0.3310	0.0990	24.967	44.142
14.60	10.00	785.34	0.7500	0.773	0.191	-0.033	0.4760	0.1310	25.673	46.251
19.60	10.00	785.34	1.0130	1.044	0.267	-0.031	0.6470	0.1770	27.058	46.570
24.60	10.00	785.34	1.0750	1.138	0.386	0.006	0.7220	0.2440	30.571	49.120
29.60	10.00	785.34	1.2810	1.372	0.522	0.036	0.8490	0.3180	32.606	47.756
34.60	10.00	785.34	1.3960	1.539	0.687	0.073	0.9350	0.4150	34.757	47.782
39.60	10.00	785.34	1.4100	1.635	0.861	0.105	0.9430	0.5060	36.393	46.690

RUDDER DYNAMOMETER e25r.pd Rudder No. 5 J=0.51

Angle	V	RPM	Cl	Cn	Cd	Cmz	Cmx	Cmy	Cpc	Cps
-35.40	10.00	1462.54	-2.9170	-3.031	1.127	0.091	-1.9150	0.7220	26.998	47.819
-30.40	10.00	1458.23	-2.5560	-2.608	0.797	0.115	-1.6373	0.5090	25.599	46.531
-25.40	10.00	1462.54	-2.1700	-2.215	0.595	0.130	-1.3640	0.3870	24.141	45.605
-20.40	10.00	1458.23	-1.7037	-1.726	0.372	0.127	-1.0497	0.2427	22.637	44.391
-15.40	10.00	1462.54	-1.2670	-1.293	0.269	0.119	-0.7590	0.1910	20.828	43.005
-10.40	10.00	1458.23	-0.8233	-0.835	0.141	0.092	-0.4650	0.1017	18.993	39.455
-5.40	10.00	1462.54	-0.4130	-0.423	0.126	0.063	-0.2050	0.1010	15.083	33.025
-0.40	10.00	1459.31	-0.0188	-0.019	0.084	0.022	0.0518	0.0700	-83.478	-284.721
4.60	10.00	1462.54	0.3730	0.383	0.130	-0.015	0.3200	0.1060	26.146	68.021
9.60	10.00	1458.23	0.7813	0.794	0.145	-0.050	0.5957	0.1027	23.665	58.606
14.60	10.00	1462.54	1.2070	1.238	0.278	-0.067	0.8860	0.1980	24.562	55.778
19.60	10.00	1458.23	1.6007	1.635	0.379	-0.077	1.1700	0.2533	25.289	55.091
24.60	10.00	1462.54	2.0170	2.086	0.605	-0.070	1.4680	0.4140	26.635	54.741
29.60	10.00	1458.23	2.3740	2.460	0.802	-0.059	1.7300	0.5347	27.611	54.399
34.60	10.00	1462.54	2.6850	2.870	1.162	-0.001	1.9770	0.7840	29.968	54.718
39.60	10.00	1462.54	2.7610	3.118	1.554	0.115	2.0020	1.0480	33.683	53.388

RUDDER DYNAMOMETER e35r.pd Rudder No. 5 J=0.35

Angle	V	RPM	Cl	Cn	Cd	Cmz	Cmx	Cmy	Cpc	Cps
-35.40	10.00	2159.10	-4.2700	-4.511	1.778	0.224	-2.8200	1.1330	25.024	48.003
-30.40	10.00	2159.10	-3.7720	-3.913	1.303	0.256	-2.4330	0.8360	23.448	46.937
-25.40	10.00	2159.10	-3.1610	-3.253	0.927	0.260	-2.0020	0.6000	22.017	46.005
-20.40	10.00	2159.10	-2.5190	-2.578	0.622	0.243	-1.5480	0.4160	20.560	44.413
-15.40	10.00	2159.10	-1.8320	-1.869	0.385	0.212	-1.0770	0.2720	18.636	41.905
-10.40	10.00	2159.10	-1.1890	-1.211	0.229	0.162	-0.6450	0.1700	16.657	37.417
-5.40	10.00	2159.10	-0.5760	-0.587	0.138	0.103	-0.2360	0.1140	12.426	24.344
-0.40	10.00	2159.10	0.0235	0.023	0.116	0.036	0.1685	0.0955	195.674	743.500
4.60	10.00	2159.10	0.5860	0.595	0.140	-0.032	0.5720	0.1130	24.659	79.870
9.60	10.00	2159.10	1.1690	1.191	0.228	-0.098	0.9890	0.1700	21.762	66.744
14.60	10.00	2159.10	1.7220	1.759	0.367	-0.151	1.3990	0.2700	21.421	63.375
19.60	10.00	2159.10	2.3190	2.375	0.567	-0.186	1.8390	0.4090	22.167	61.215
24.60	10.00	2159.10	2.9120	3.003	0.854	-0.202	2.2790	0.6060	23.259	59.892
29.60	10.00	2159.10	3.5320	3.691	1.253	-0.195	2.7560	0.8820	24.724	59.233
34.60	10.00	2159.10	4.1140	4.362	1.718	-0.157	3.2020	1.2210	26.396	58.817

39.60	10.00	2159.10	4.5100	4.896	2.229	-0.086	3.5060	1.5830	28.235	58.295

RUDDER DYNAMOMETER e16r.pd Rudder No 6 j=0.94

Angle	V	RPM	Cl	Cn	Cd	Cmz	Cmx	Cmy	Cpc	Cps
-35.40	10.00	783.56	-0.8310	-1.021	0.593	-0.091	-0.7150	0.3690	38.966	60.612
-30.40	10.00	783.56	-0.8670	-1.003	0.503	-0.086	-0.7480	0.3320	38.570	63.639
-25.40	10.00	783.56	-1.0390	-1.075	0.318	-0.026	-0.7710	0.2180	32.497	56.016
-20.40	10.00	783.56	-1.1130	-1.113	0.199	0.035	-0.7940	0.1480	26.863	53.977
-15.40	10.00	783.56	-0.8250	-0.826	0.117	0.035	-0.5700	0.0970	25.786	52.141
-10.40	10.00	783.56	-0.5660	-0.568	0.063	0.035	-0.3800	0.0560	23.878	50.054
-5.40	10.00	783.56	-0.3090	-0.310	0.031	0.020	-0.1960	0.0370	23.437	46.659
-0.40	10.00	783.56	-0.0425	-0.043	0.025	-0.010	-0.0010	0.0340	51.930	-14.536
4.60	10.00	783.56	0.2130	0.215	0.042	-0.025	0.1940	0.0380	18.603	73.621
9.60	10.00	783.56	0.4870	0.493	0.077	-0.041	0.3960	0.0520	21.794	63.510
14.60	10.00	783.56	0.7500	0.759	0.133	-0.046	0.5940	0.0830	23.988	60.964
19.60	10.00	783.56	0.9820	0.997	0.212	-0.045	0.7730	0.1290	25.543	59.959
24.60	10.00	783.56	1.1840	1.200	0.297	-0.029	0.9410	0.1910	27.638	60.411
29.60	10.00	783.56	1.3140	1.356	0.432	0.015	1.0710	0.2750	31.123	61.183
34.60	10.00	783.56	1.0500	1.231	0.646	0.073	0.8310	0.4090	35.938	56.956
39.60	10.00	783.56	1.0530	1.308	0.779	0.099	0.8490	0.4960	37.619	56.695

RUDDER DYNAMOMETER e26r.pd j=0.51

Angle	V	RPM	Cl	Cn	Cd	Cmz	Cmx	Cmy	Cpc	Cps
-35.40	10.00	1462.50	-2.1200	-2.513	1.354	-0.232	-1.4660	0.8800	39.261	50.353
-30.40	10.00	1463.46	-2.4660	-2.605	0.945	-0.117	-1.7023	0.6457	34.506	51.403
-25.40	10.00	1462.50	-2.5610	-2.549	0.549	0.068	-1.7270	0.4110	27.352	50.611
-20.40	10.00	1463.46	-2.0563	-2.038	0.318	0.097	-1.3530	0.2503	25.244	49.005
-15.40	10.00	1462.50	-1.5690	-1.559	0.171	0.089	-0.9880	0.1530	24.295	46.211
-10.40	10.00	1463.46	-1.0213	-1.017	0.071	0.072	-0.6193	0.0753	22.890	43.768
-5.40	10.00	1462.50	-0.5570	-0.556	0.014	0.029	-0.2770	0.0450	24.848	32.936
-0.40	10.00	1463.22	-0.0560	-0.056	-0.010	-0.007	0.0615	0.0257	43.909	-131.933
4.60	10.00	1462.50	0.3980	0.393	-0.042	-0.049	0.4190	0.0390	17.518	89.545
9.60	10.00	1463.46	0.8733	0.872	0.069	-0.075	0.7697	0.0700	21.454	70.815
14.60	10.00	1462.50	1.3330	1.327	0.147	-0.094	1.1300	0.1520	22.961	67.731

19.60	10.00	1463.46	1.7837	1.792	0.334	-0.095	1.4513	0.2487	24.741	63.429
24.60	10.00	1462.50	2.1780	2.204	0.537	-0.048	1.7430	0.4360	27.836	62.642
29.60	10.00	1463.46	2.3533	2.472	0.863	0.033	1.9020	0.6417	31.350	62.209
34.60	10.00	1462.50	2.5250	2.754	1.189	0.123	2.0430	0.9170	34.492	62.478
39.60	10.00	1462.50	2.5280	2.971	1.605	0.183	1.9310	1.1730	36.184	57.744

RUDDER DYNAMOMETER e36r.pd j=0.34

Angle	V	RPM	Cl	Cn	Cd	Cmz	Cmx	Cmy	Cpc	Cps
-35.40	10.00	2163.22	-4.6560	-4.951	1.994	-0.108	-3.1610	1.4200	32.209	51.163
-30.40	10.00	2163.22	-4.3130	-4.404	1.353	0.061	-2.8930	1.0000	28.658	50.651
-25.40	10.00	2163.22	-3.9520	-3.917	0.808	0.202	-2.6110	0.6220	24.867	49.519
-20.40	10.00	2163.22	-3.1780	-3.127	0.426	0.198	-2.0270	0.3800	23.697	47.493
-15.40	10.00	2163.22	-2.3970	-2.352	0.154	0.174	-1.4730	0.1990	22.645	45.153
-10.40	10.00	2163.22	-1.5710	-1.541	-0.022	0.123	-0.9000	0.0760	22.046	40.825
-5.40	10.00	2163.22	-0.7680	-0.755	-0.110	0.059	-0.3400	0.0140	22.272	27.525
-0.40	10.00	2163.22	-0.0090	-0.008	-0.146	-0.029	0.2180	-0.0130	403.368	-2880.419
4.60	10.00	2163.22	0.7080	0.696	-0.123	-0.092	0.7920	-0.0020	16.856	95.953
9.60	10.00	2163.22	1.4310	1.406	-0.027	-0.154	1.3430	0.0570	19.063	77.290
14.60	10.00	2163.22	2.1610	2.123	0.127	-0.206	1.8990	0.1660	20.342	71.008
19.60	10.00	2163.22	2.8550	2.814	0.369	-0.250	2.4410	0.3460	21.151	68.365
24.60	10.00	2163.22	3.4870	3.461	0.698	-0.252	2.9360	0.5760	22.766	66.556
29.60	10.00	2163.22	4.0170	4.119	1.267	-0.157	3.3740	0.9690	26.231	65.335
34.60	10.00	2163.22	4.4450	4.698	1.830	-0.028	3.6350	1.4530	29.443	63.750

Table I Particulars of Six All-Movable Rudder Models

Rudder Number	1	2	3	4	5	6
Mean Chord c mm	667	667	667	667	800	556
Span S mm	1000	1000	1200	1300	1000	1000
Geometric Aspect Ratio AR_G	3.0	3.0	3.6	3.9	2.5	3.6
Taper Ratio C_T/C_R	0.80	1.0	1.0	1.0	1.0	1.0
Thickness/Chord Ratio t/c	0.20	0.20	0.20	0.20	0.20	0.20
Section	NACA0020 Root and Tip with square tips					

Table II Overall Modified Wageningen B4.40 Series Propeller Details

Number of Blades	4
Range of revolutions rpm	0 to 3000
Diameter mm	800
Boss Diameter (max) mm	200
Mean Pitch Ratio	0.95 (set for tests)
Blade Area Ratio	0.40
Rake (deg)	0°
Blade Thickness Ratio t/D	0.050
Sections shape	Based on Wageningen B series
Blade Outline shape	Based on Wageningen but with reduced skew

Table III Parameters varied during experimental programme.

Parameters Test	Rudder No.		X1/D	X/D	Y/D	Z/D	λ	ξ	AR	P/D
Base	2		0.25	0.39	0.0	0.75	1.0	0.8	3.0	0.95
Pitch										0.69
										1.34
Lateral					- 0.25		0.866	0.693		0.95
					+0.25		0.866	0.693		
Vertical					0.0	1.125	0.5	0.5		
Coverage	4					1.125	1.0	0.615	3.9	
Aspect ratio	5		0.30						2.5	
	6		0.21						3.6	
Pivot	2	0.46				0.75	1.0	0.8	3.0	

Figure 1 Series of all-movable rudders for parametric investigation.

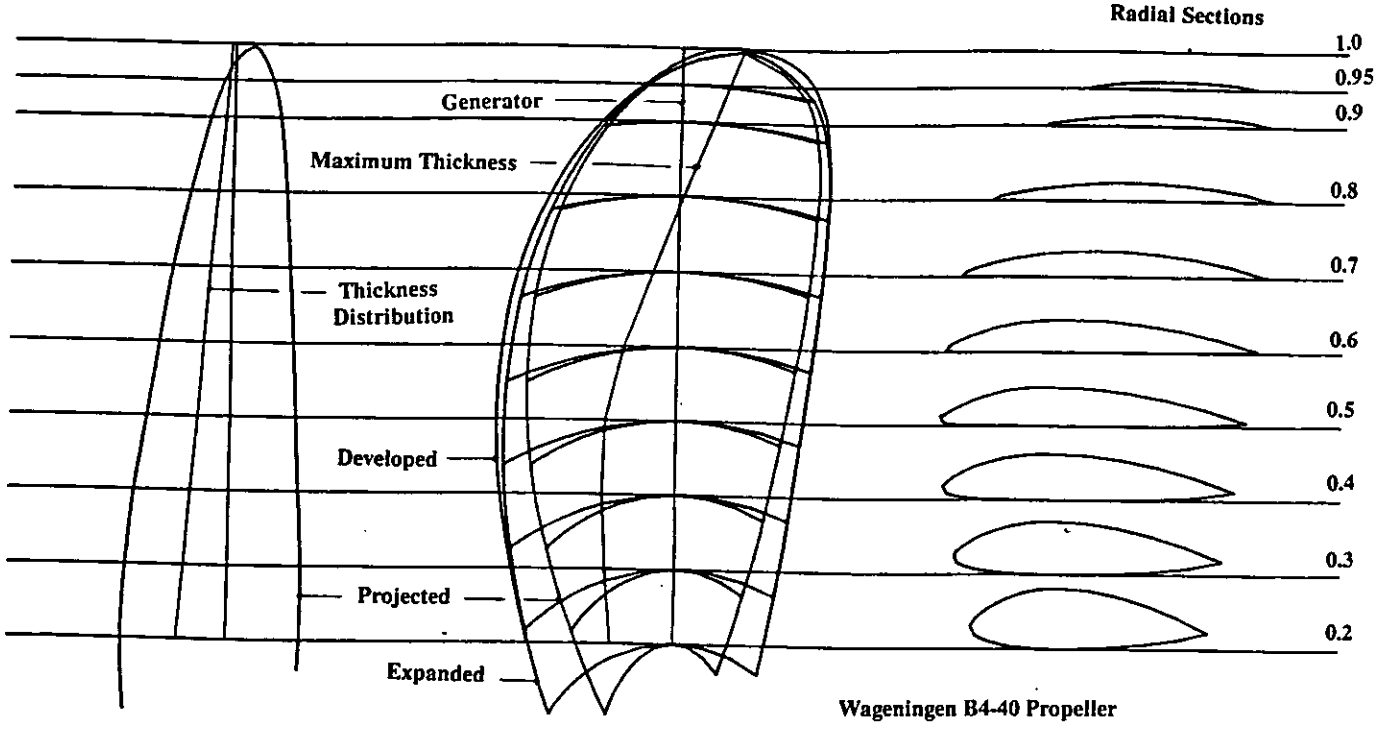

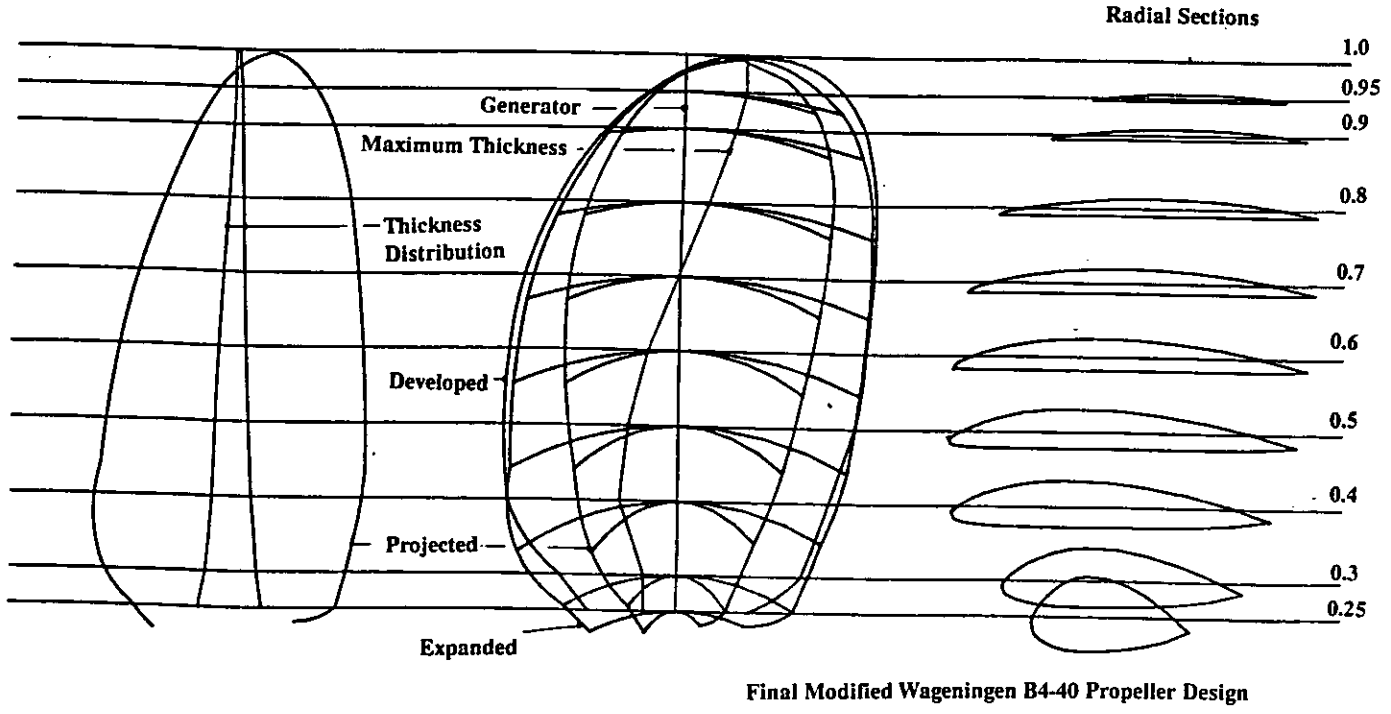

Figure 2 Comparison of Basis and Modified Wageningen B4.40 Propeller

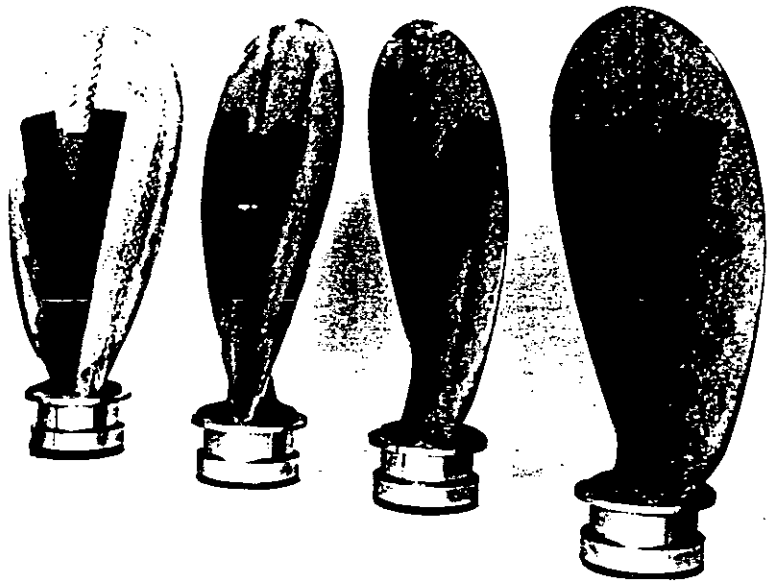

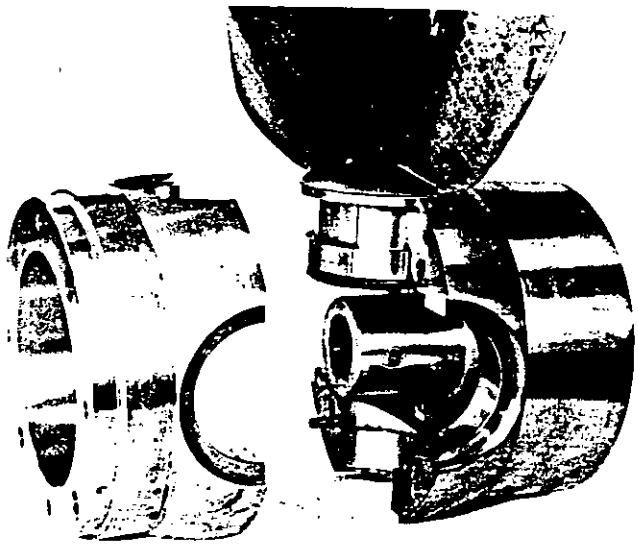

Figure 3 Views of Propeller Blades, Hub and final Assembly

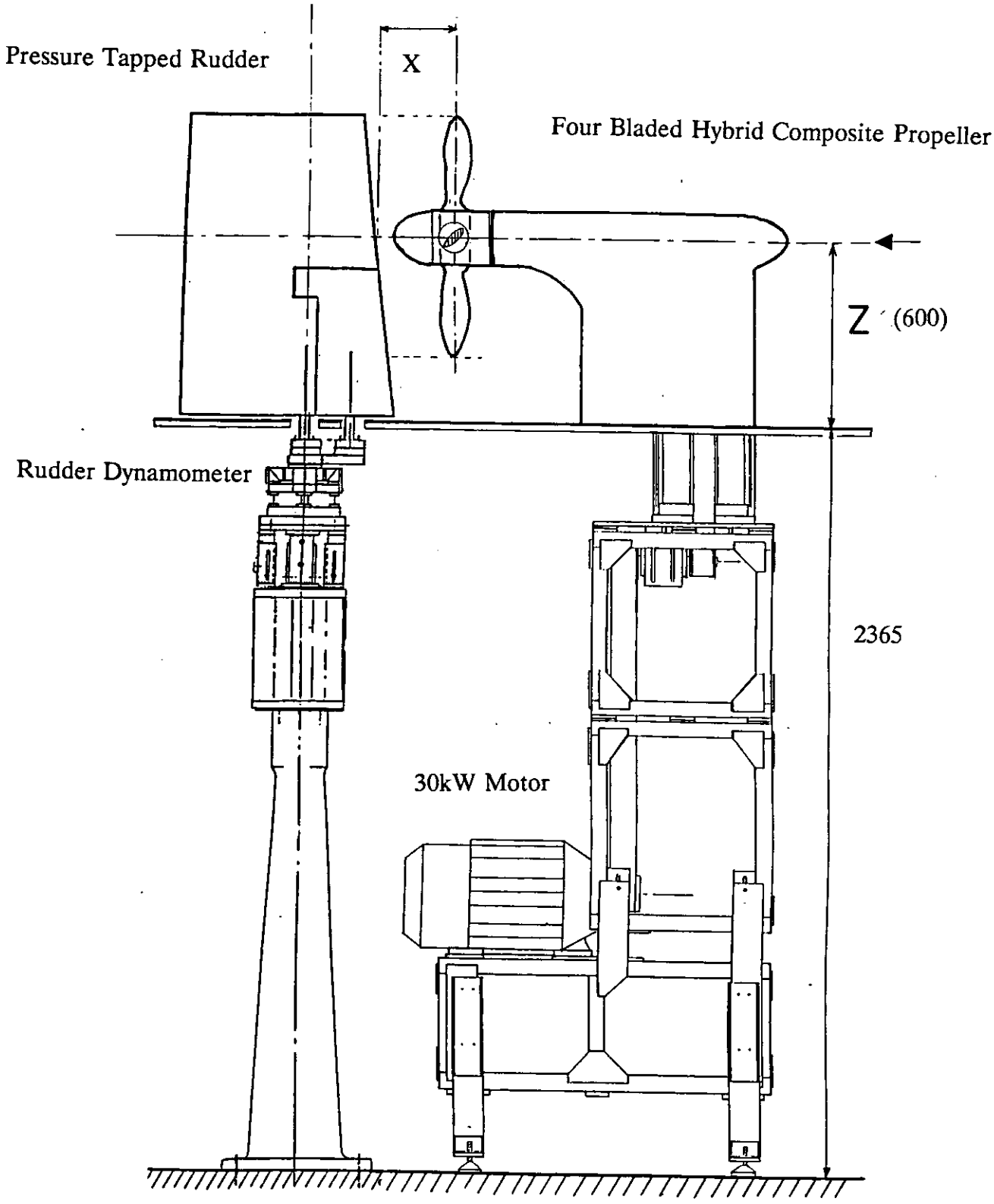

All dimensions in mm

Figure 4 Overall Test Rig for Investigation of Rudder and Propeller Interaction

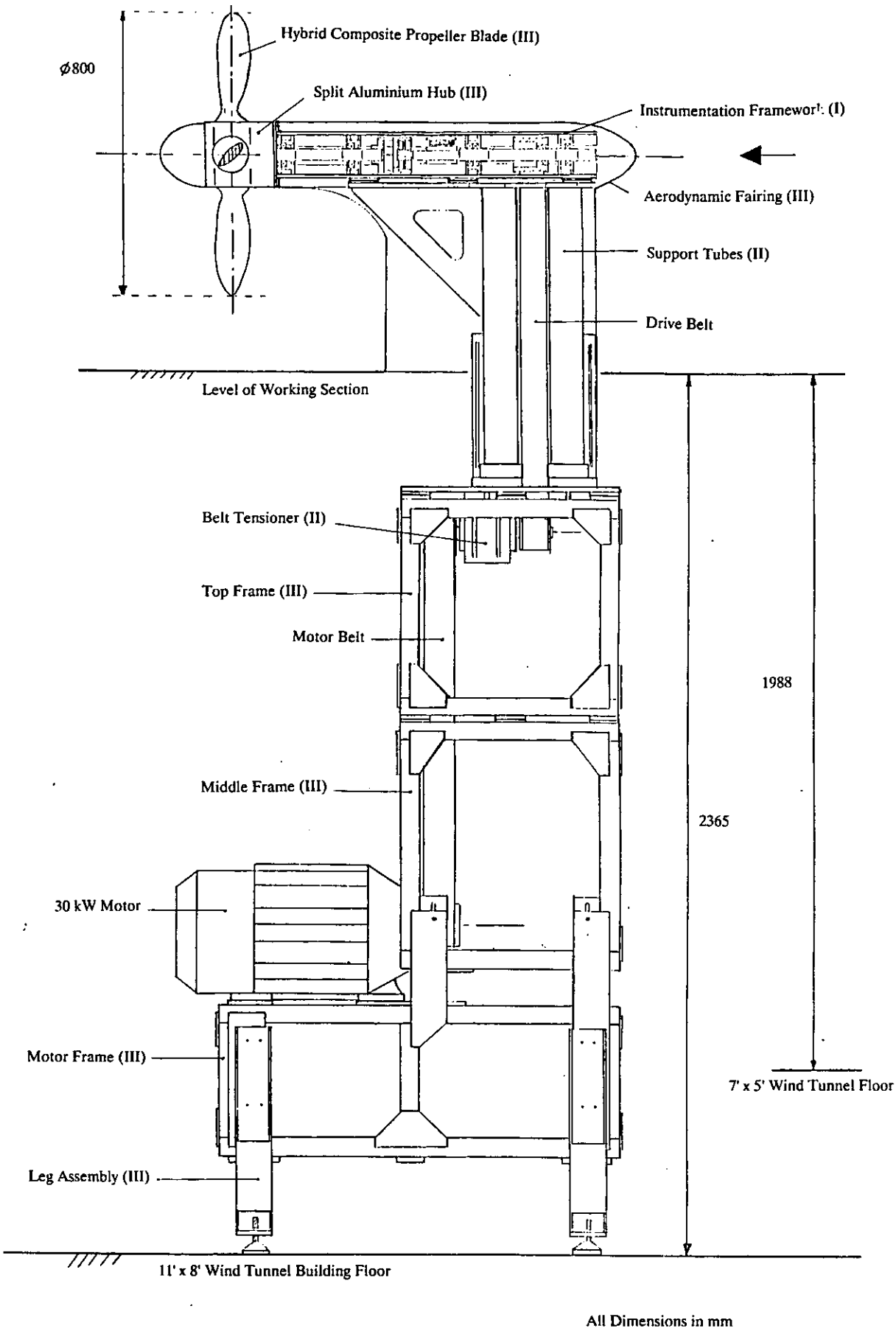

Figure 5 Side View of Installed Propeller Rig

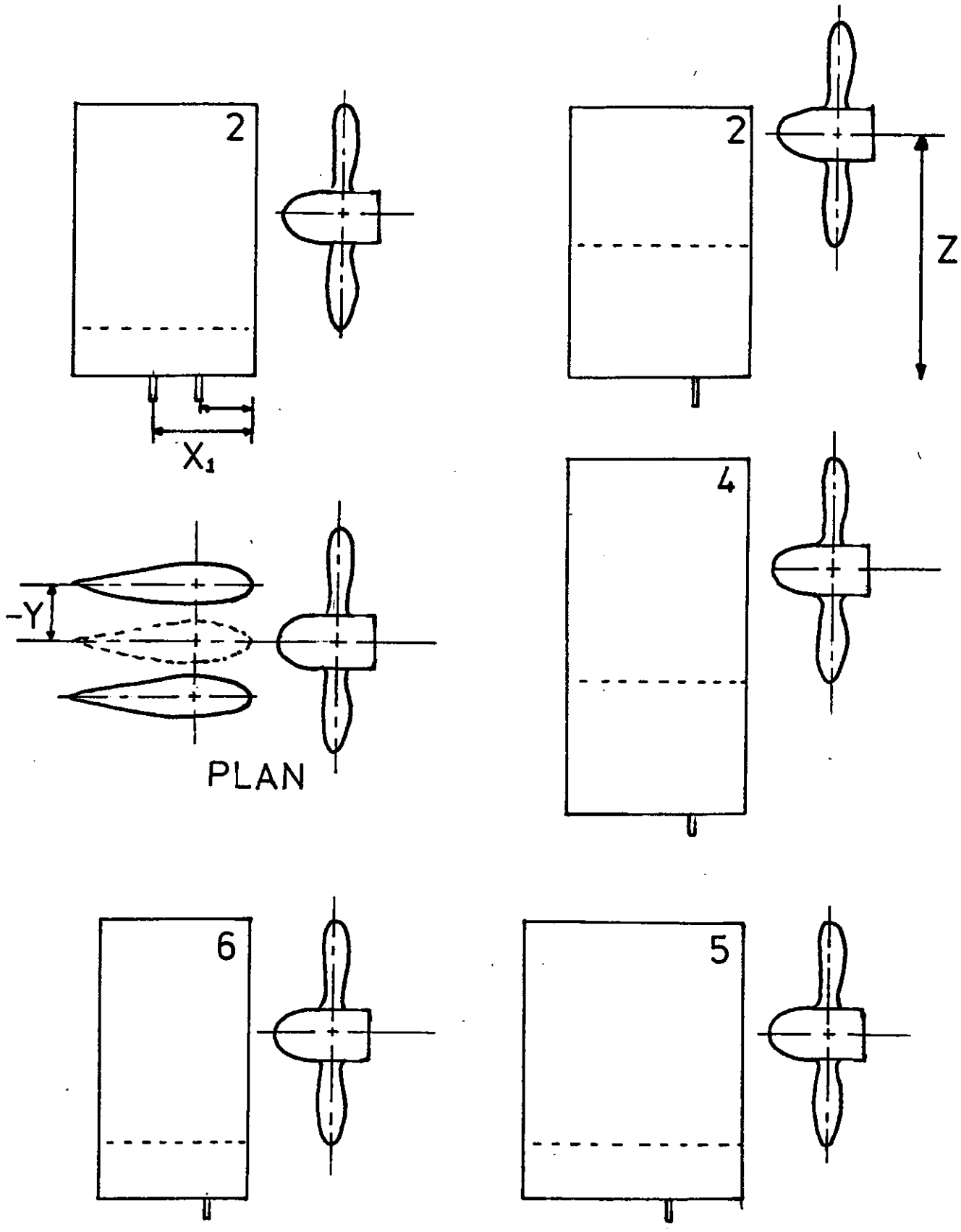

Figure 6 Views of relative position of rudder and propeller used in parametric study.

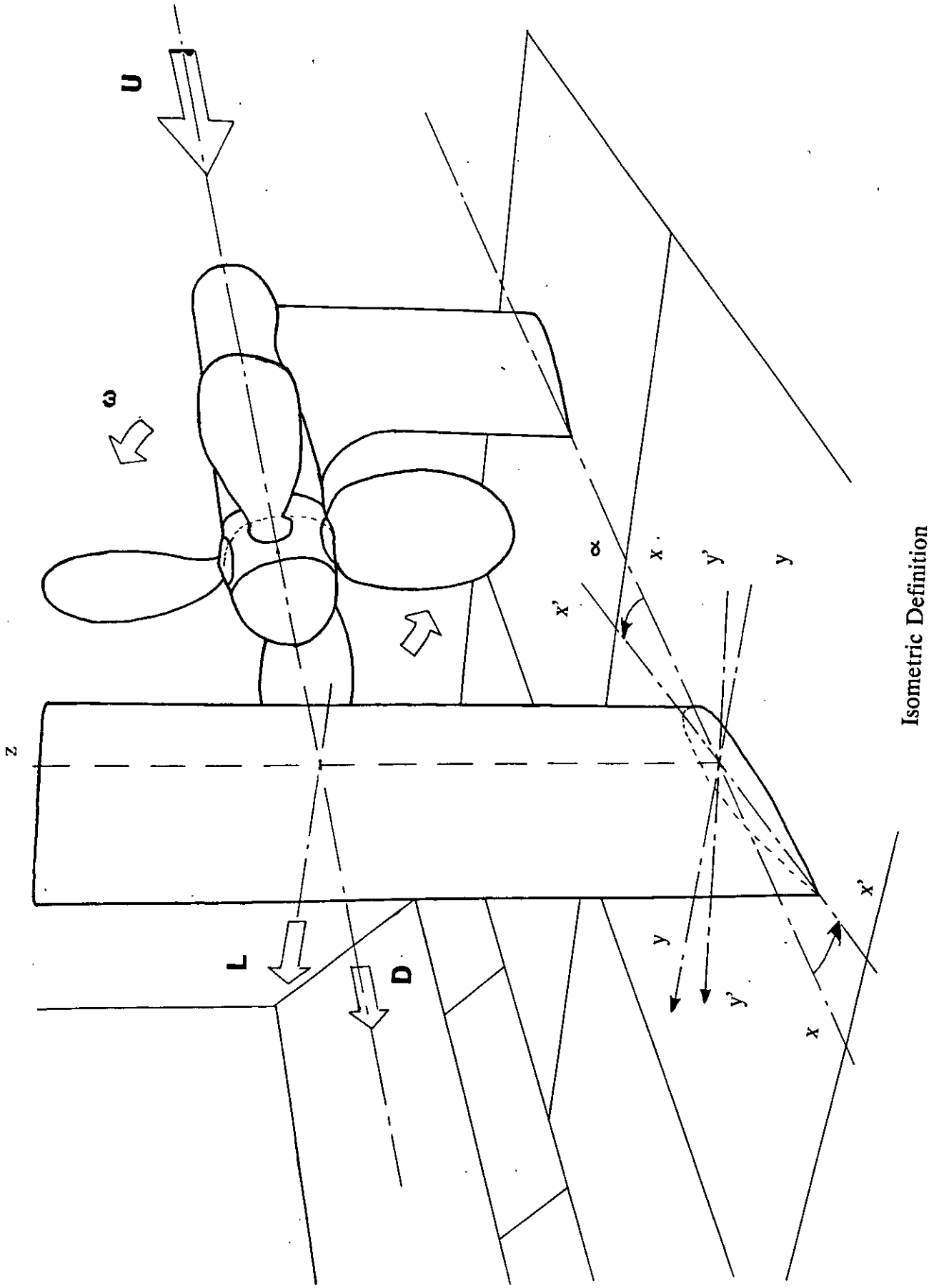

Figure 7 Rudder and Propeller Test Definition

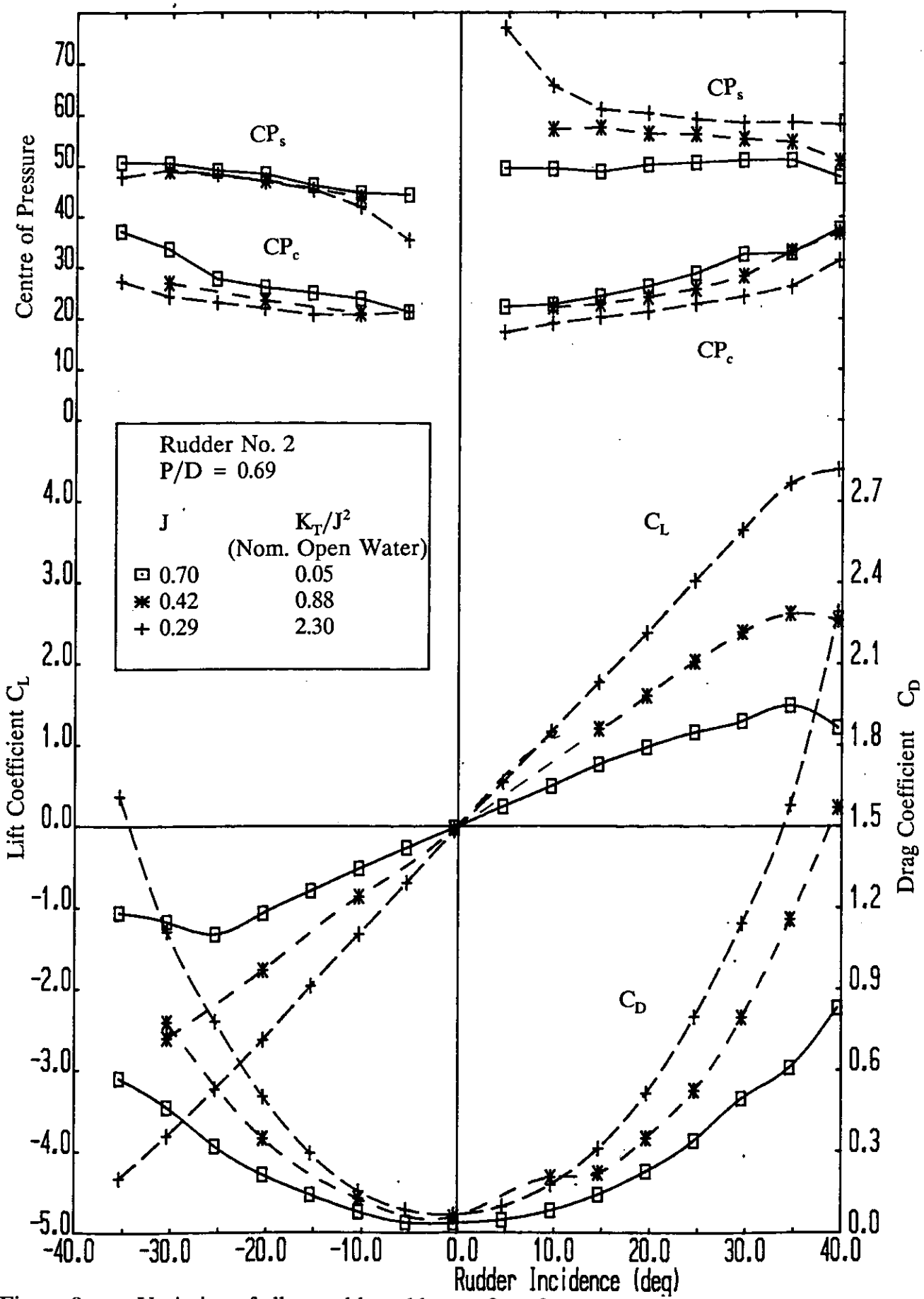

Figure 8 Variation of all-movable rudder no. 2 performance characteristic for three propeller advance ratio with a propeller pitch ratio setting of P/D=0.69.

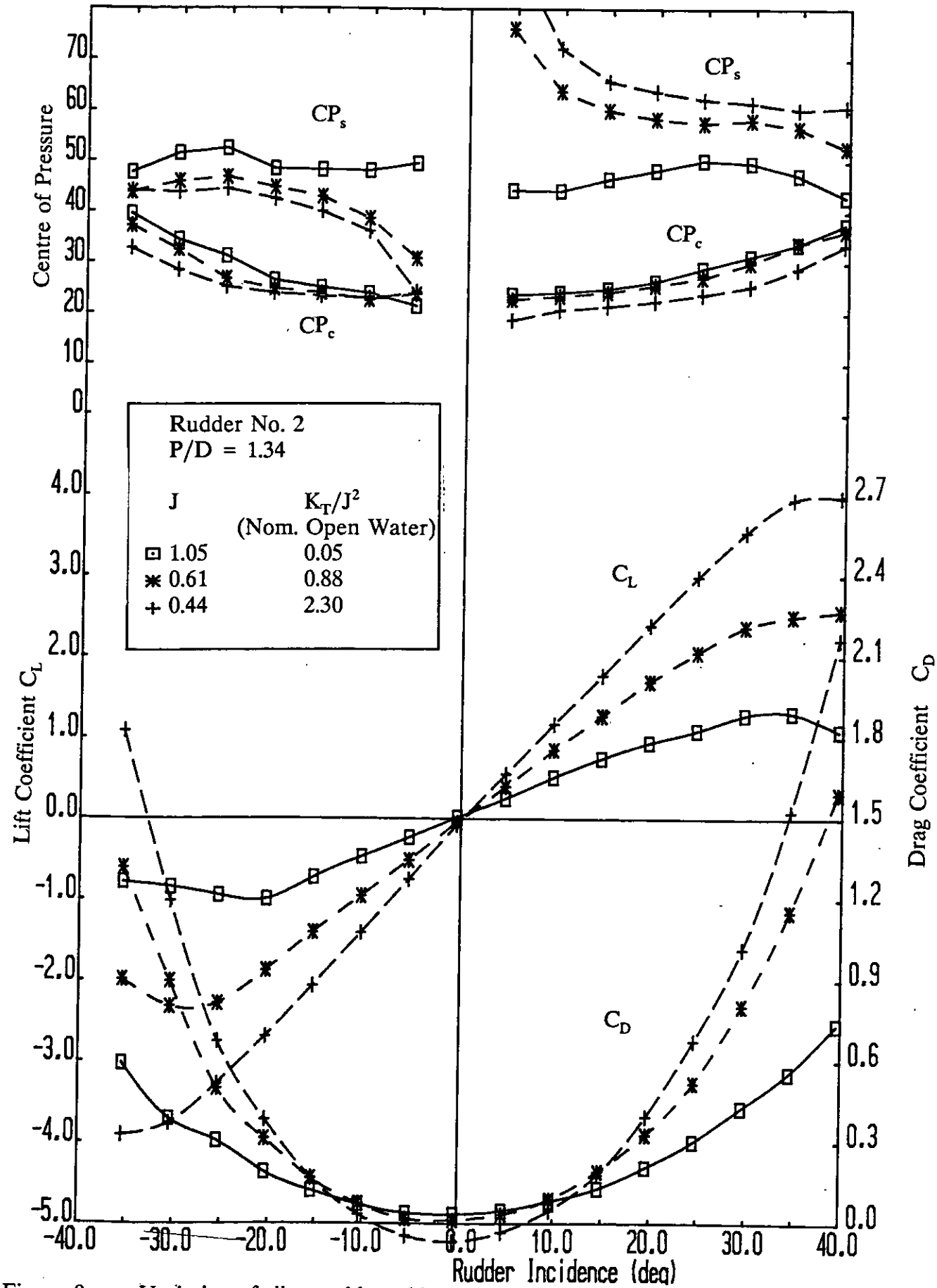

Figure 9 Variation of all-movable rudder no. 2 performance characteristic for three propeller advance ratio with a propeller pitch ratio setting of P/D = 1.34.

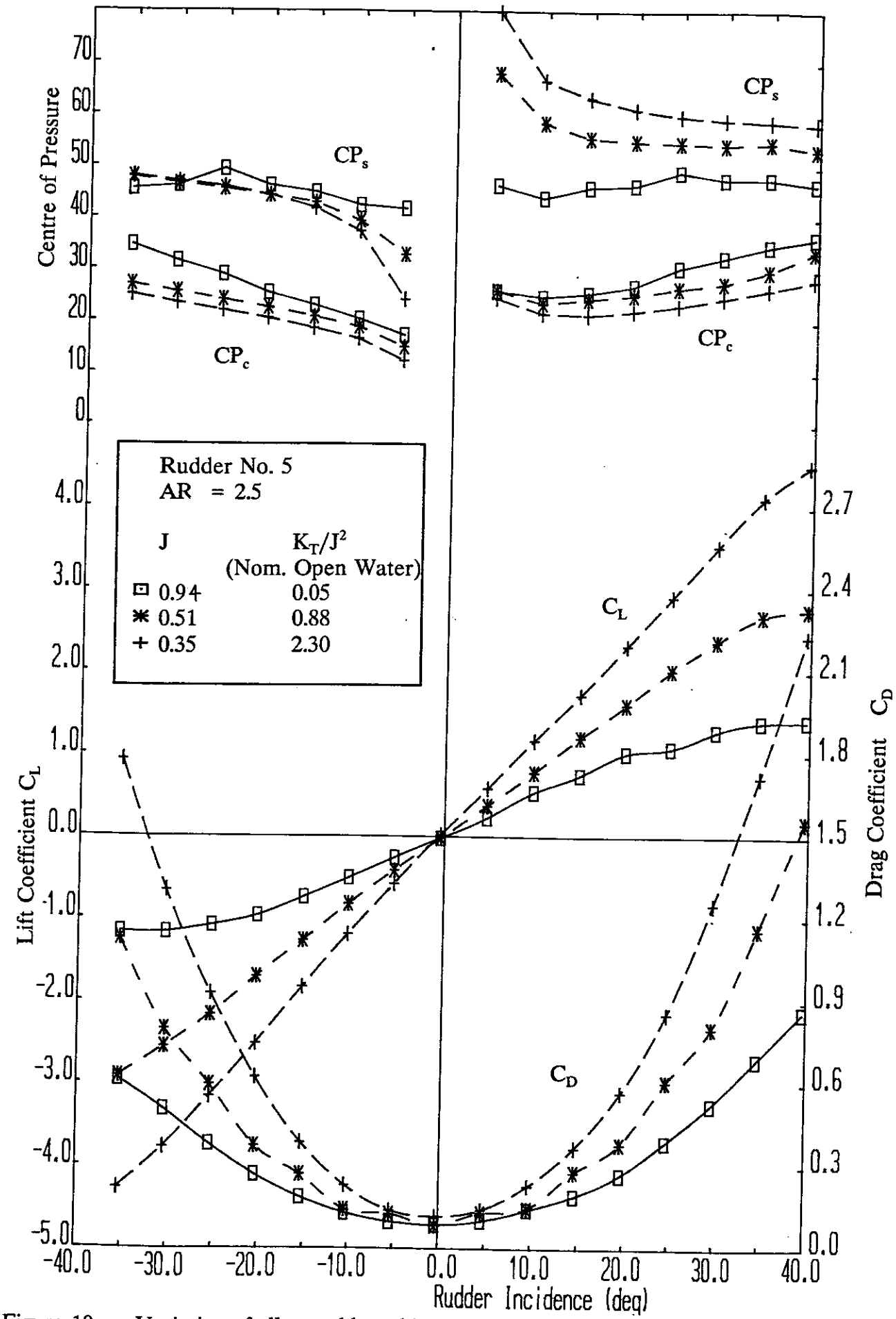

Figure 10 Variation of all-movable rudder no. 5 performance characteristic for three propeller advance ratio.

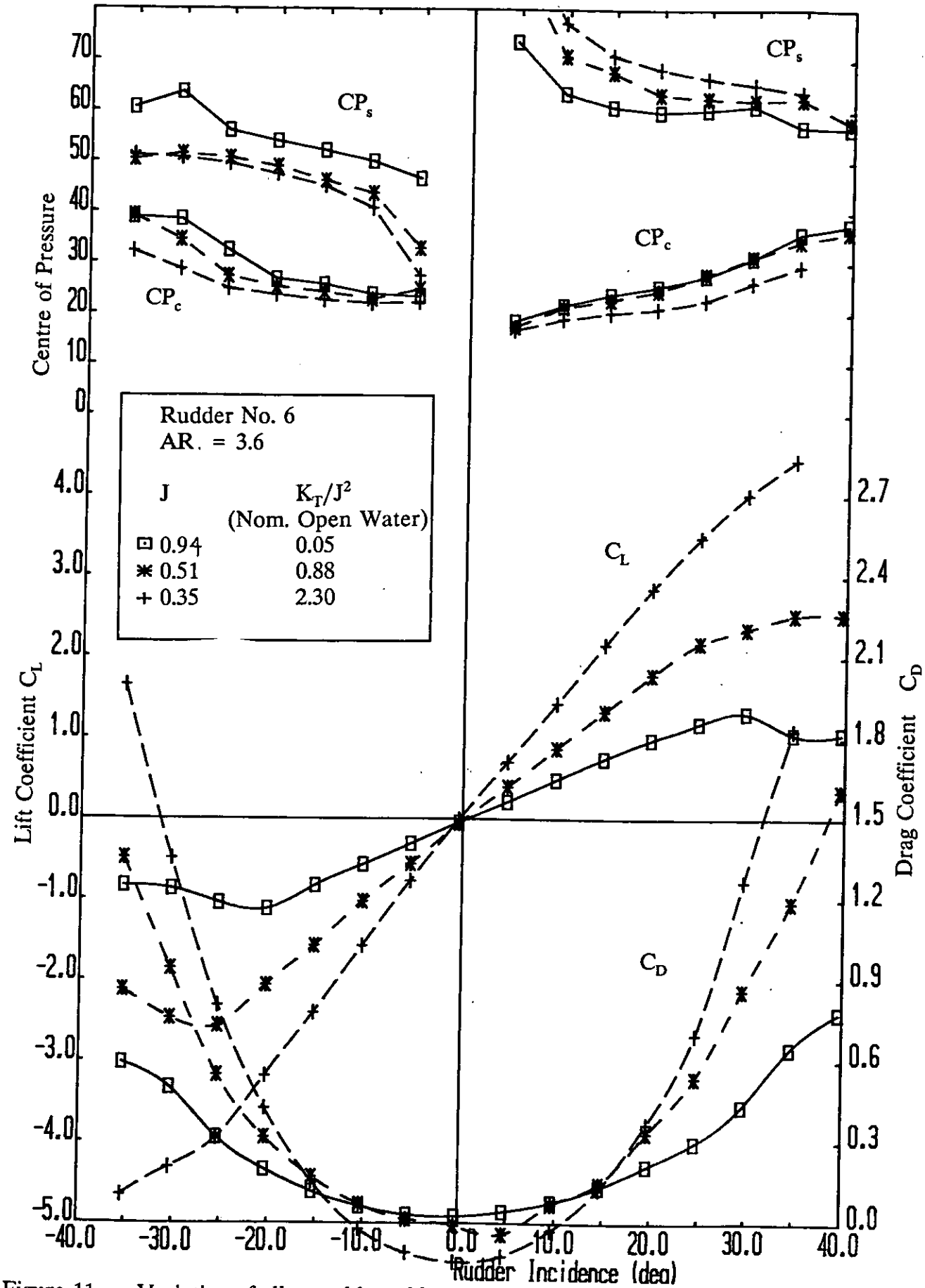

Figure 11 Variation of all-movable rudder no. 6 performance characteristic for three propeller advance ratio.

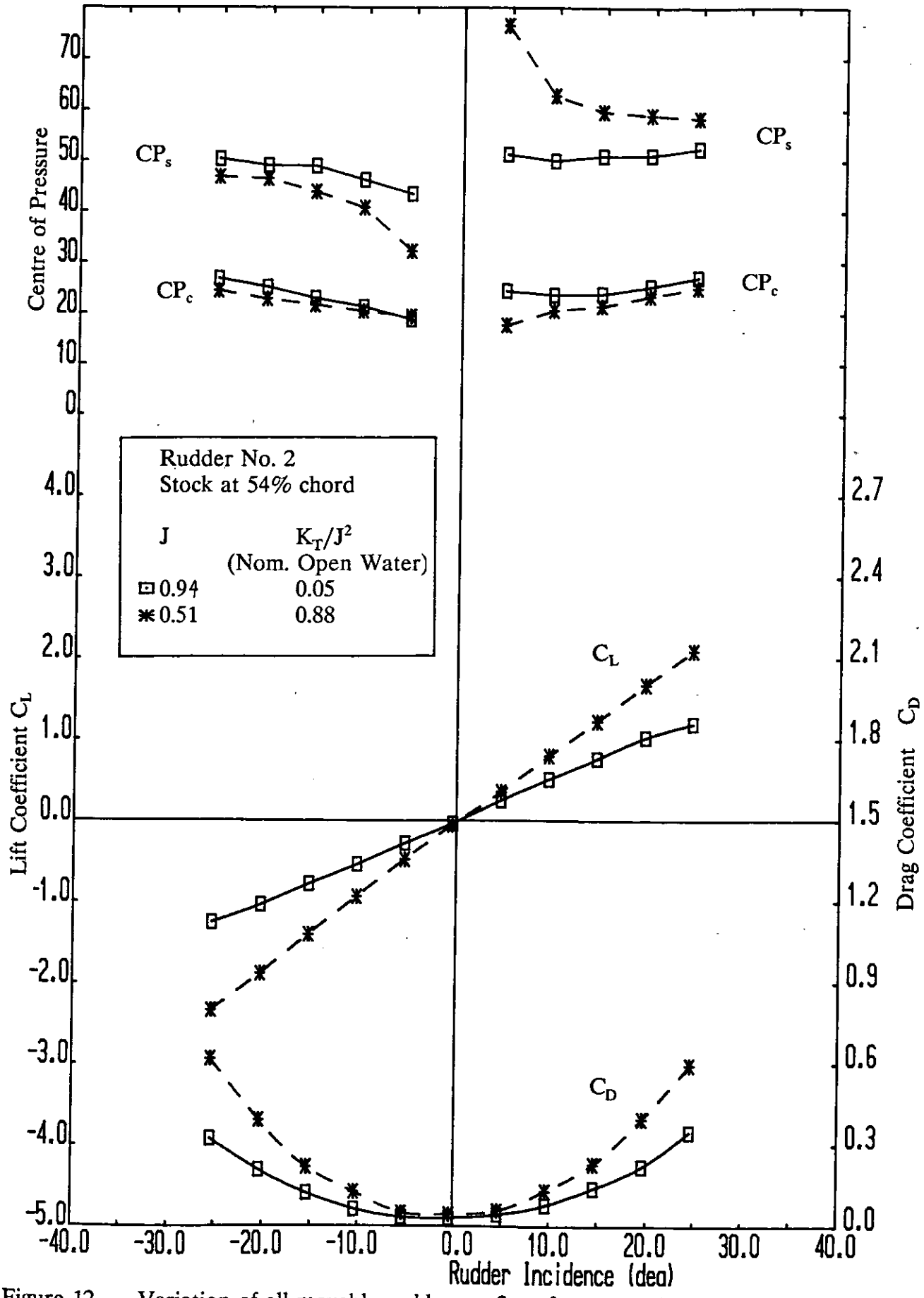

Figure 12 Variation of all-movable rudder no. 2 performance characteristic for two propeller advance ratio with rudder stock at 54% of rudder chord.

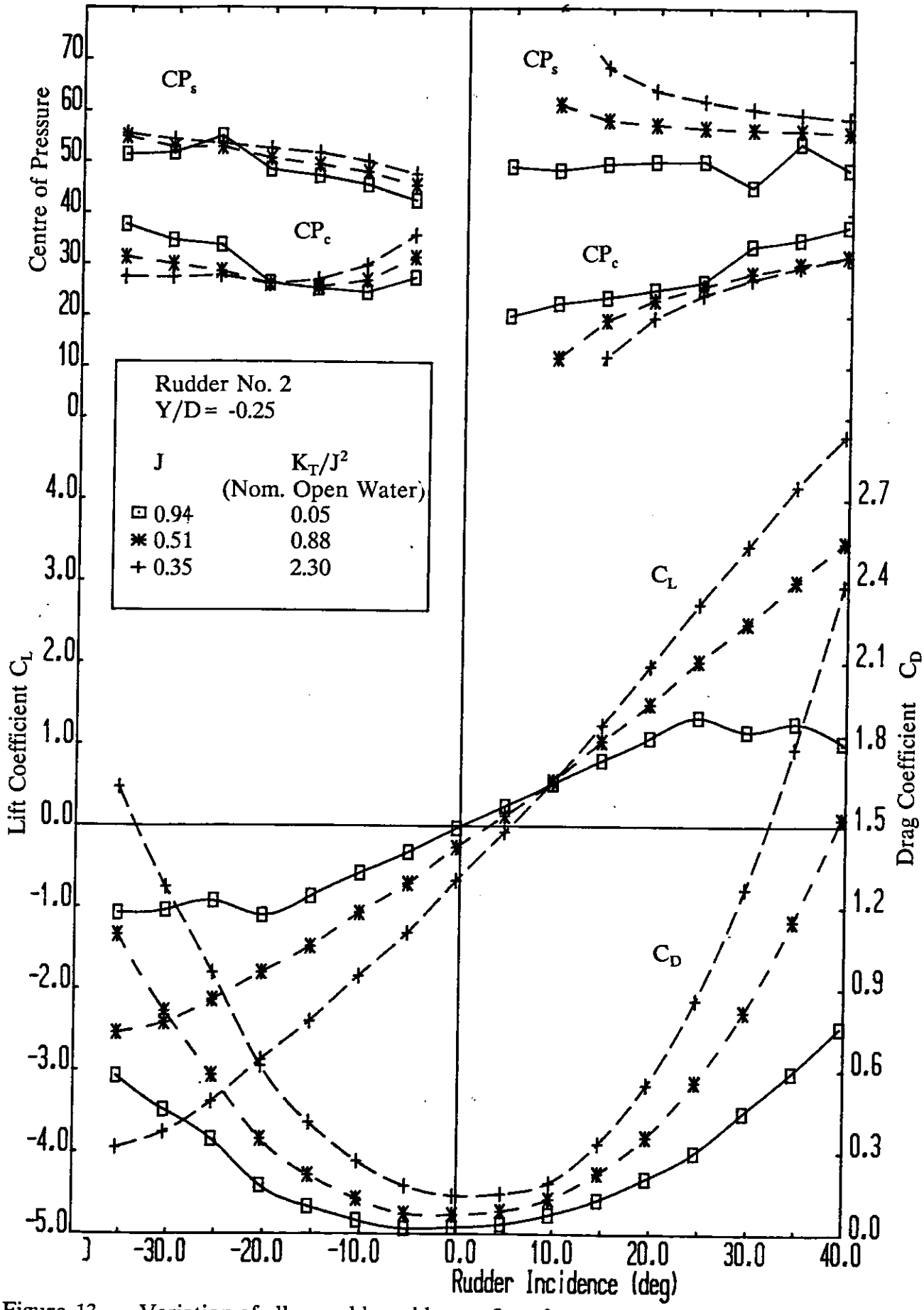

Figure 13 Variation of all-movable rudder no. 2 performance characteristic for three propeller advance ratio for a lateral separation of rudder from propeller axis of Y/D= -0.25.

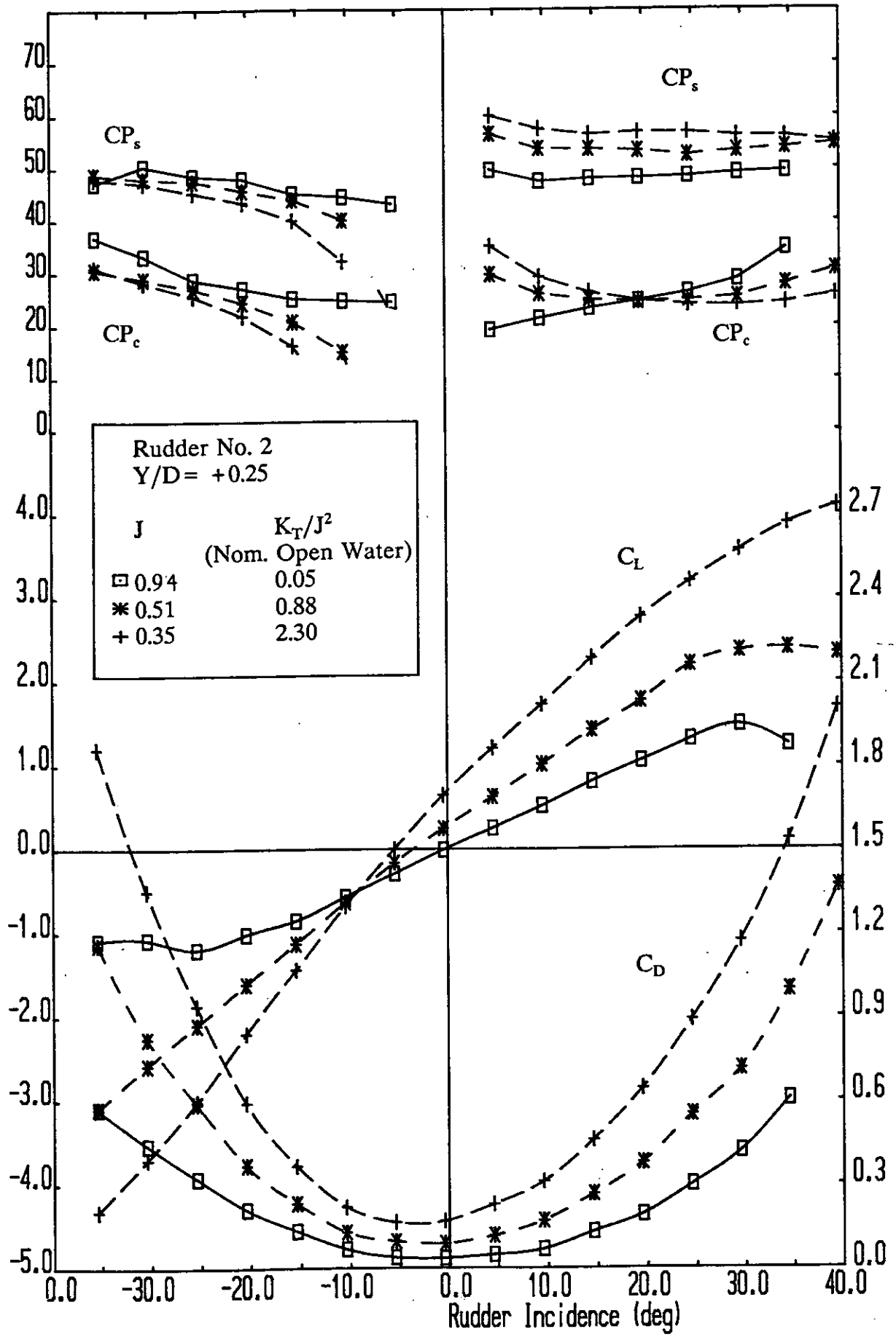

Figure 14 Variation of all-movable rudder no. 2 performance characteristic for three propeller advance ratio for a lateral separation of rudder from propeller axis of Y/D= +0.25.

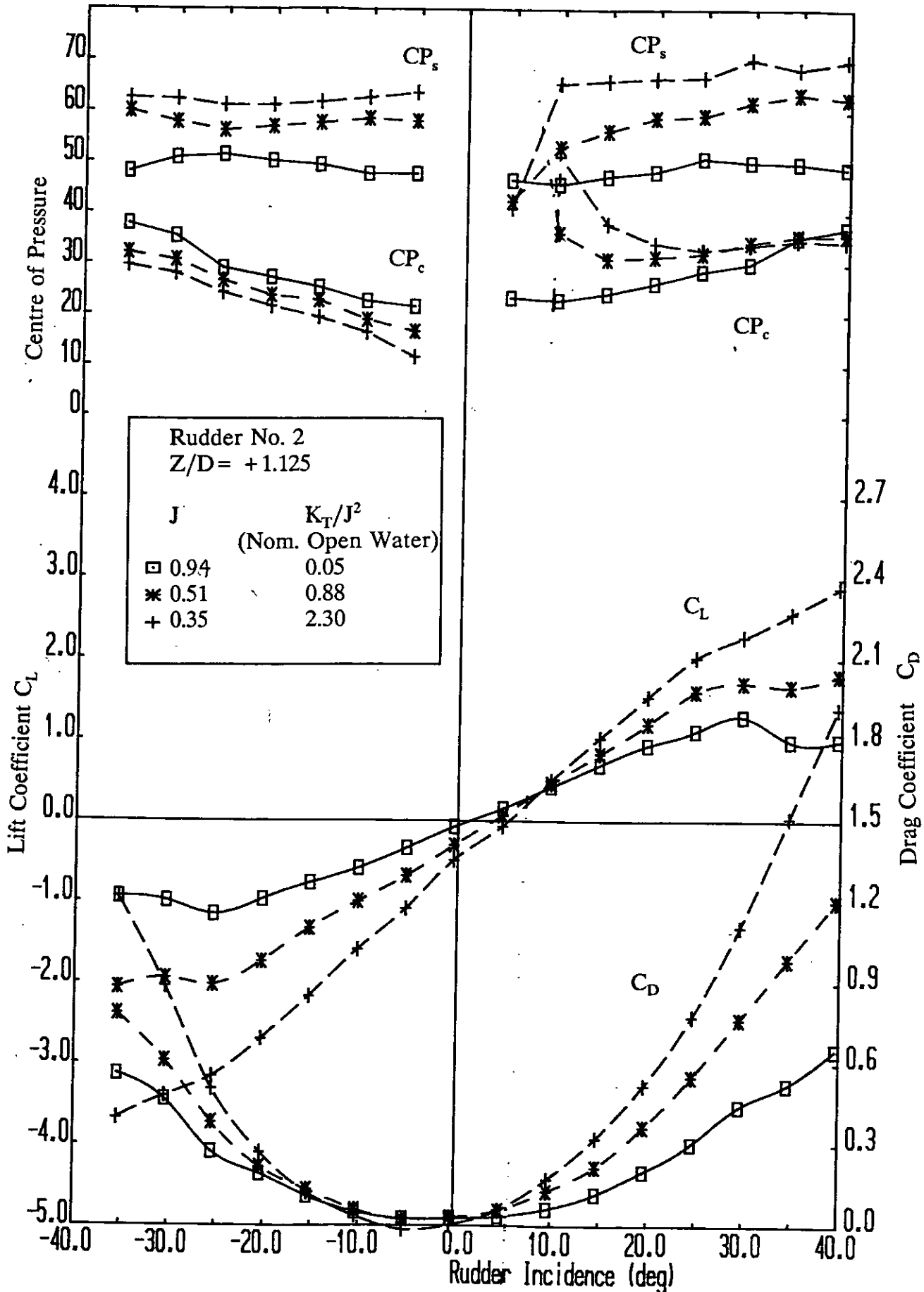

Figure 15 Variation of all-movable rudder no. 2 performance characteristic for three propeller advance ratio with the propeller axis height of 900mm.

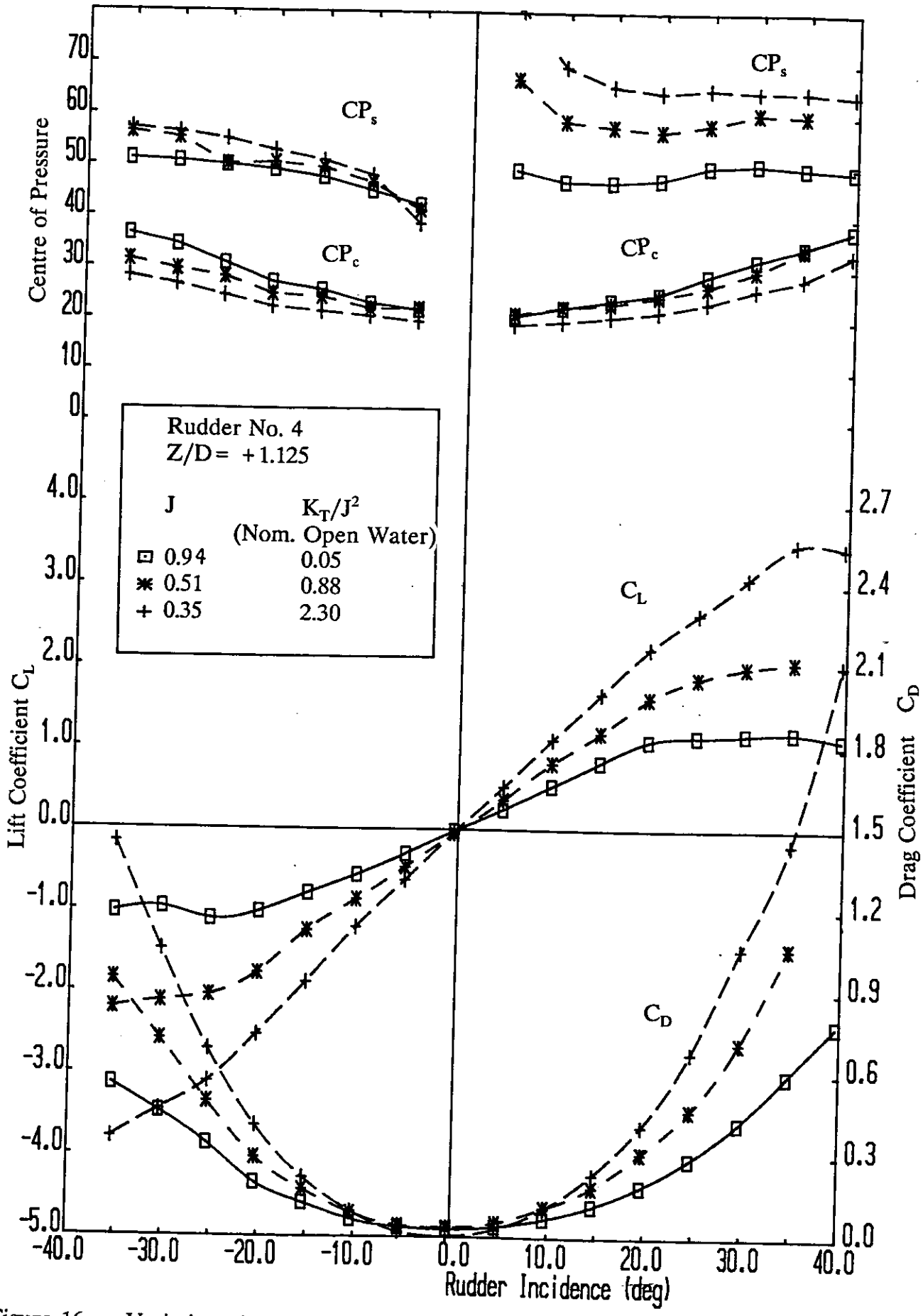

Figure 16 Variation of all-movable rudder no. 4 performance characteristic for three propeller advance ratio with the propeller axis height of 900mm.

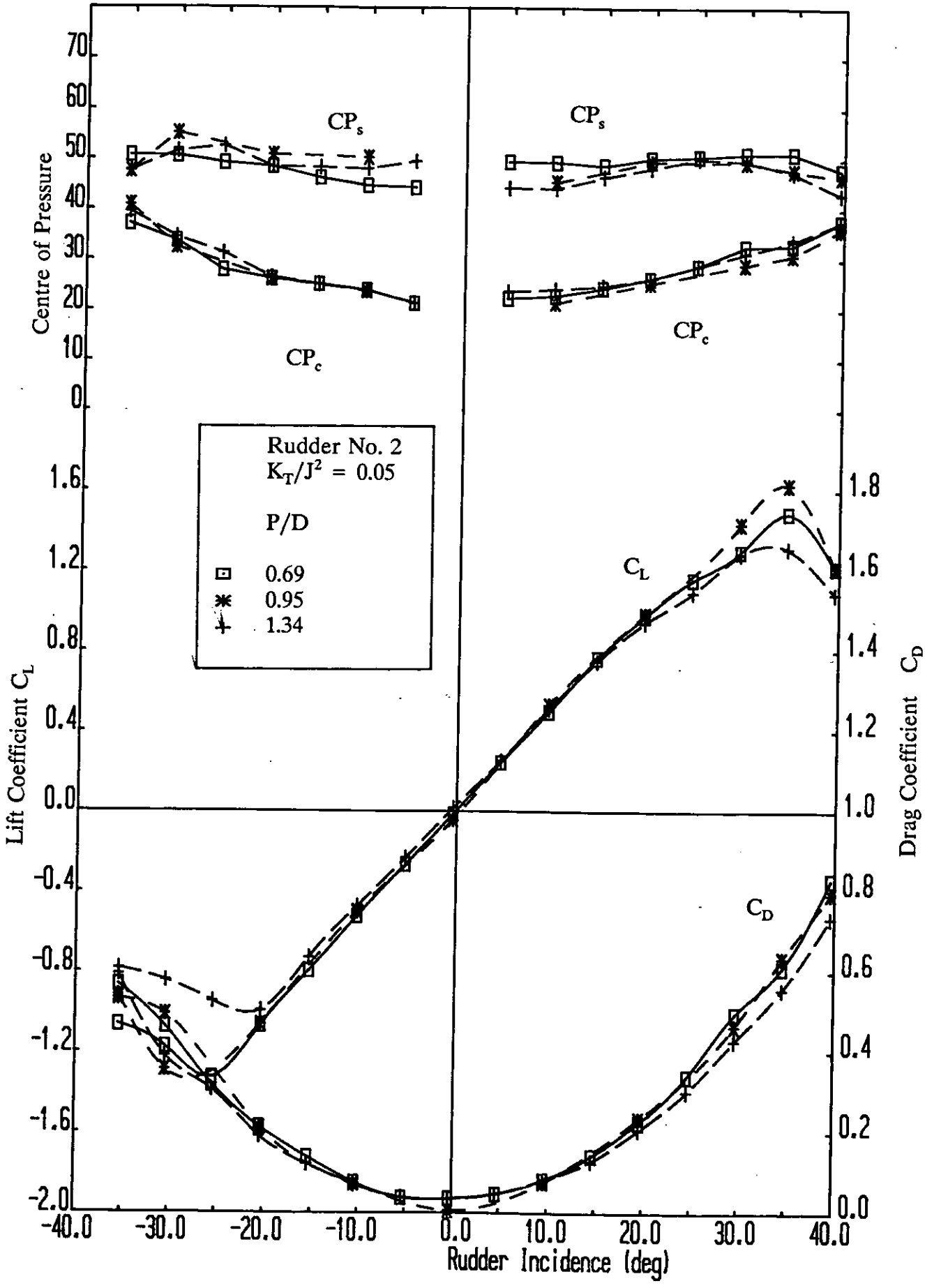

Figure 17 Effect of propeller pitch ratio setting on the performance characteristic of rudder no. 2 with a nominal open-water thrust loading K_T/J^2 = 0.05.

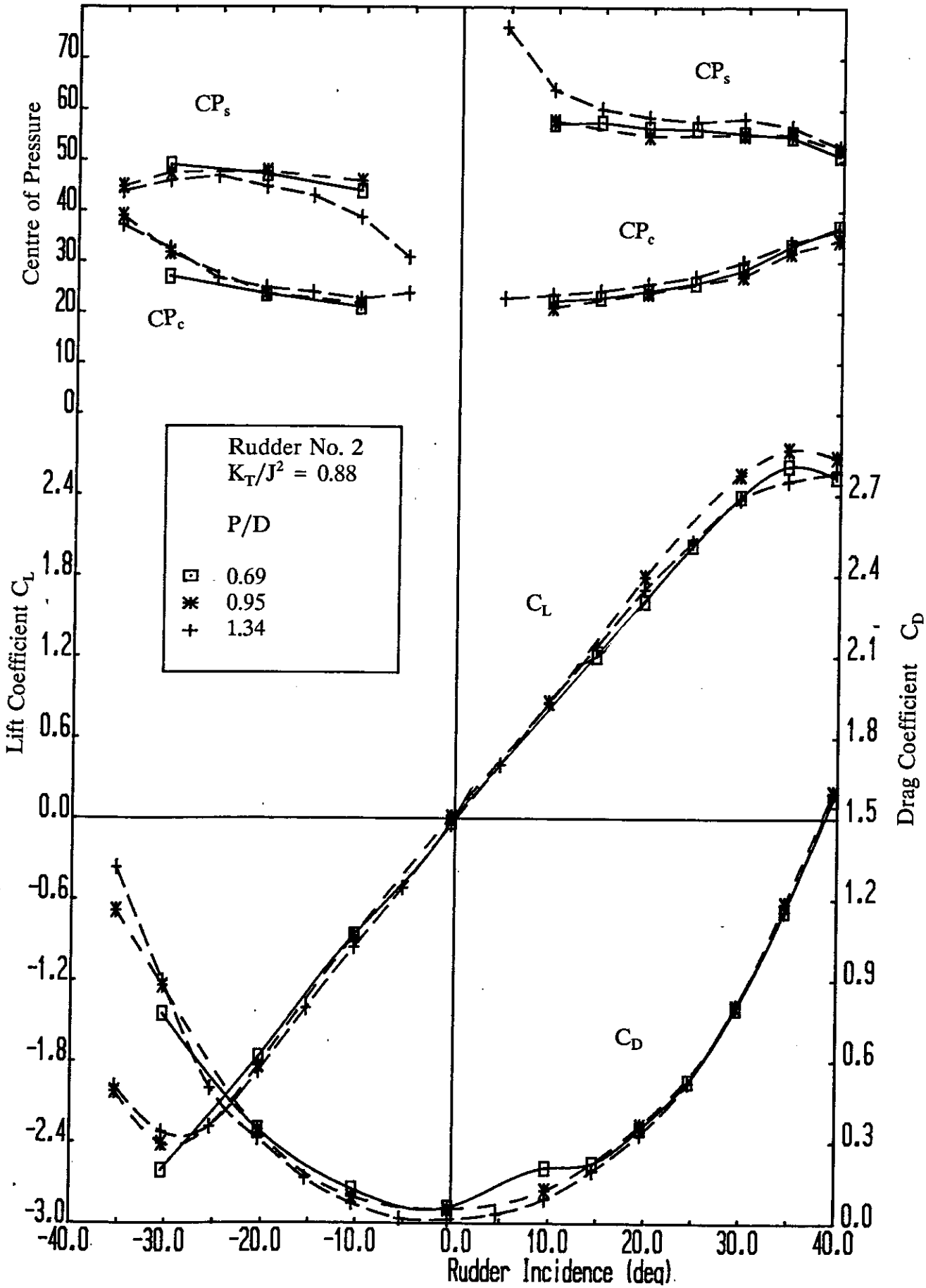

Figure 18 Effect of propeller pitch ratio setting on the performance characteristic of rudder no. 2 with a nominal open-water thrust loading K_T/J^2 = 0.88.

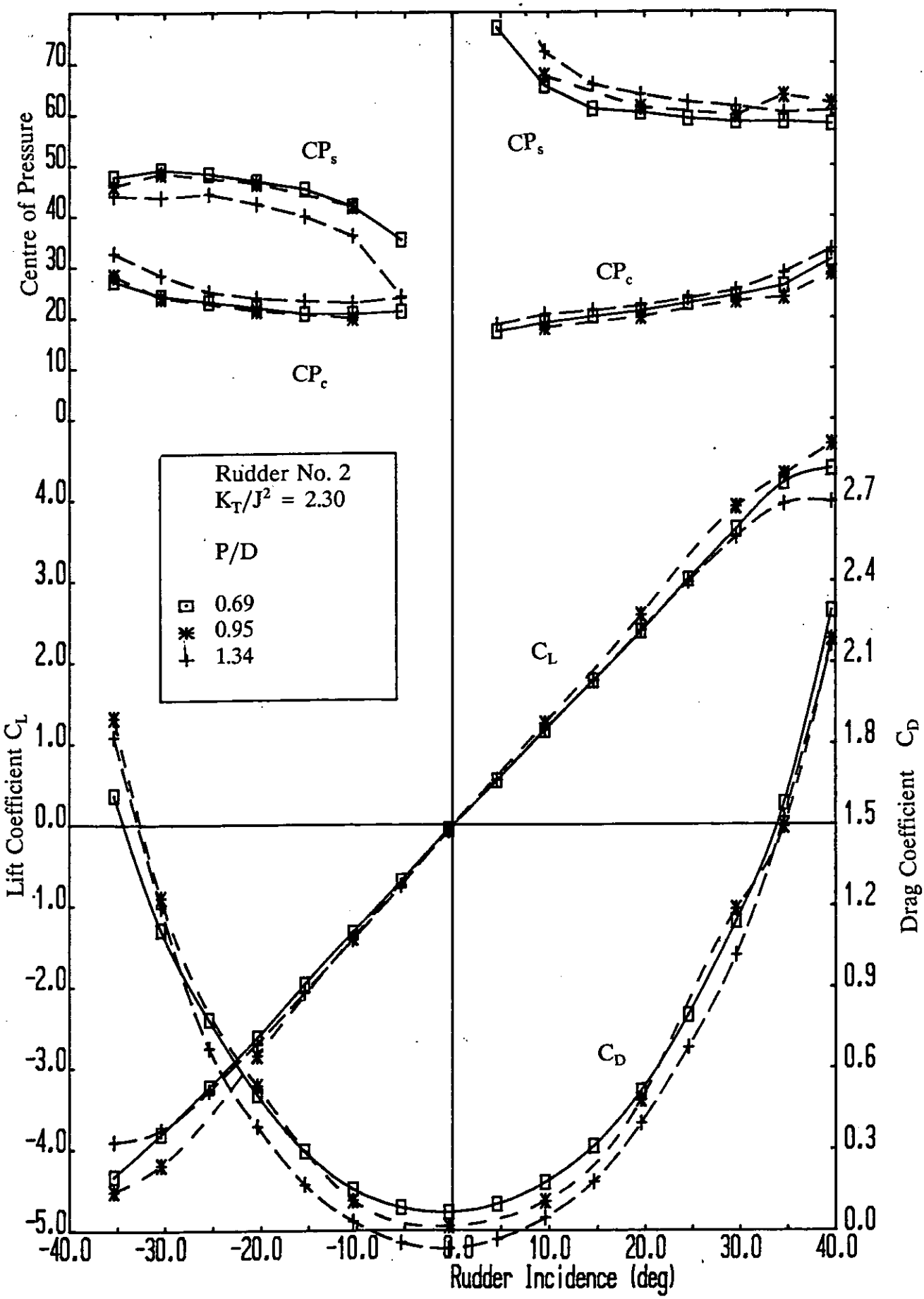

Figure 19 Effect of propeller pitch ratio setting on the performance characteristic of rudder no. 2 with a nominal open-water thrust loading K_T/J^2 = 2.30.

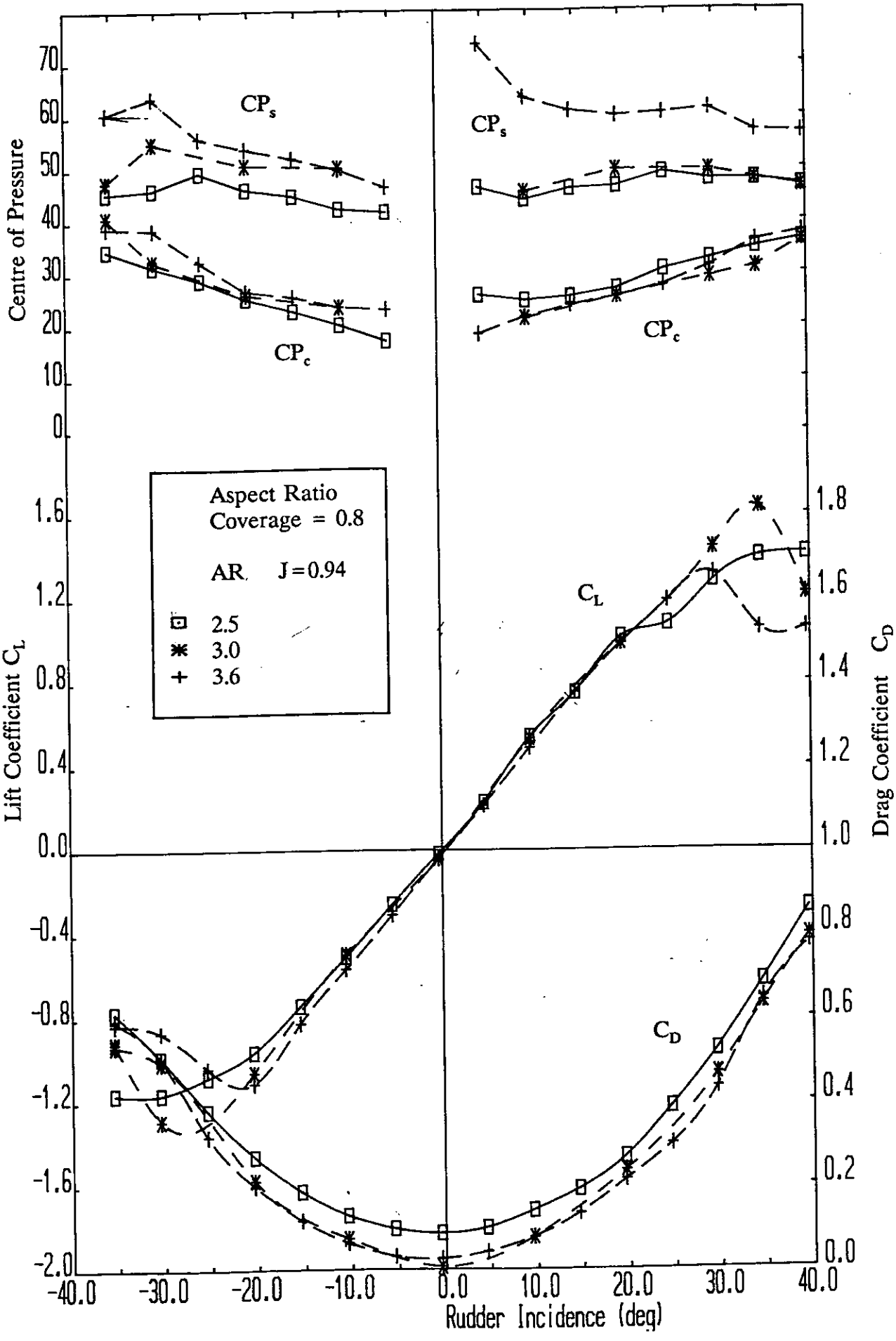

Figure 20 Effect of rudder aspect ratio on the performance characteristic of all-movable rudders with a coverage $\zeta = 0.8$ for an advance ratio J=0.94.

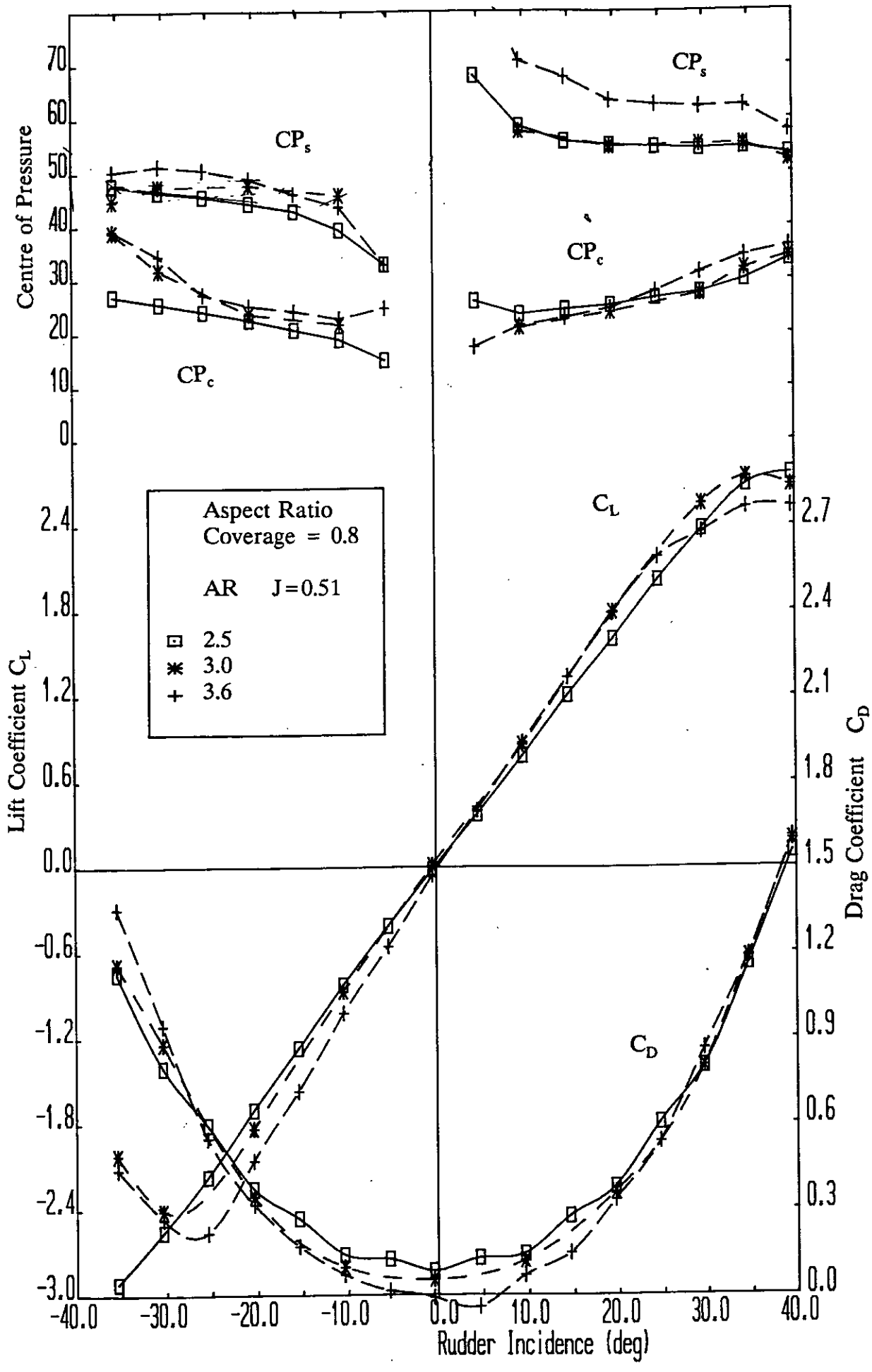

Figure 21 Effect of rudder aspect ratio on the performance characteristic of all-movable rudders with a coverage $\zeta = 0.8$ for an advance ratio J=0.51.

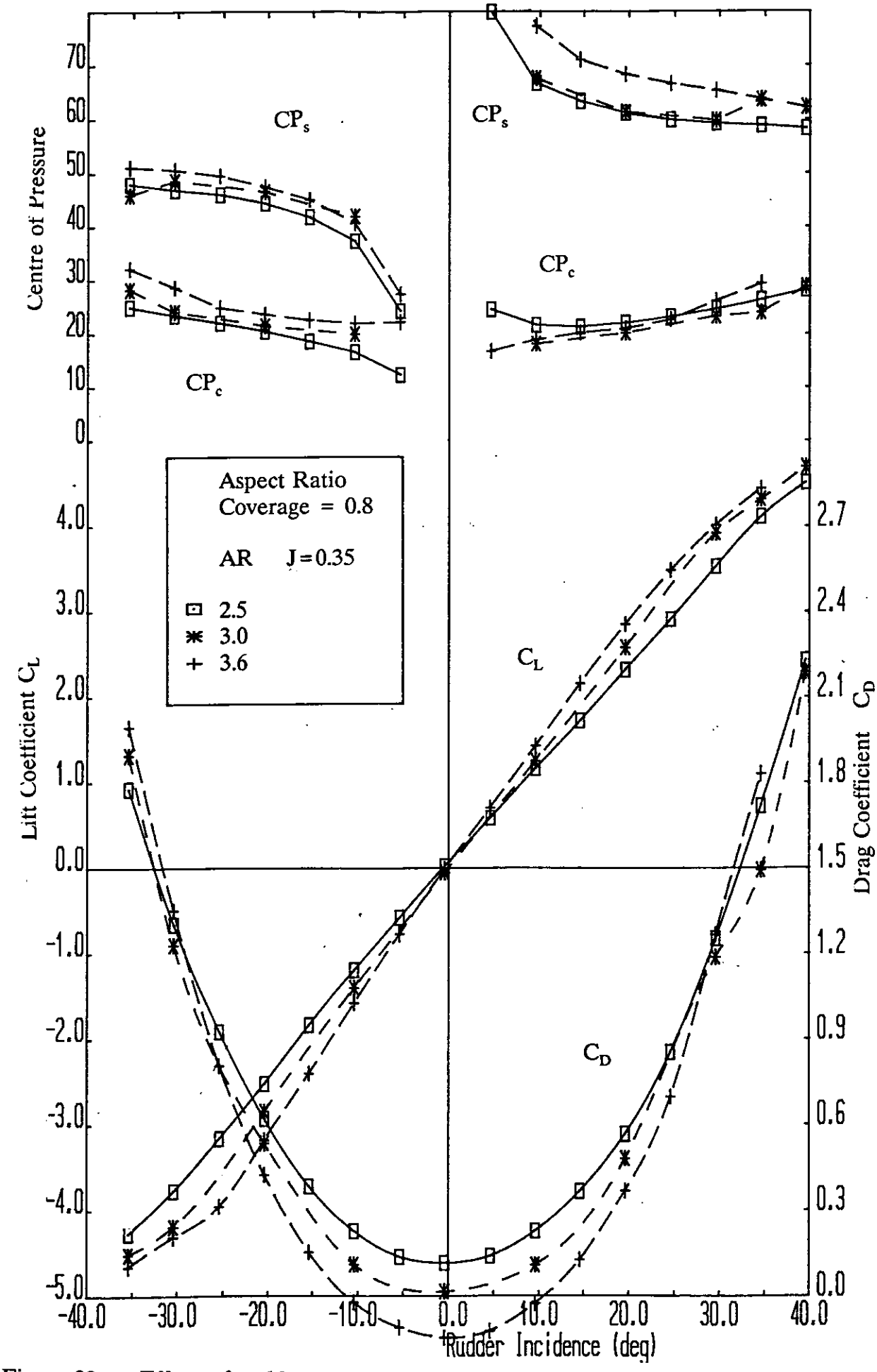

Figure 22 Effect of rudder aspect ratio on the performance characteristic of all-movable rudders with a coverage $\varsigma = 0.8$ for an advance ratio J=0.35.

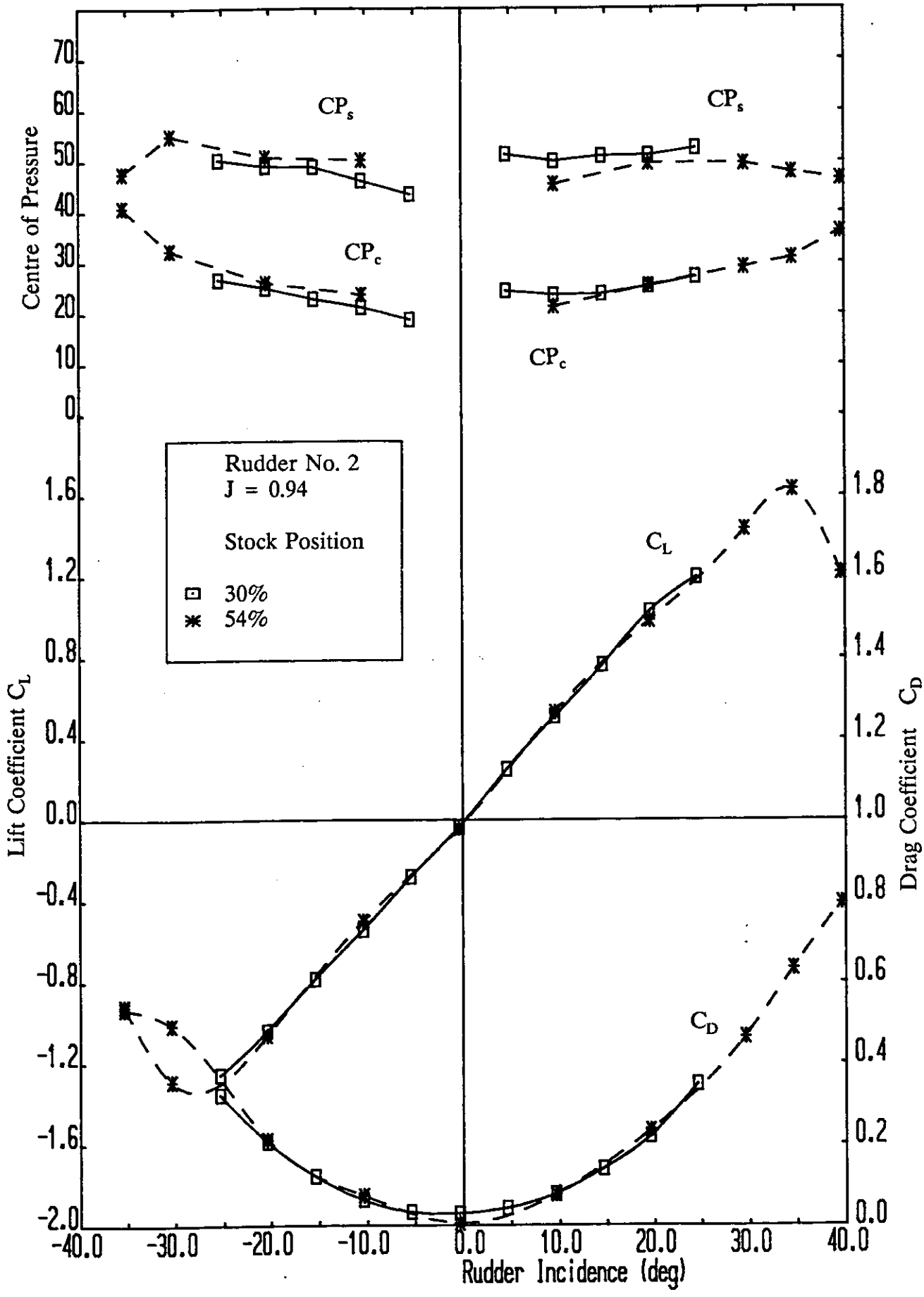

Figure 23 Effect of rudder stock position on the performance characteristic of all-movable rudder no. 2 for an advance ratio J=0.94.

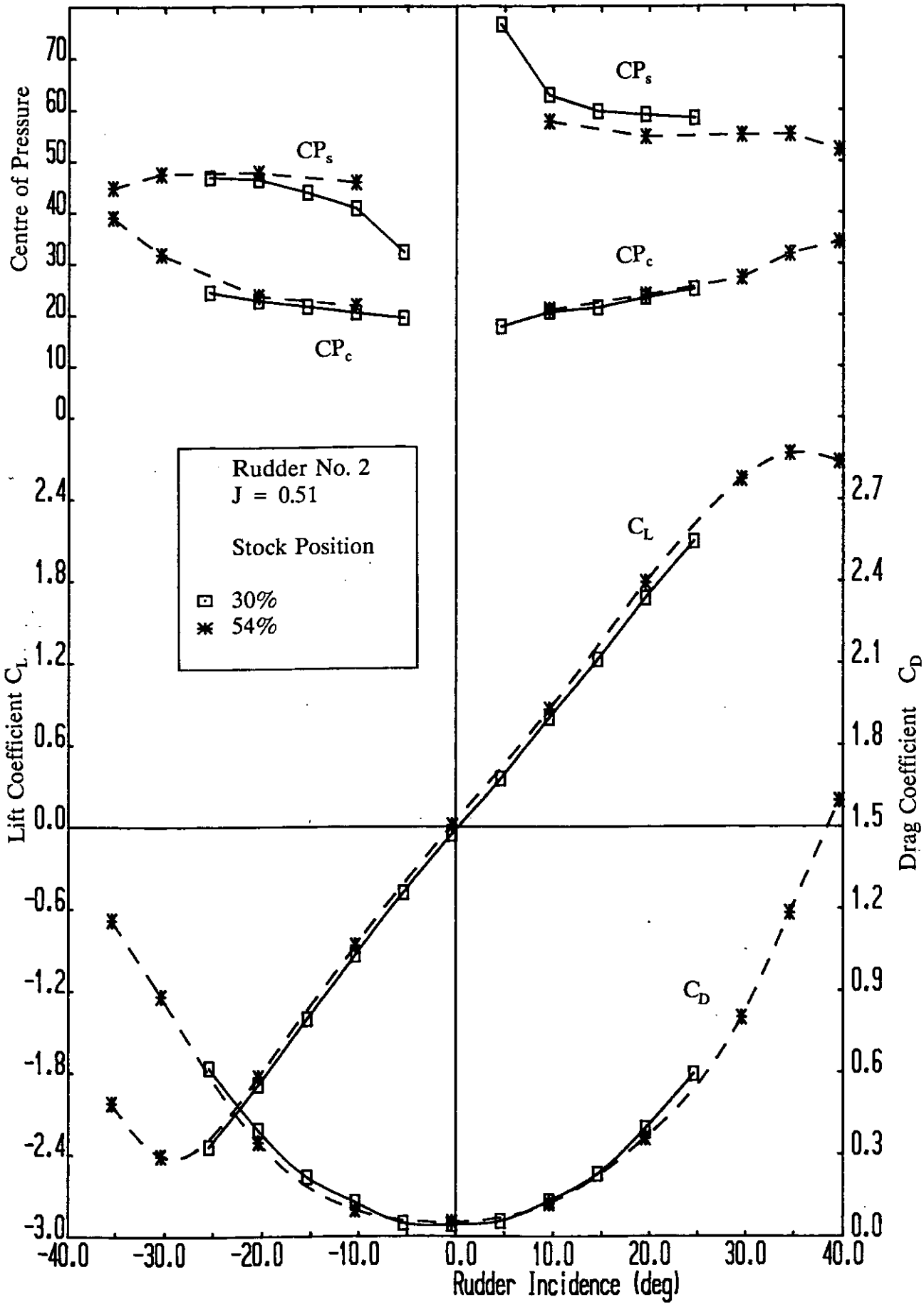

Figure 24 Effect of rudder stock position on the performance characteristic of all-movable rudder no. 2 for an advance ratio J=0.51.

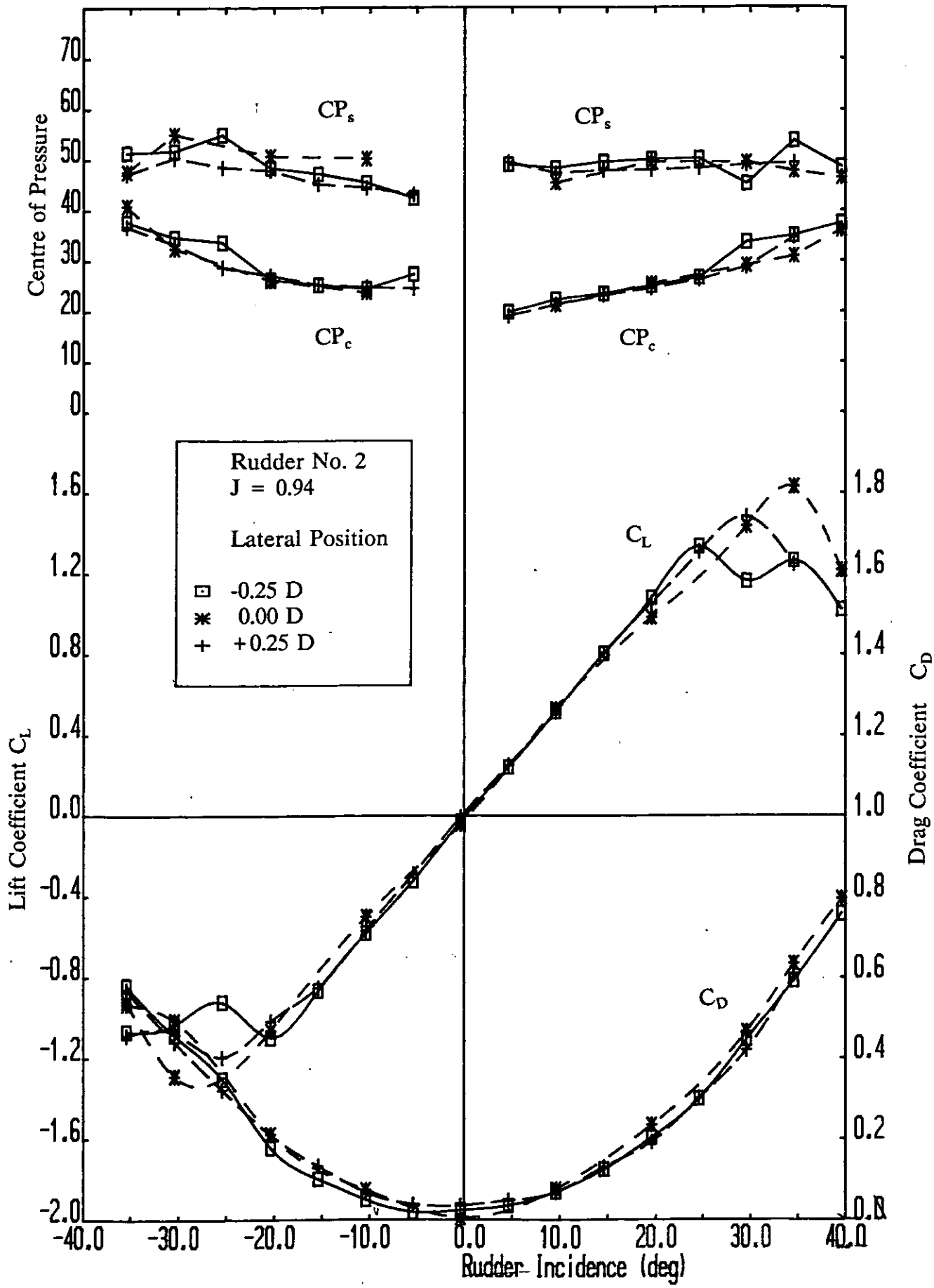

Figure 25 Effect of lateral separation of rudder and propeller on the performance characteristic of all-movable rudder no. 2 for an advance ratio J=0.94.

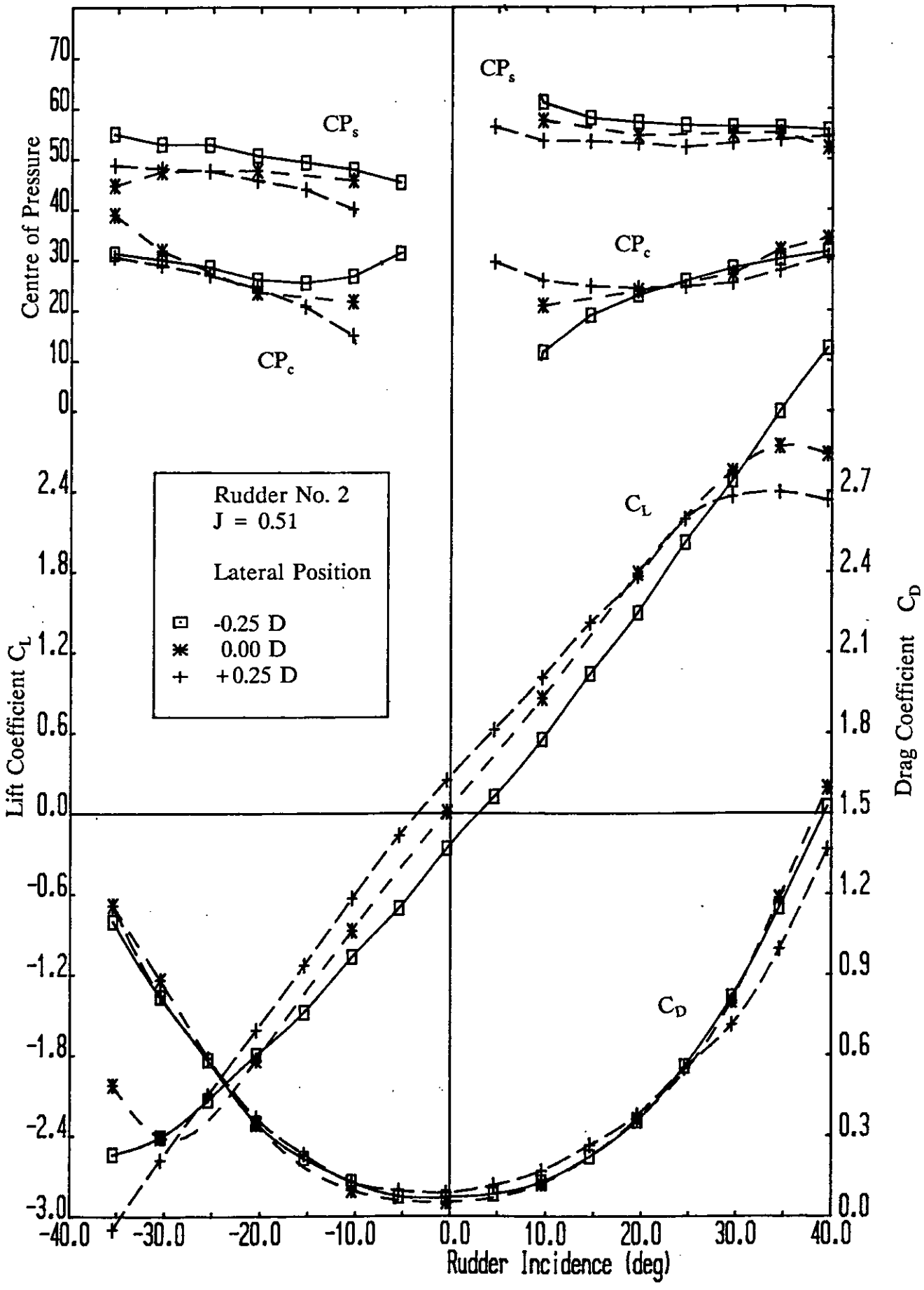

Figure 26 Effect of lateral separation of rudder and propeller on the performance characteristic of all-movable rudder no. 2 for an advance ratio J=0.51.

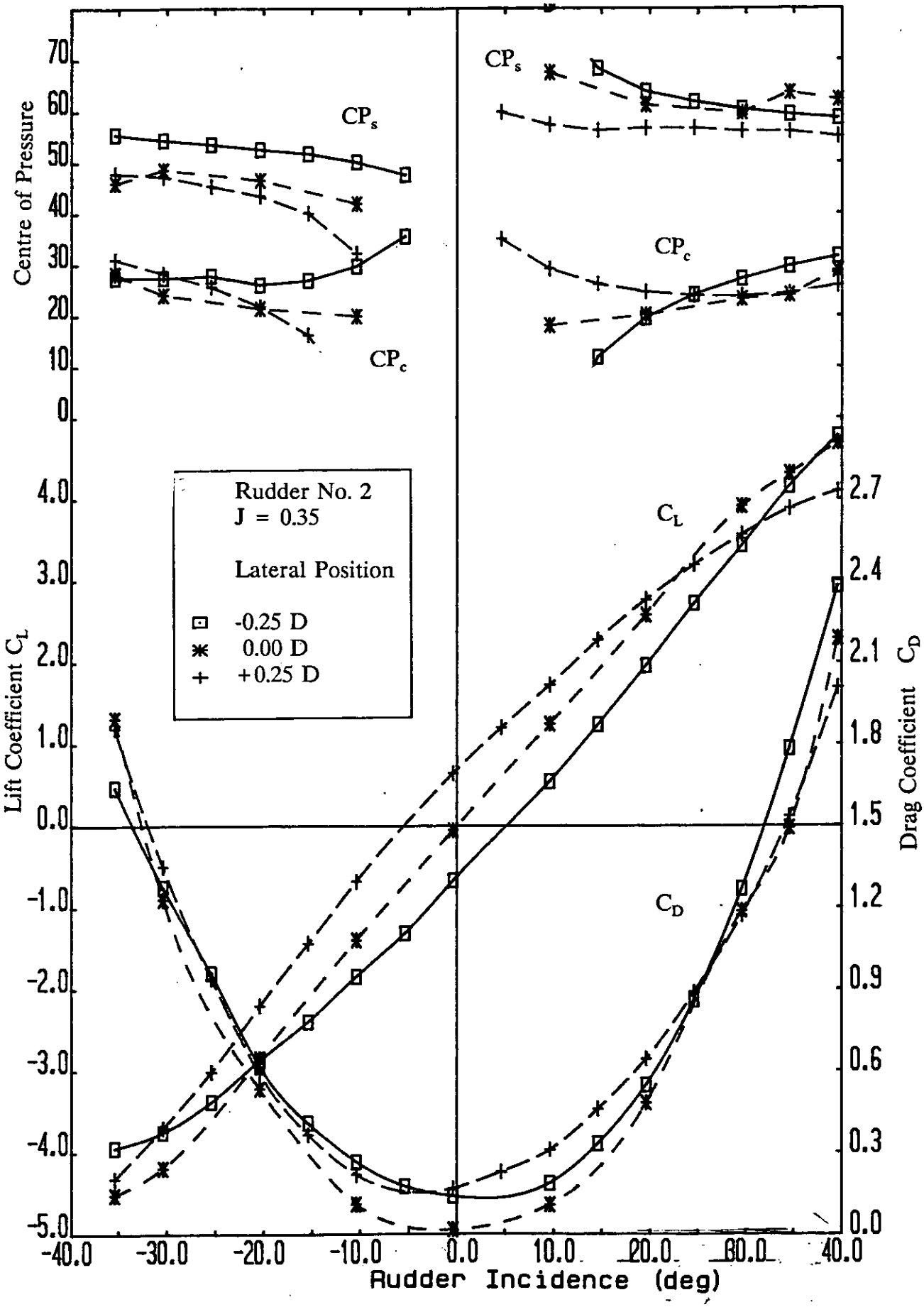

Figure 27 Effect of lateral separation of rudder and propeller on the performance characteristic of all-movable rudder no. 2 for an advance ratio J=0.35.

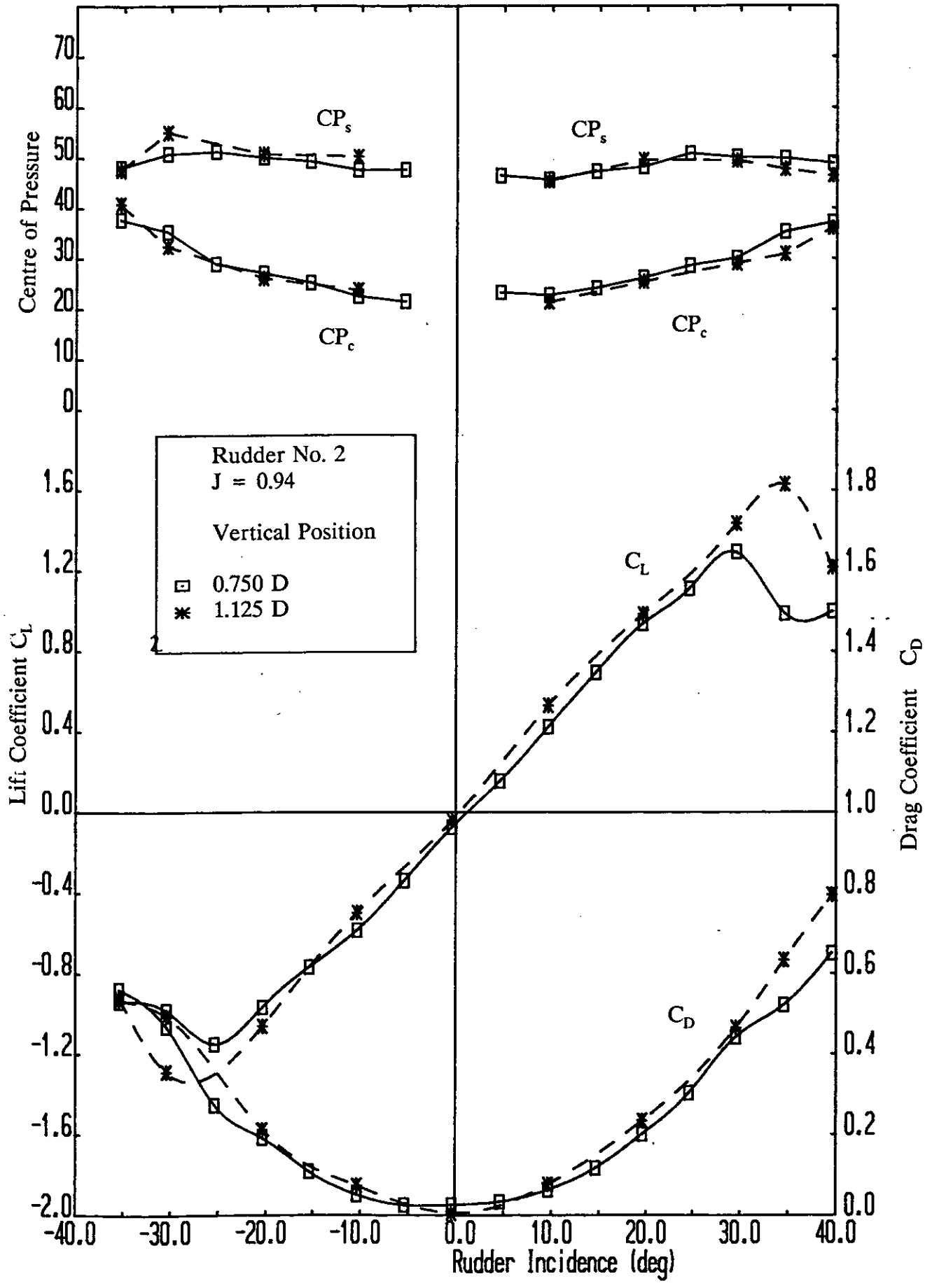

Figure 28 Effect of the height of propeller axis on the performance characteristic of all-movable rudder no. 2 for an advance ratio J=0.94.

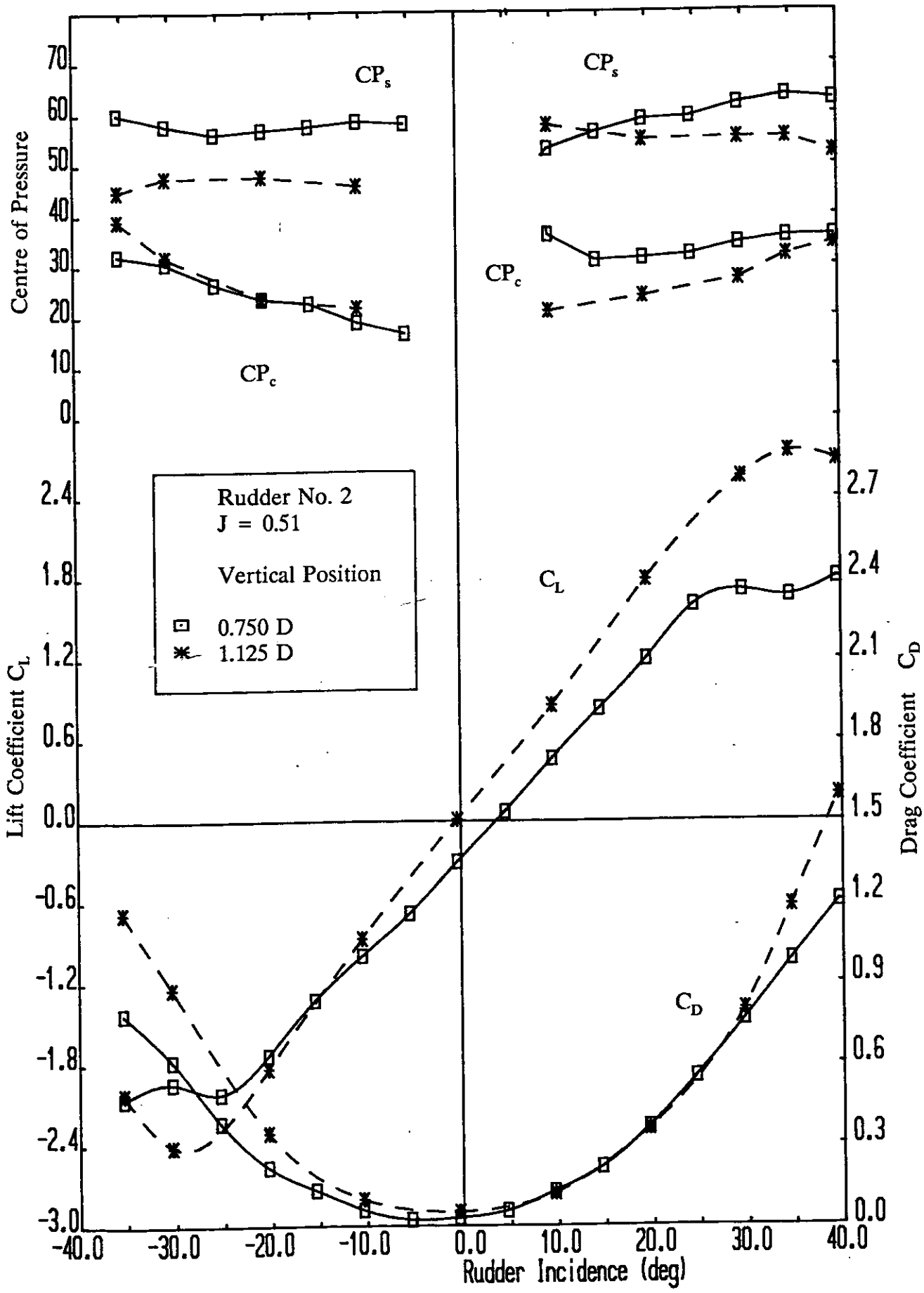

Figure 29 Effect of the height of propeller axis on the performance characteristic of all-movable rudder no. 2 for an advance ratio J=0.51.

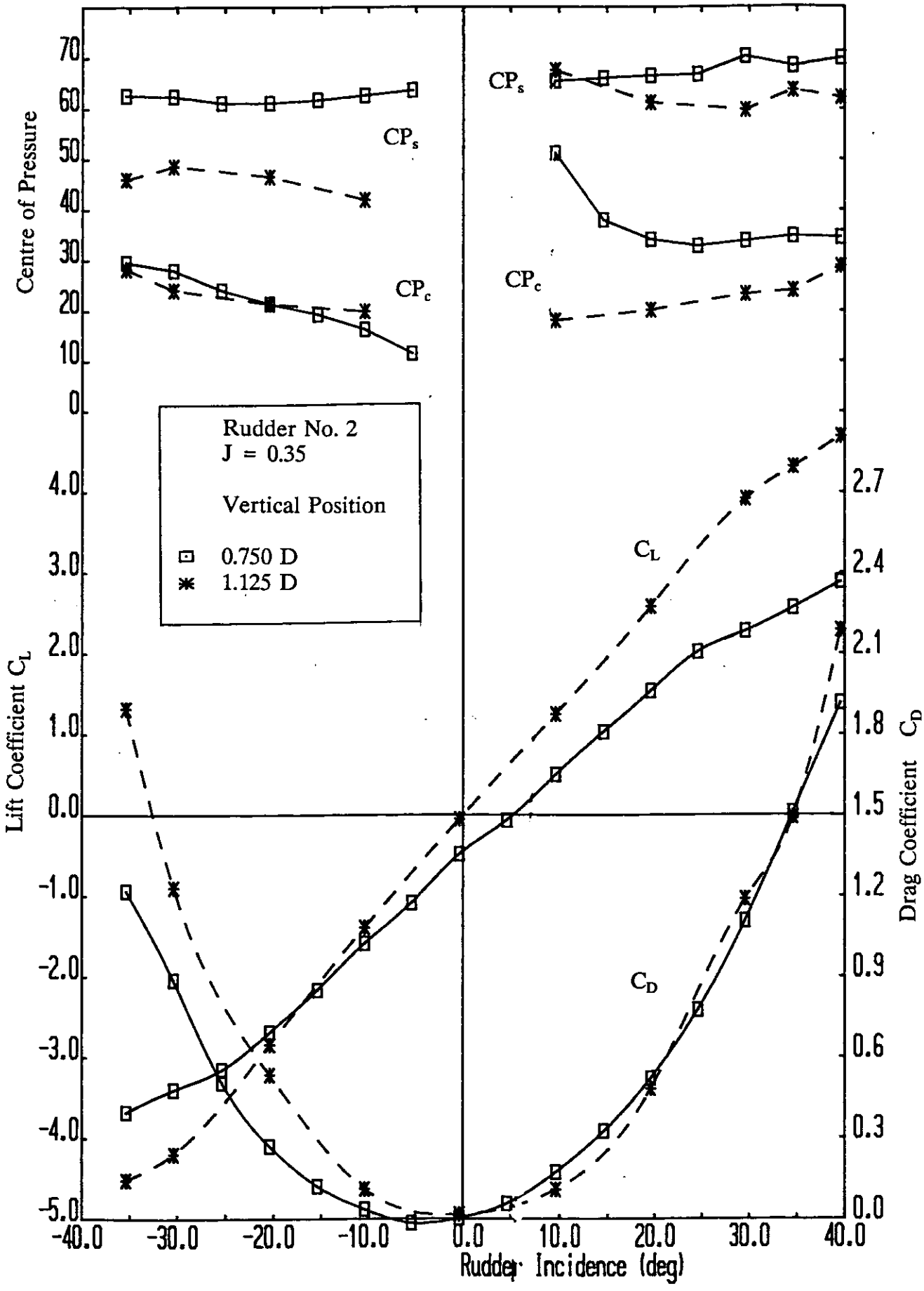

Figure 30 Effect of the height of propeller axis on the performance characteristic of all-movable rudder no. 2 for an advance ratio J=0.35.

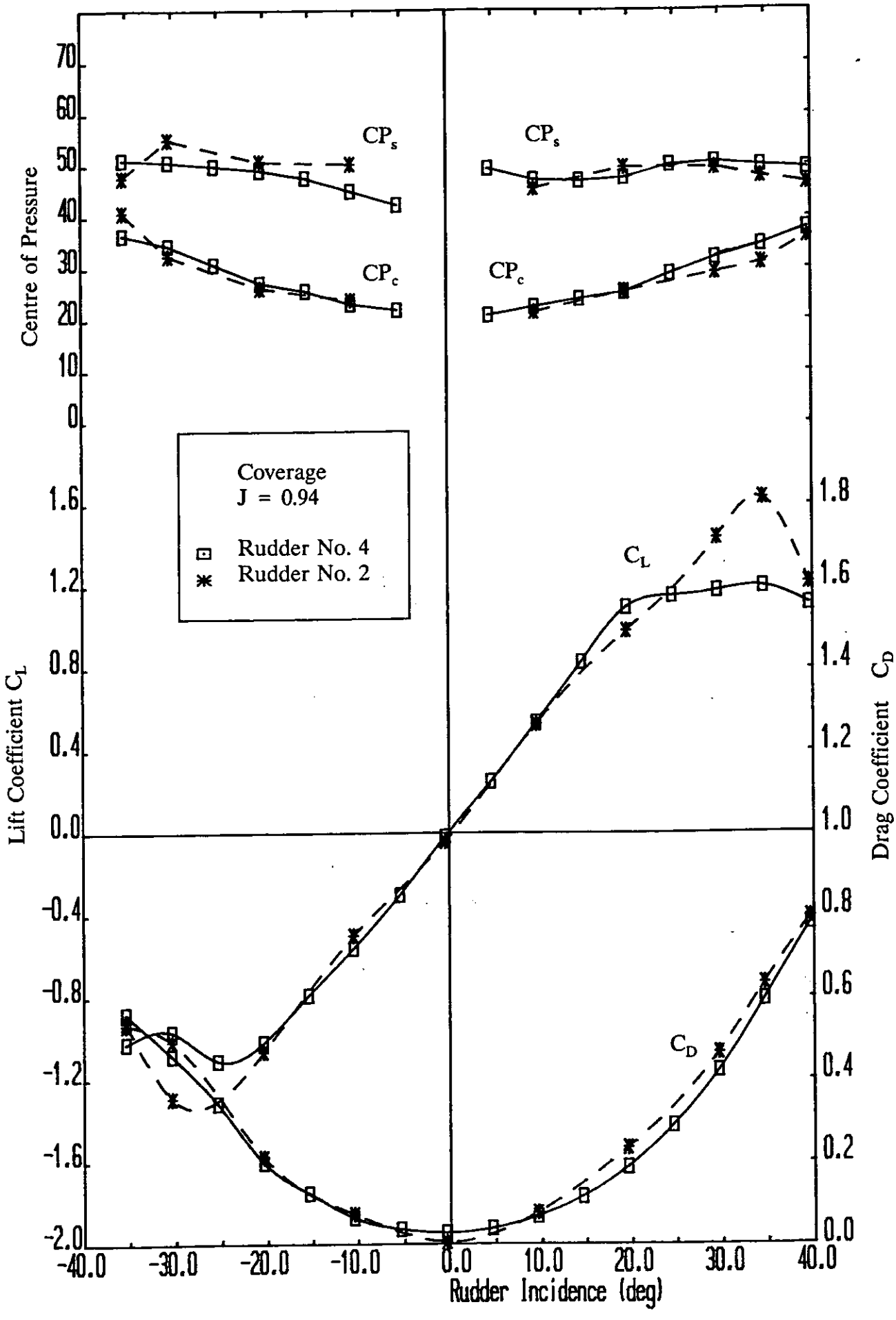

Figure 31 Effect of coverage of the rudder span by the propeller race on the performance characteristic for an advance ratio J=0.94.

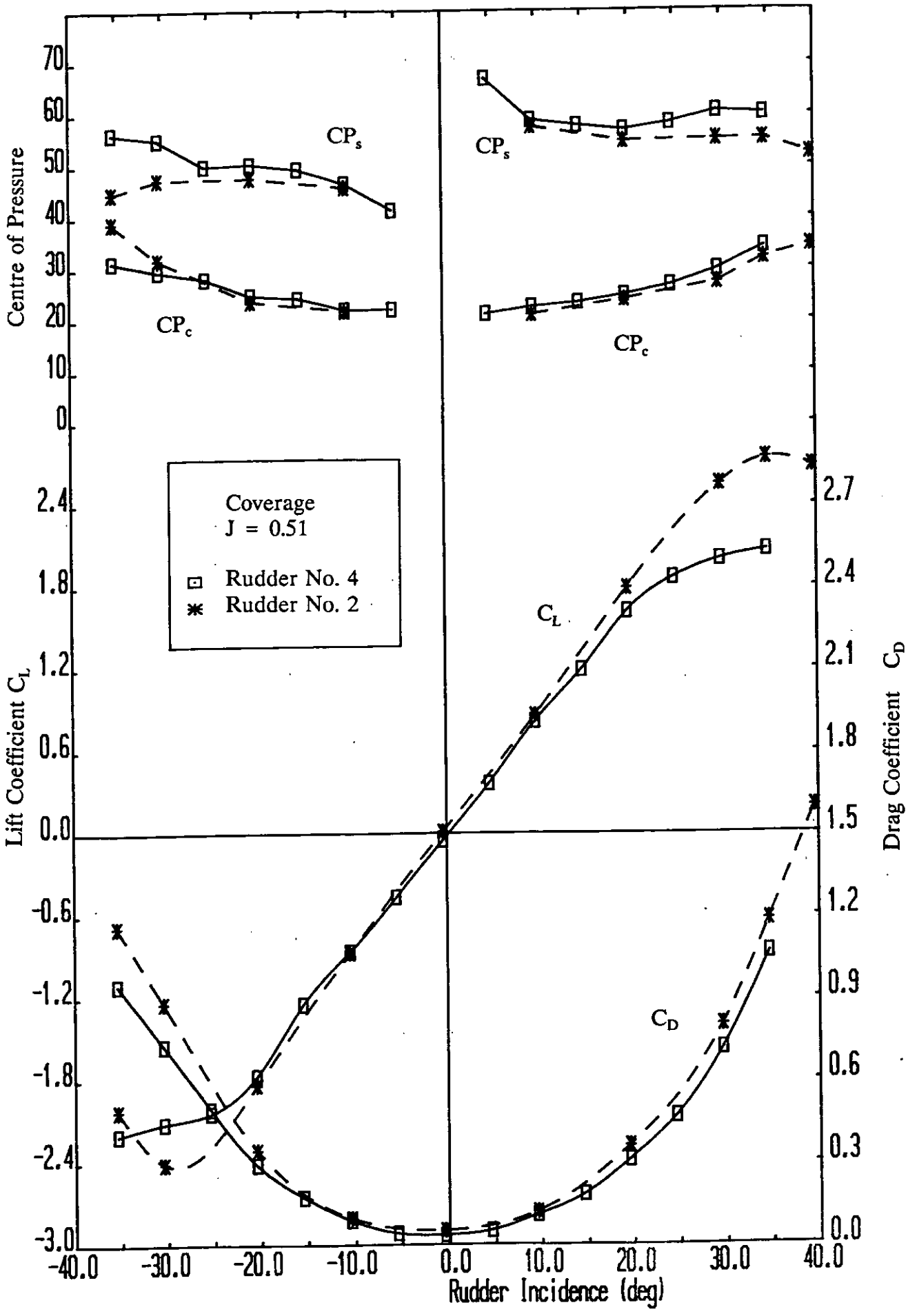

Figure 32 Effect of coverage of the rudder span by the propeller race on the performance characteristic for an advance ratio J=0.51.

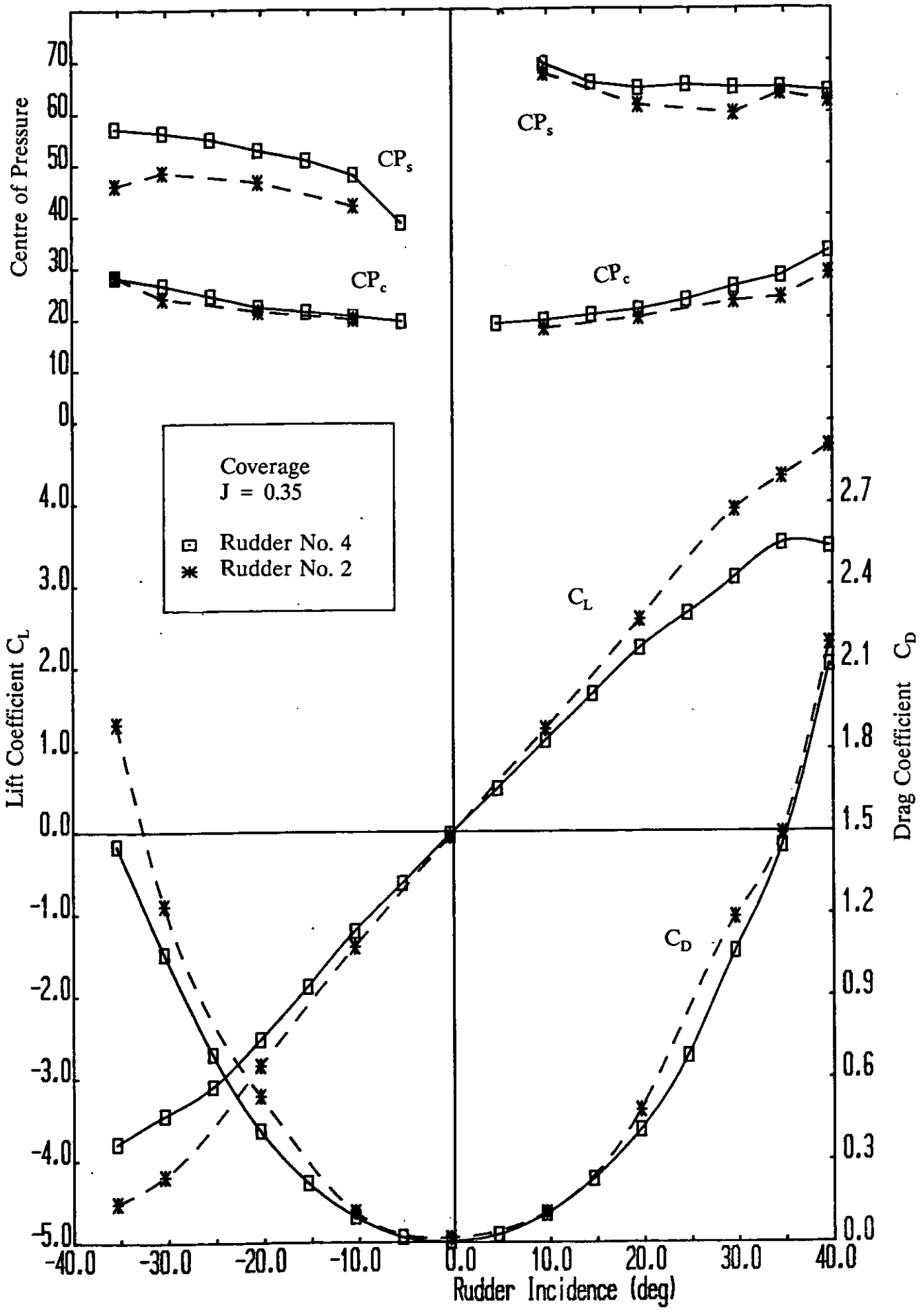

Figure 33 Effect of coverage of the rudder span by the propeller race on the performance characteristic for an advance ratio J=0.35.

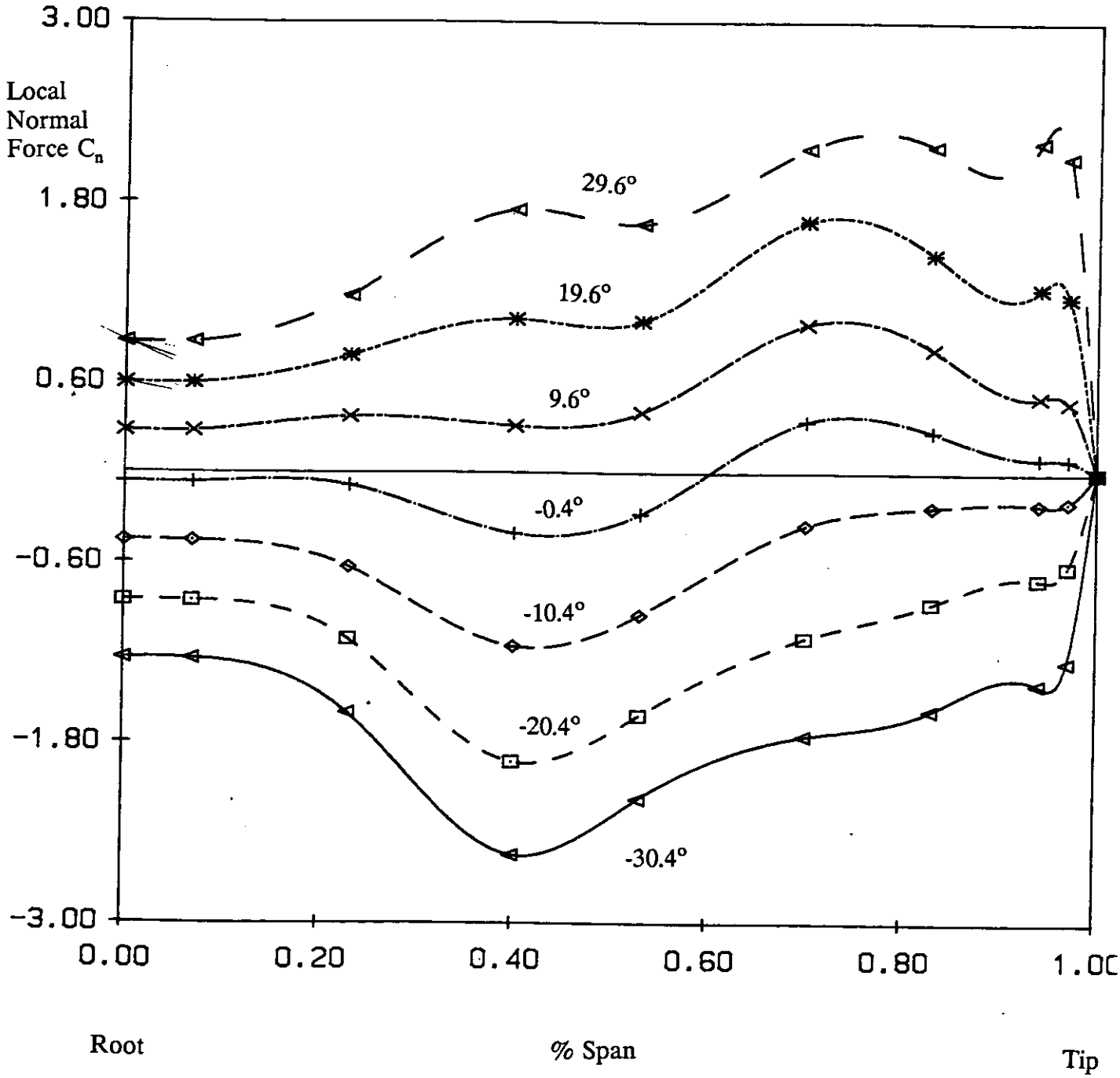

Figure 34 Variation with rudder incidence of the spanwise distribution of local section C_N of all-movable rudder no. 2 with a propeller ratio setting P/D=0.69 at an advance ratio J=0.42.

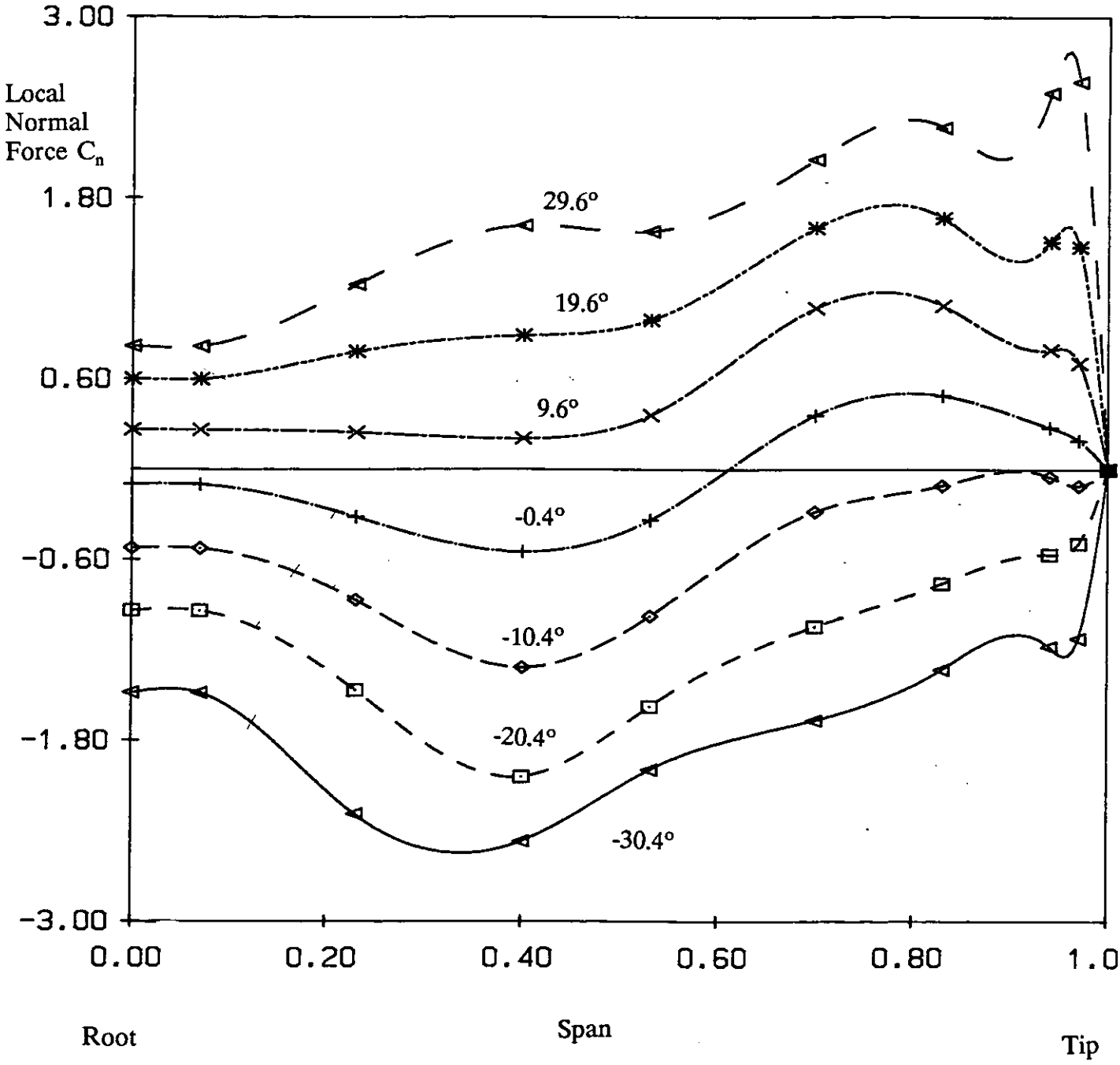

Figure 35 Variation with rudder incidence of the spanwise distribution of local section C_N of all-movable rudder no. 2 with a propeller ratio setting P/D = 1.34 at an advance ratio J = 0.61.

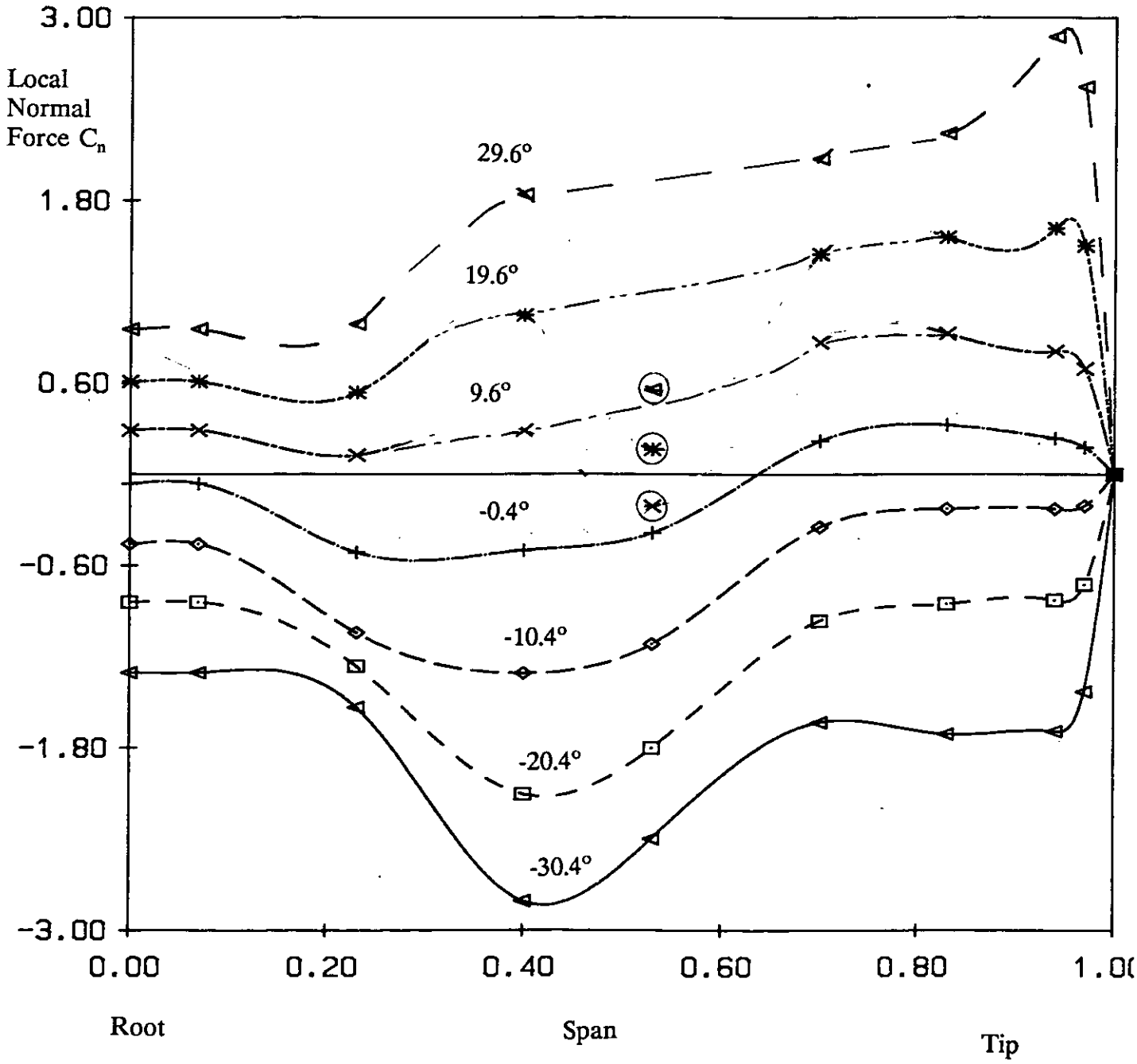

Figure 36 Variation with rudder incidence of the spanwise distribution of local section C_N of all-movable rudder no. 5 for an advance ratio J=0.51.

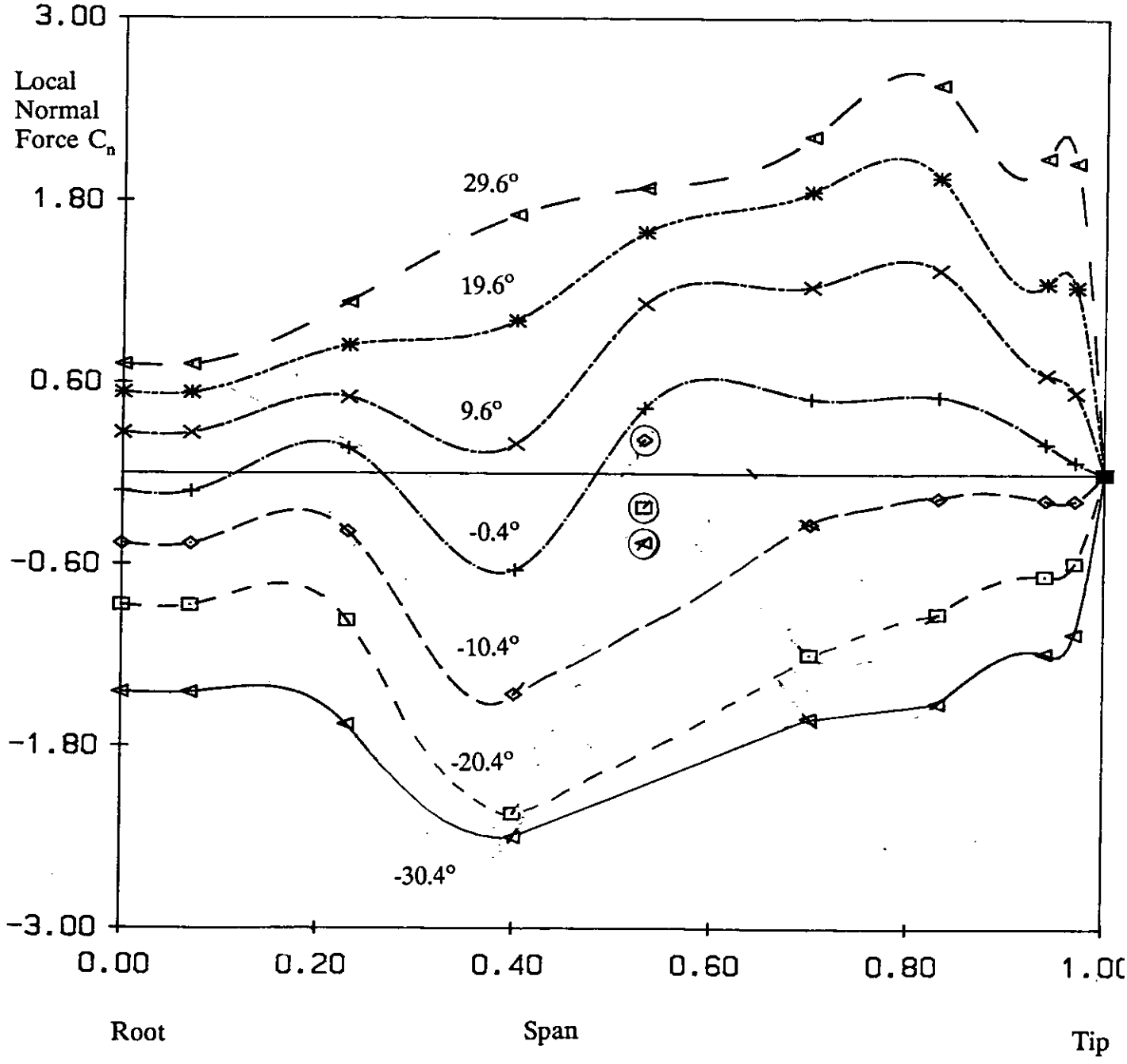

Figure 37 Variation with rudder incidence of the spanwise distribution of local section C_N of all-movable rudder no. 6 for an advance ratio J=0.51.

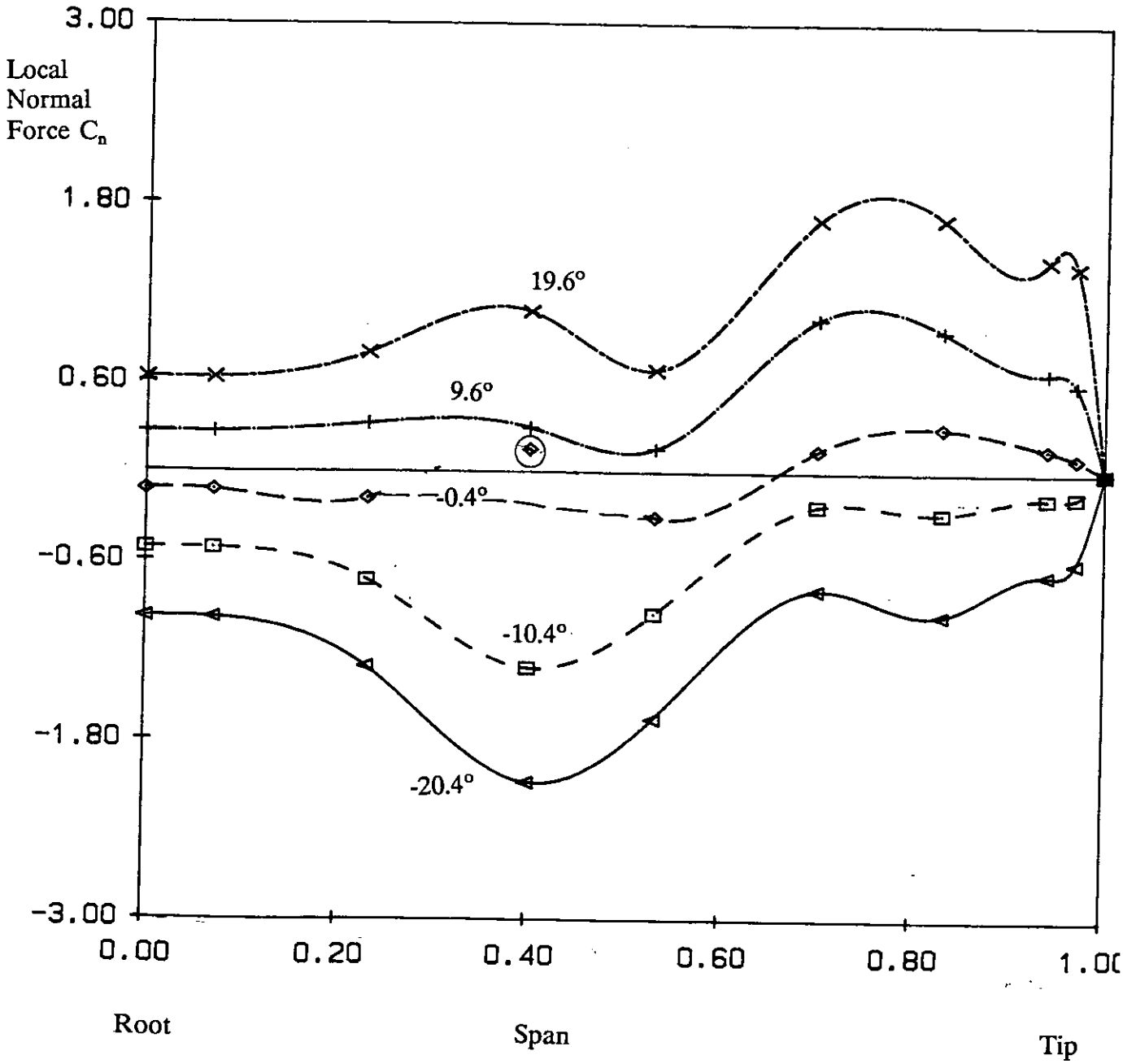

Figure 38 Variation with rudder incidence of the spanwise distribution of local section C_N of all-movable rudder no. 2 with a rudder stock position at 54% chord at an advance ratio J=0.51.

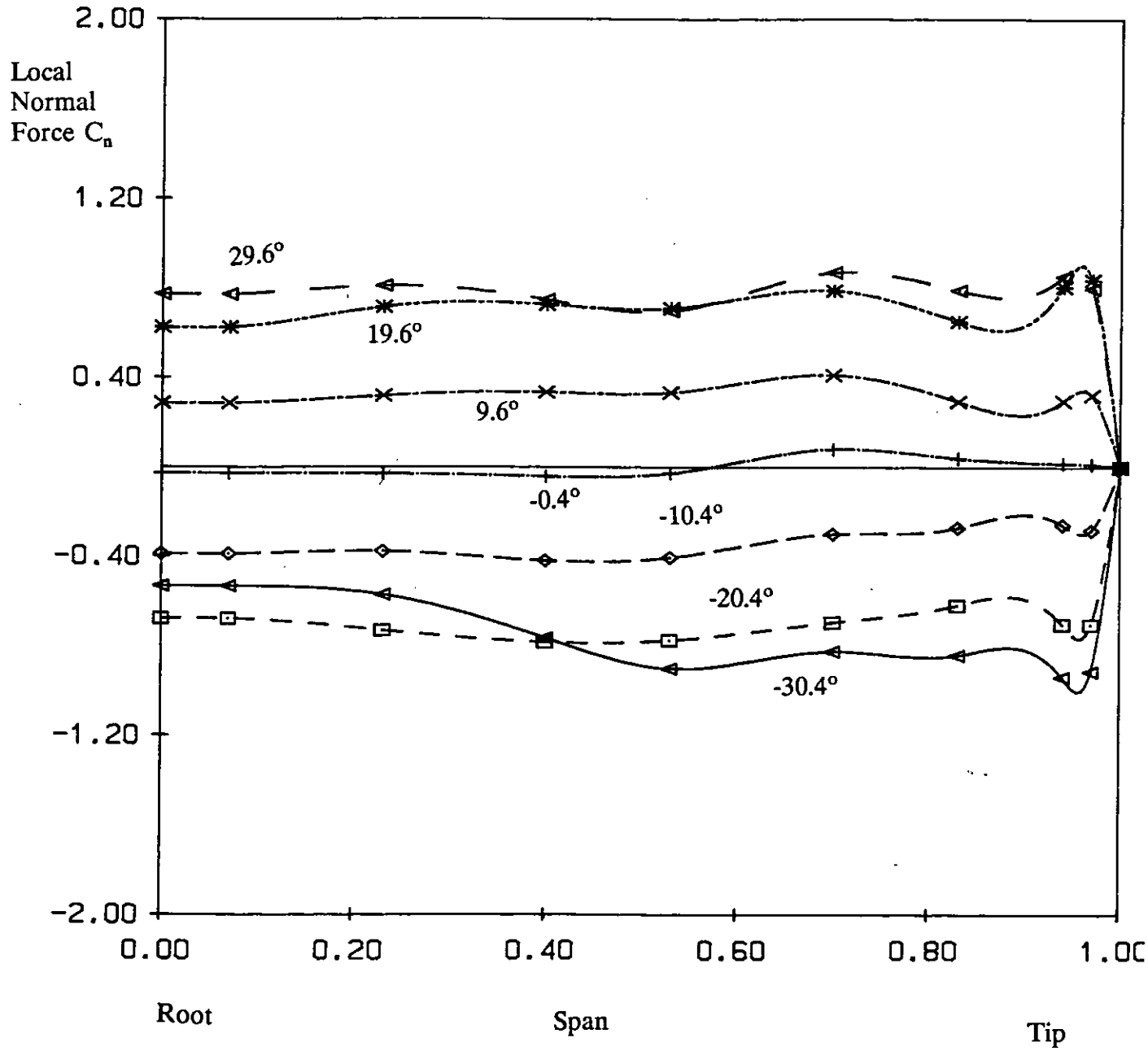

Figure 39 Variation with rudder incidence of the spanwise distribution of local section C_N of all-movable rudder no. 2 at a lateral separation Y/D = -0.25 at an advance ratio J=0.94.

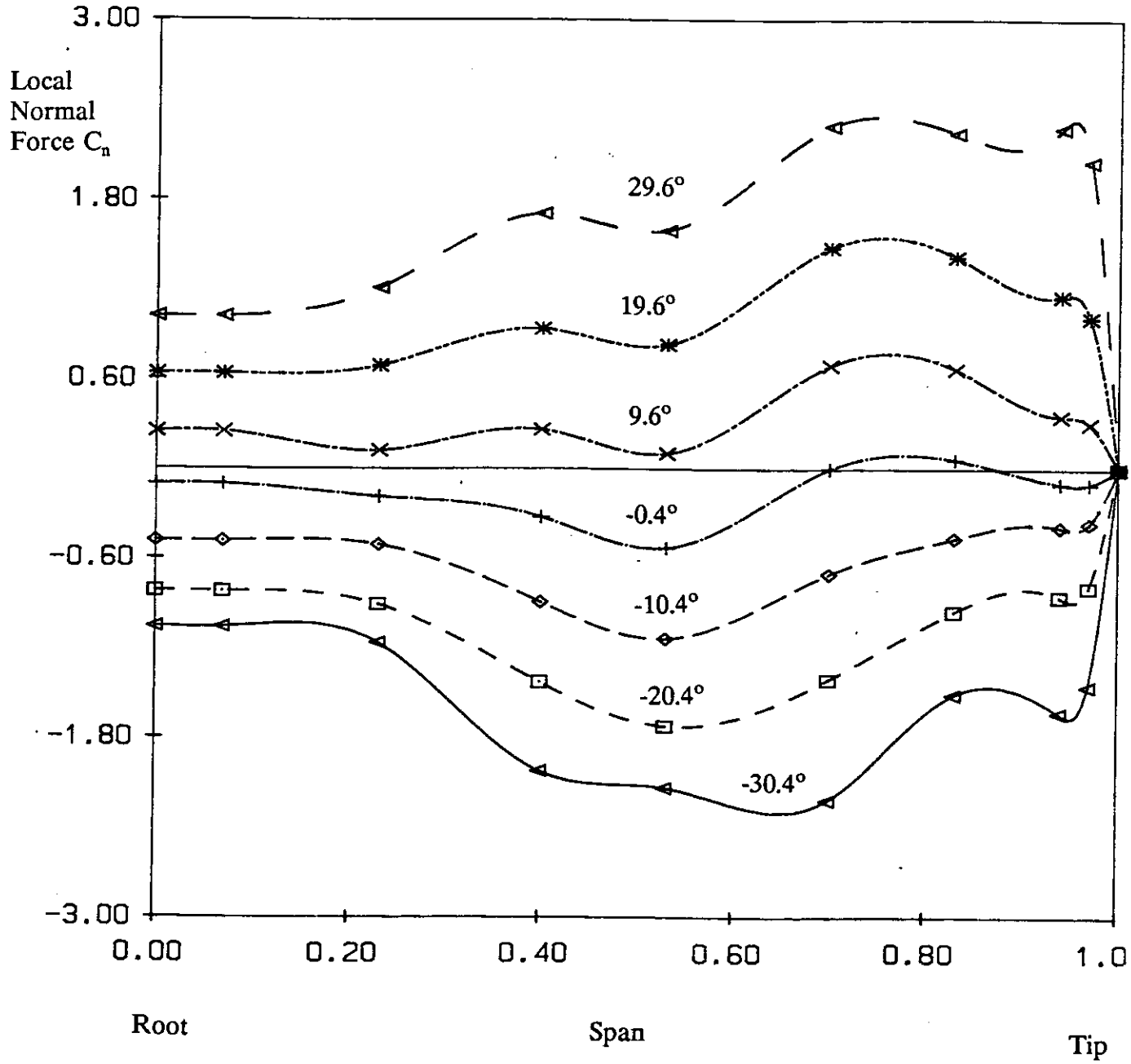

Figure 40 Variation with rudder incidence of the spanwise distribution of local section C_N of all-movable rudder no. 2 at a lateral separation Y/D = -0.25 at an advance ratio J=0.51.

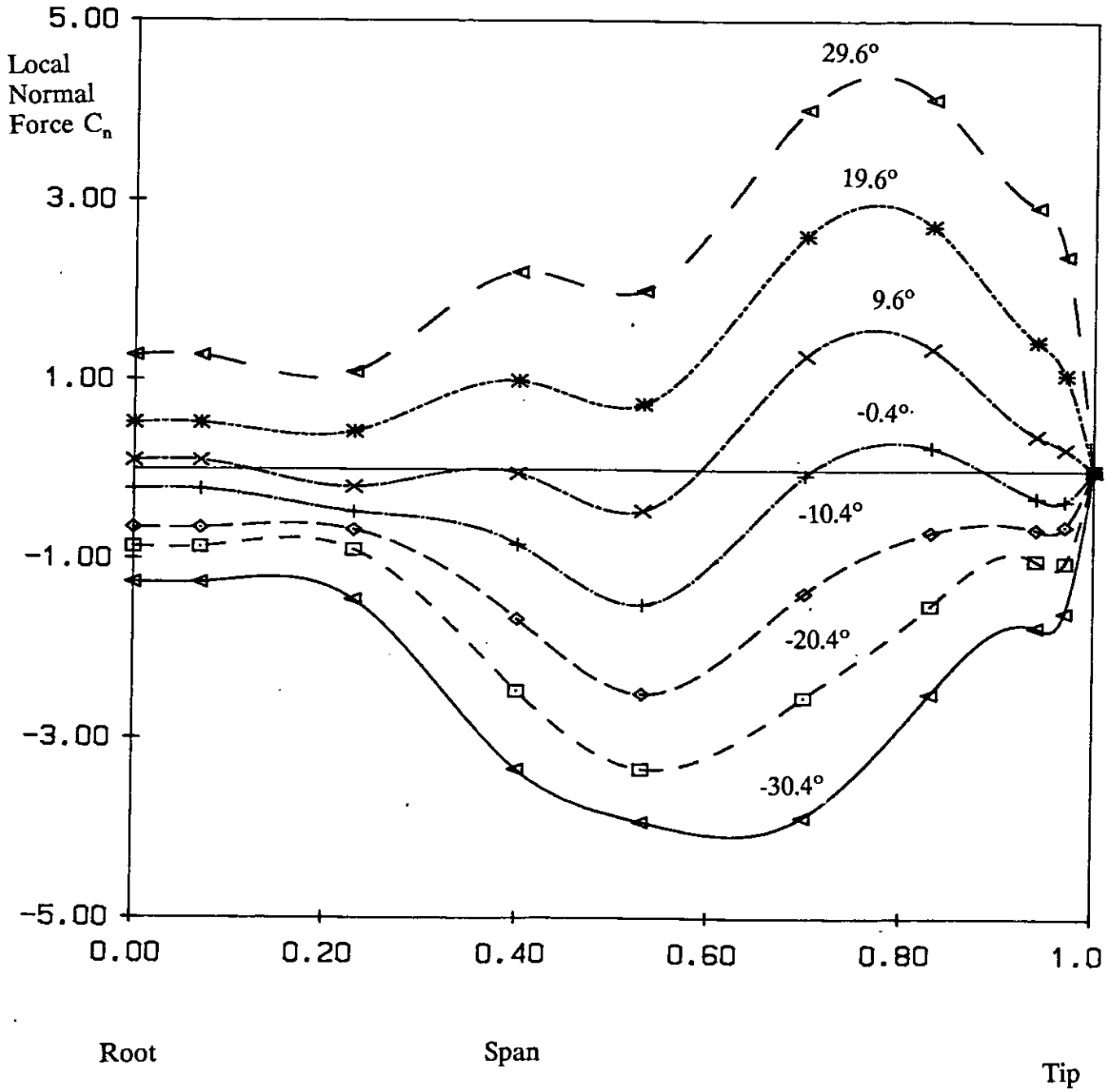

Figure 41 Variation with rudder incidence of the spanwise distribution of local section C_N of all-movable rudder no. 2 at a lateral separation Y/D = -0.25 at an advance ratio J=0.35.

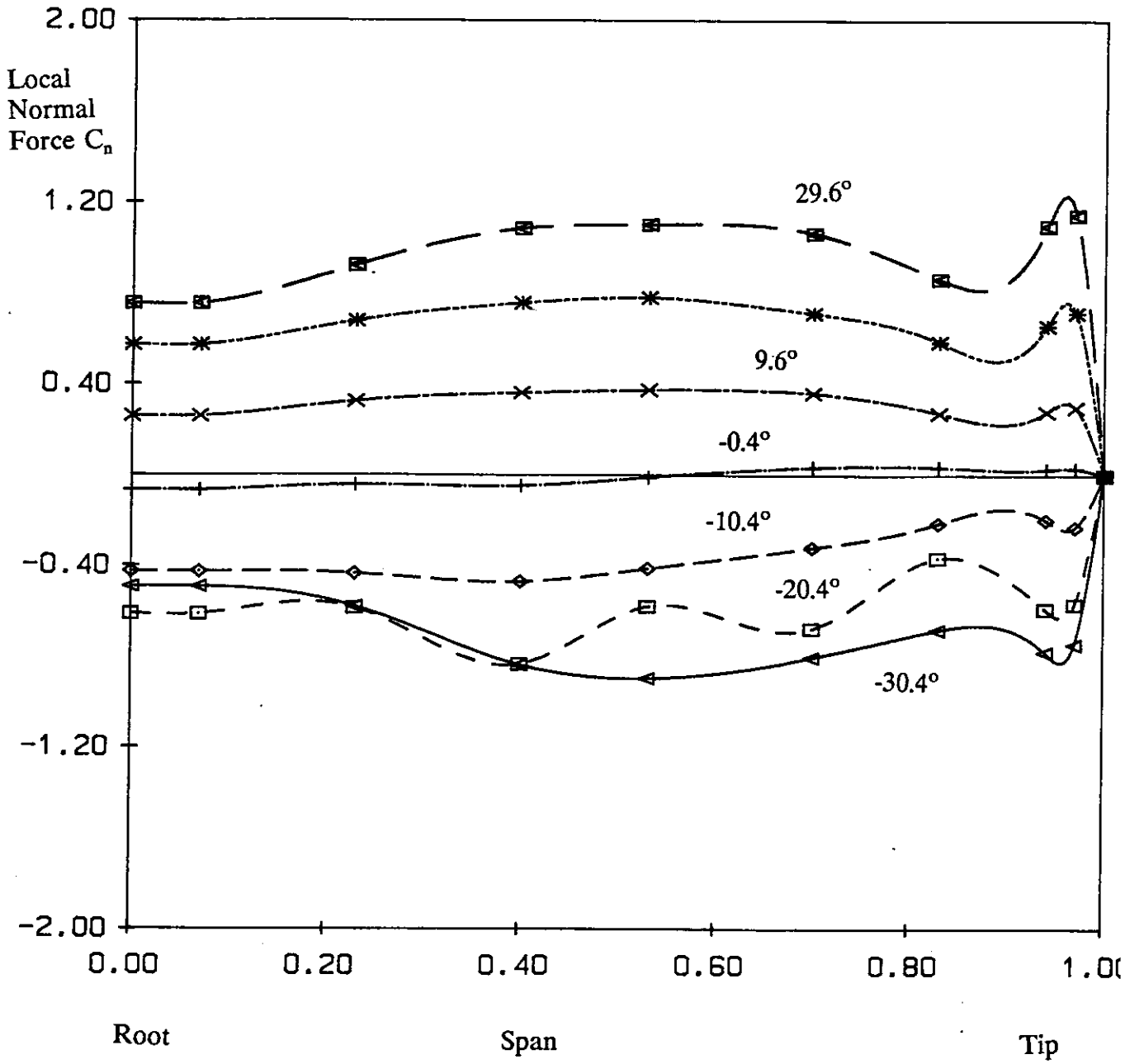

Figure 42 Variation with rudder incidence of the spanwise distribution of local section C_N of all-movable rudder no. 2 at a lateral separation Y/D = +0.25 at an advance ratio J=0.94.

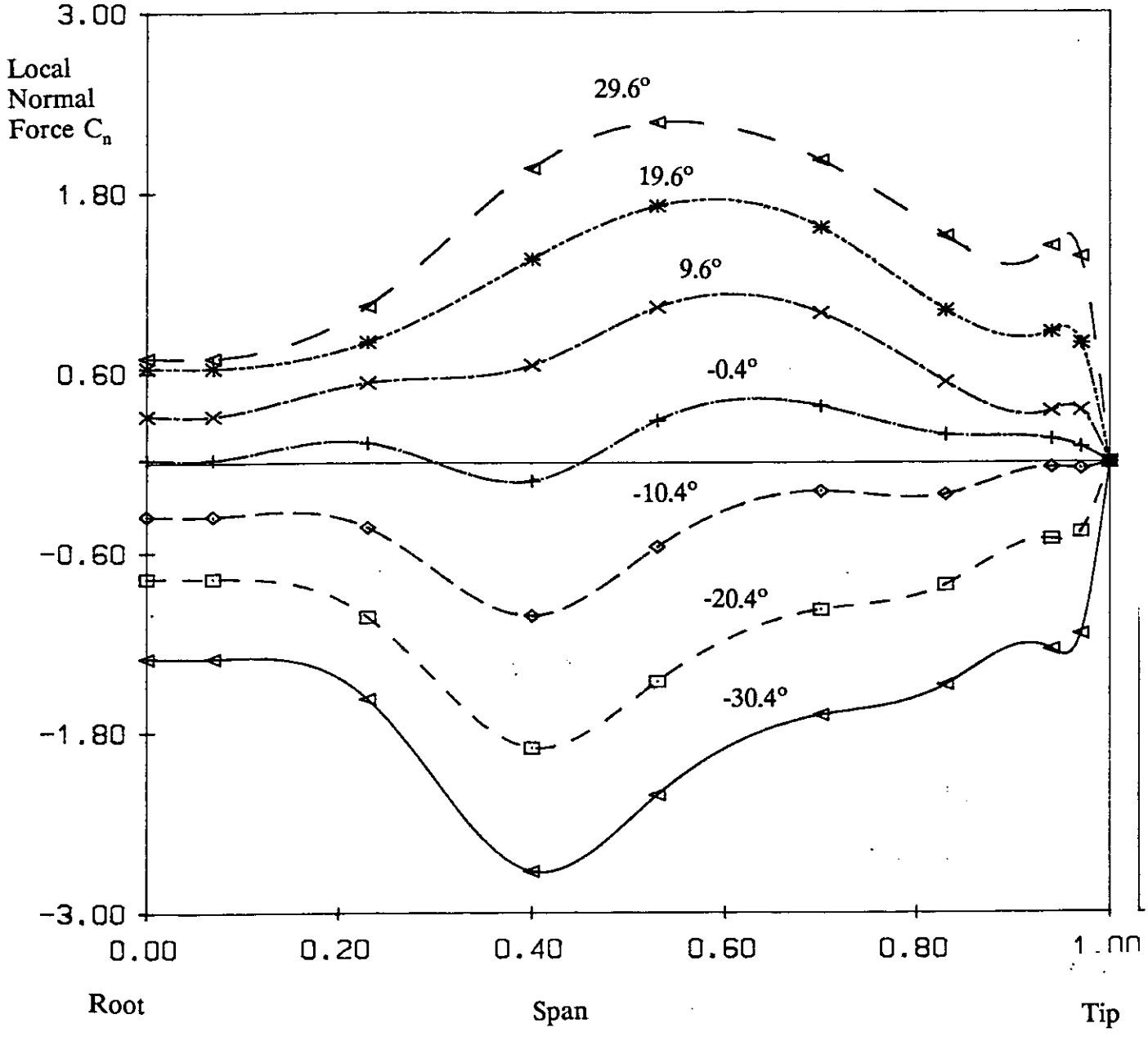

Figure 43 Variation with rudder incidence of the spanwise distribution of local section C_N of all-movable rudder no. 2 at a lateral separation Y/D = +0.25 at an advance ratio J=0.51.

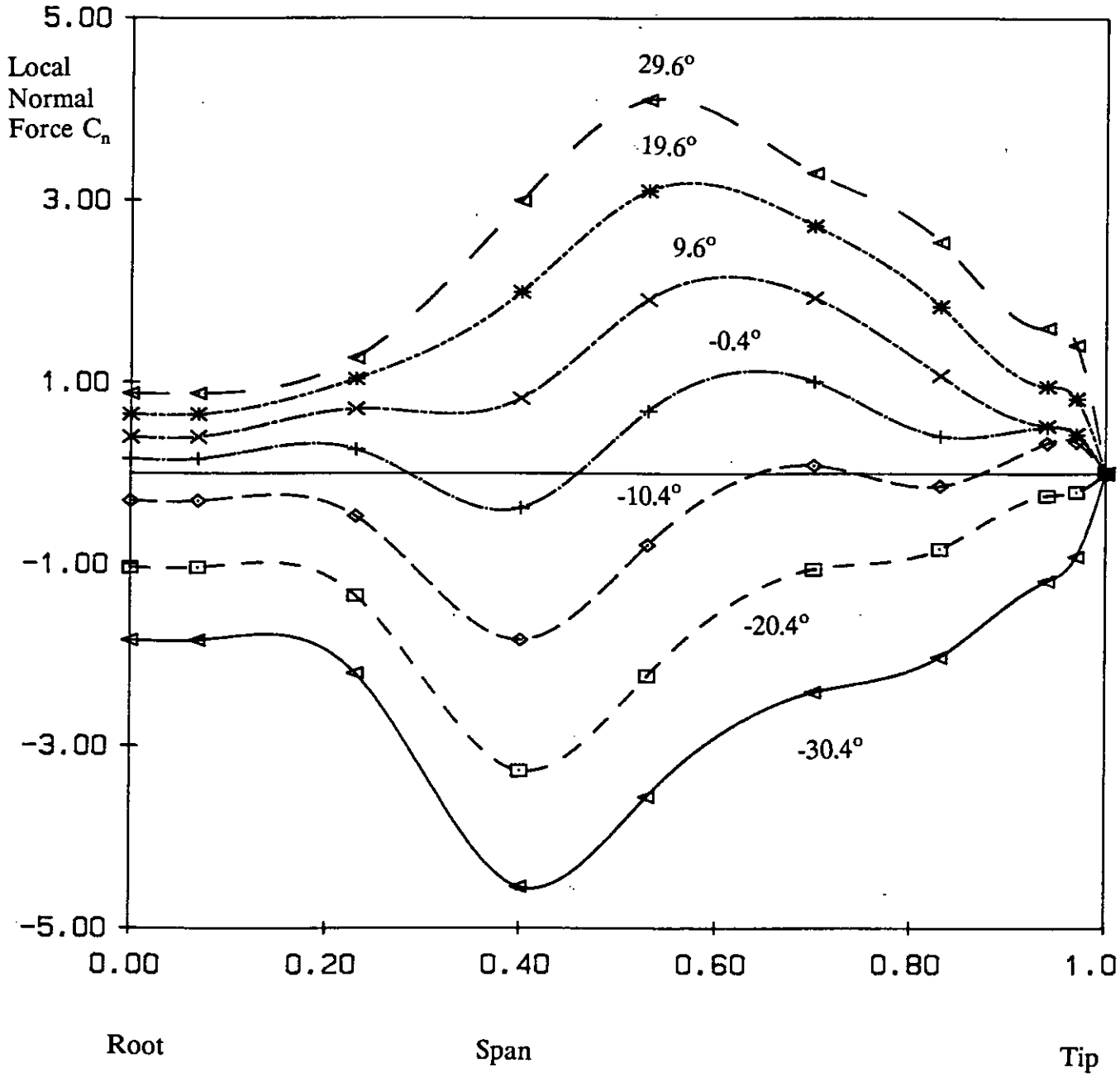

Figure 44 Variation with rudder incidence of the spanwise distribution of local section C_N of all-movable rudder no. 2 at a lateral separation Y/D = +0.25 at an advance ratio J=0.35.

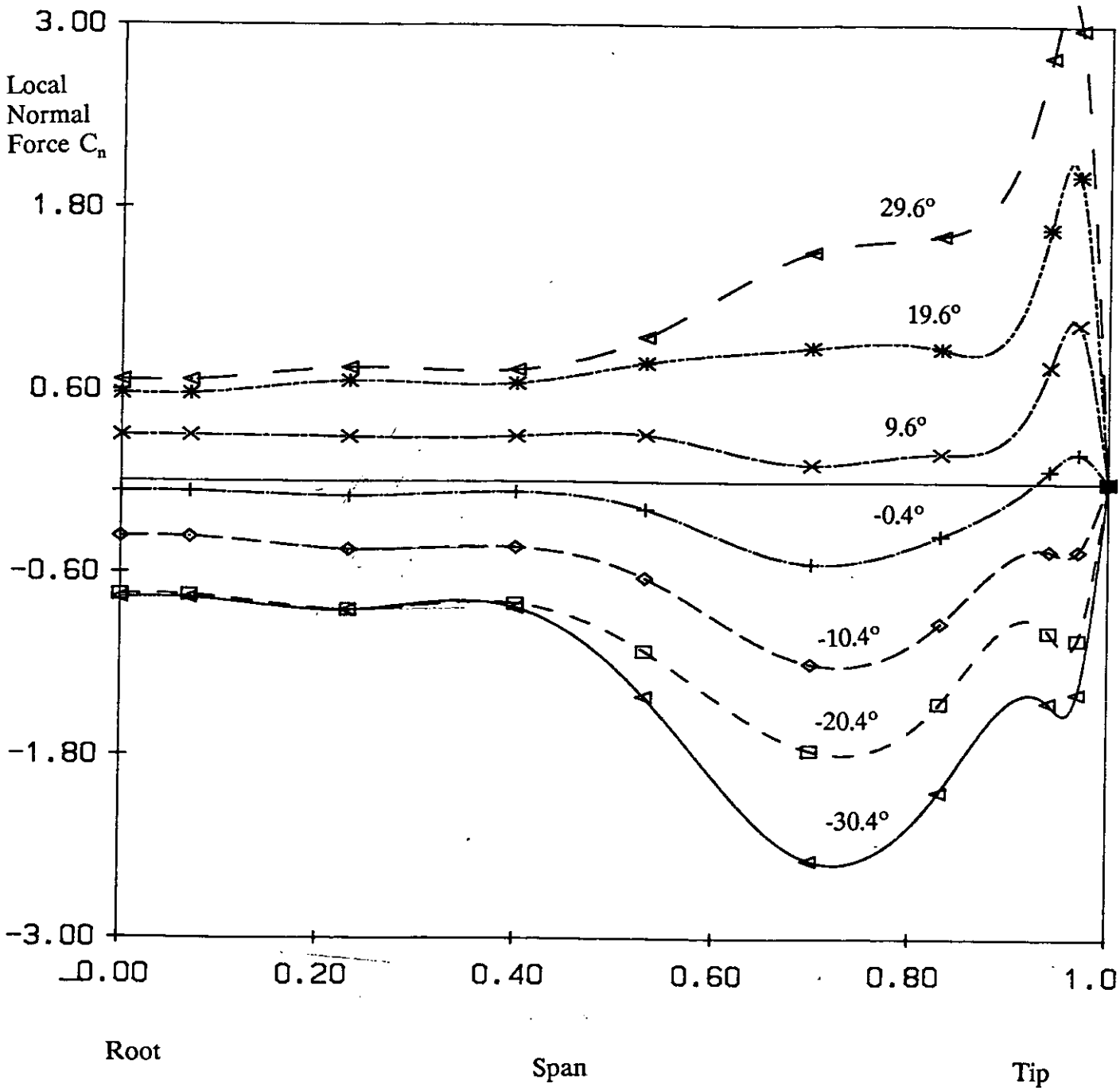

Figure 45 Variation with rudder incidence of the spanwise distribution of local section C_N of all-movable rudder no. 2 with the propeller axis height of 900mm for an advance ratio J=0.51.

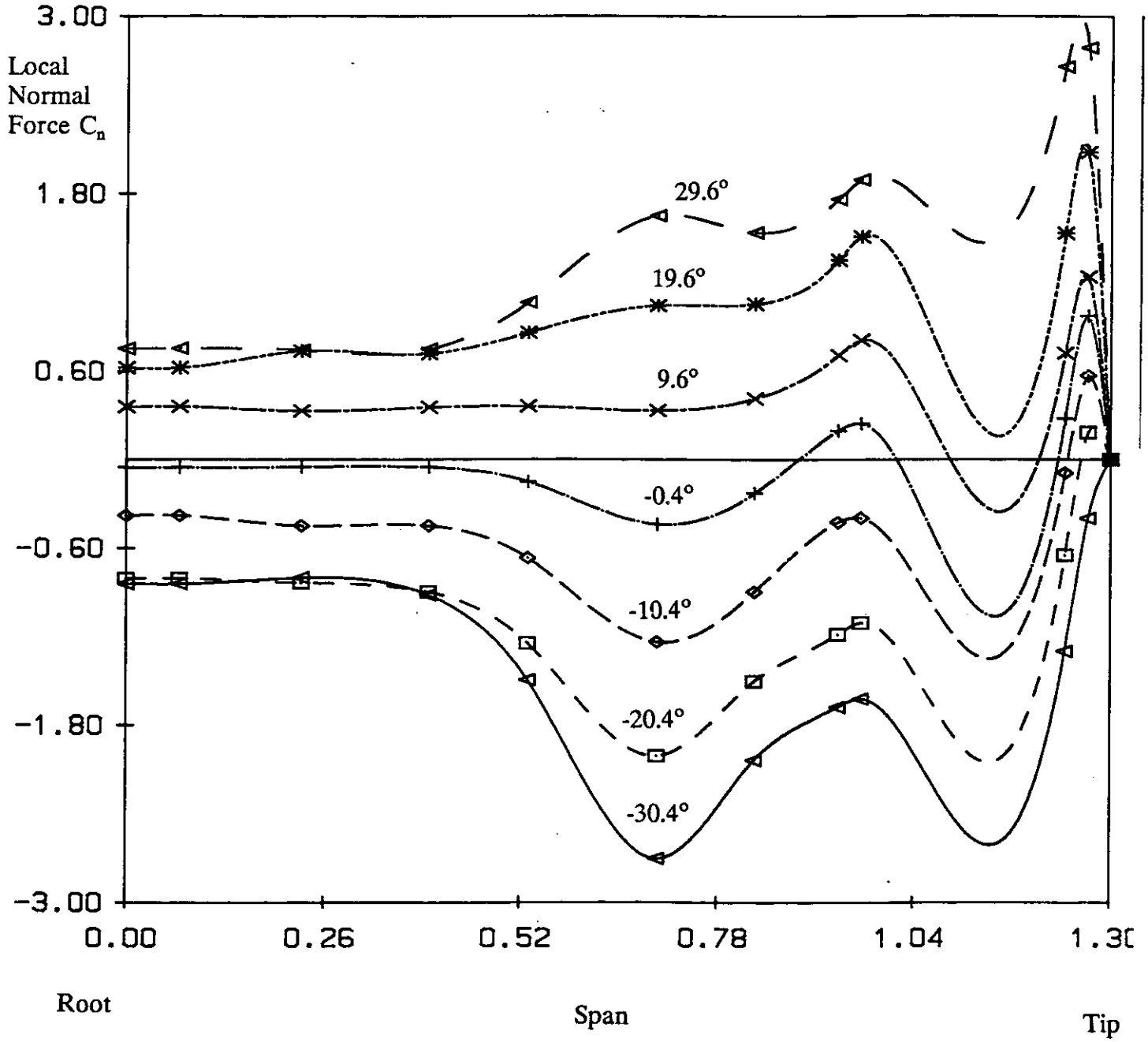

Figure 46 Variation with rudder incidence of the spanwise distribution of local section C_N of all-movable rudder no. 4 with the propeller axis height of 900mm for an advance ratio J=0.51.

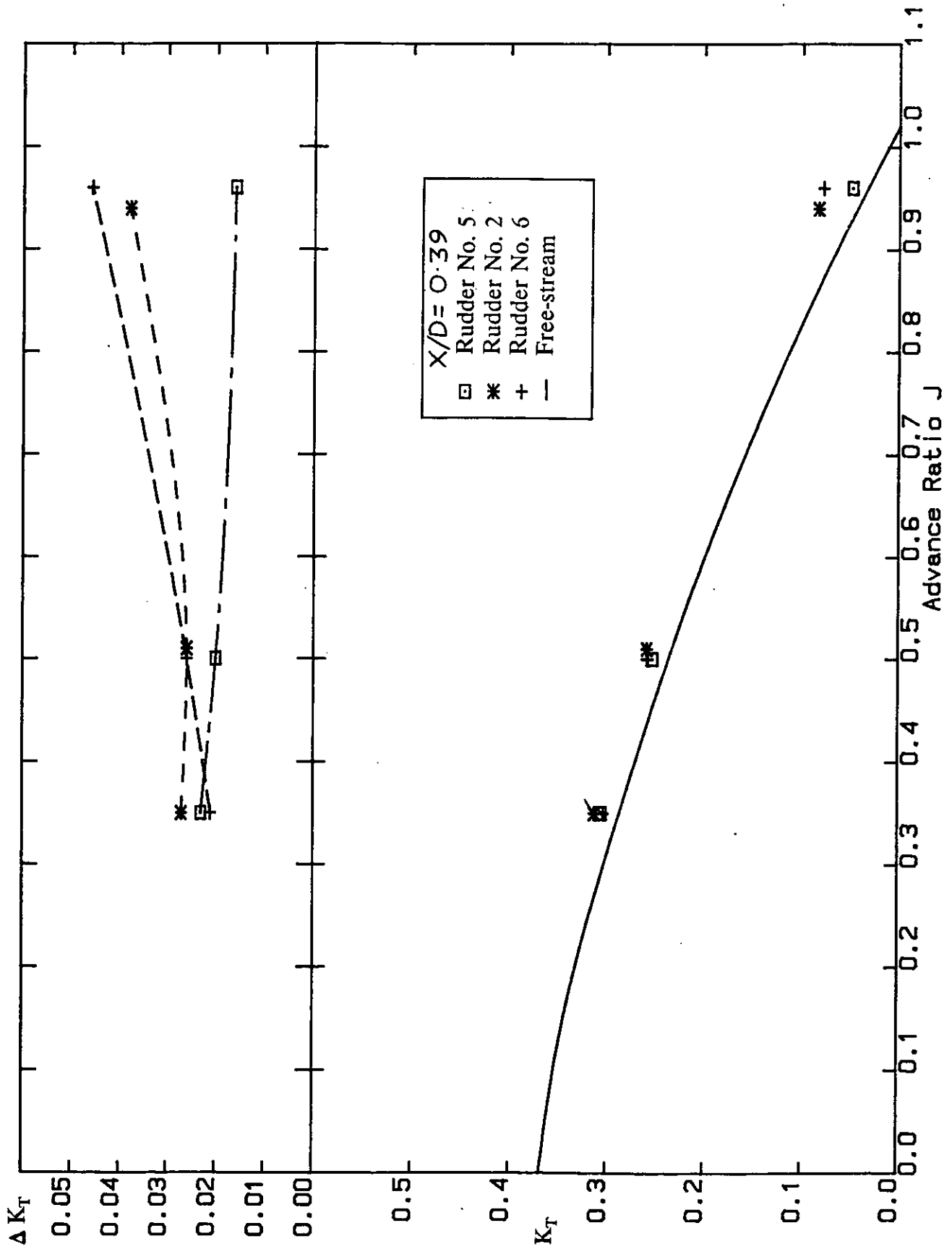

Figure 47 Comparison of propeller thrust and thrust increment against advance ratio for all-movable rudder no's 2, 5 and 6.

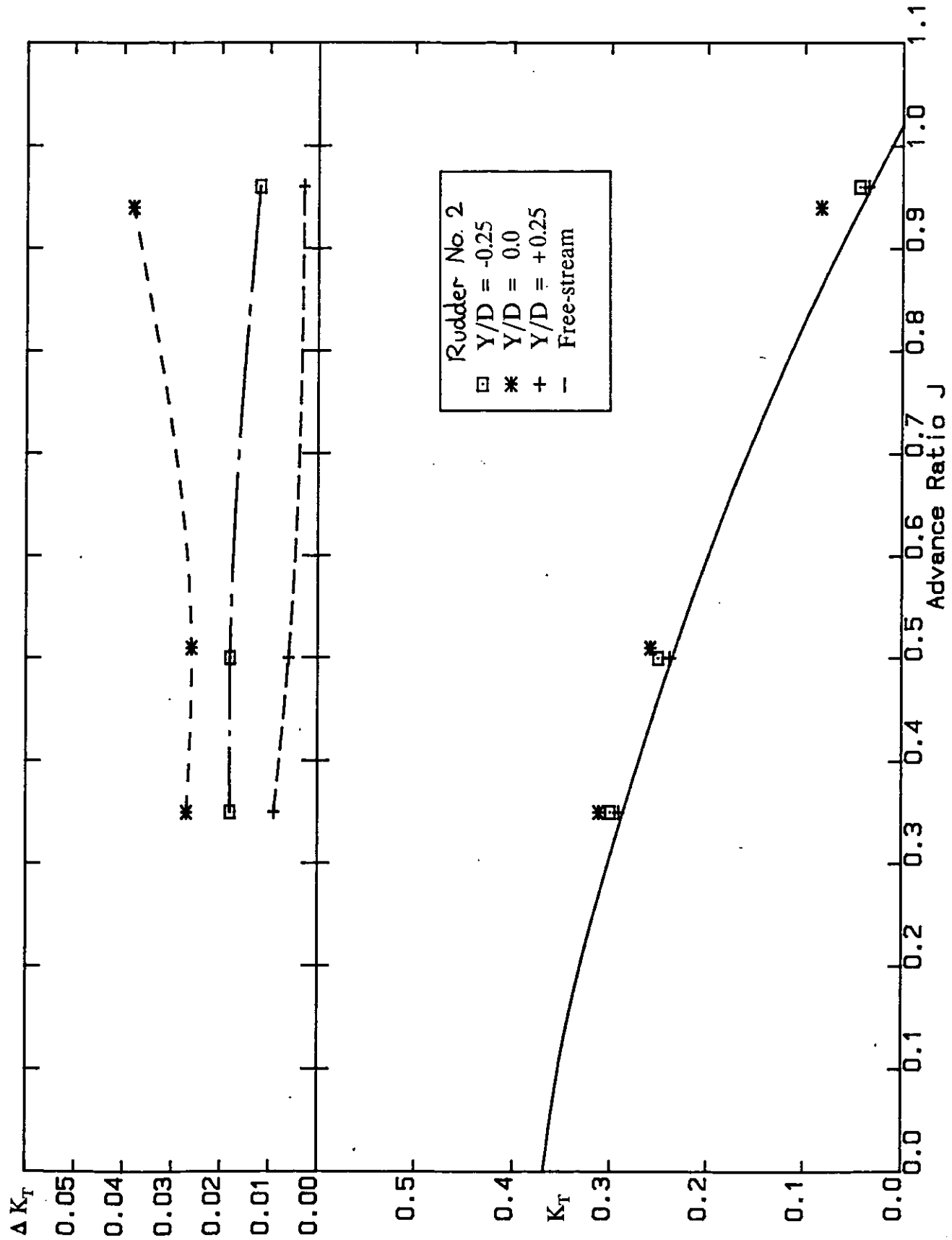

Figure 48 Comparison of propeller thrust and thrust increment against advance ratio for a lateral separation of rudder and propeller of Y/D = -0.25, 0.0, +0.25.

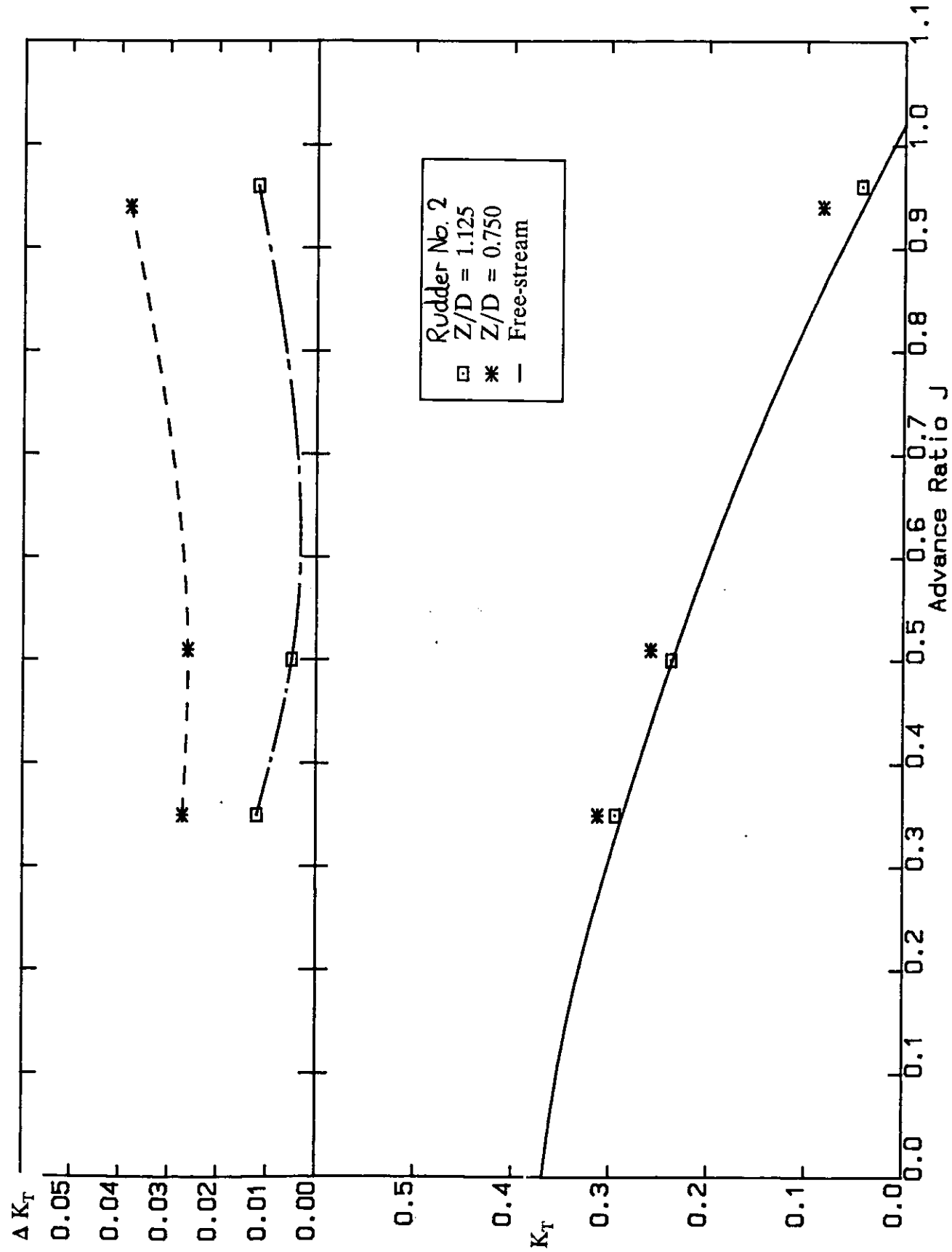

Figure 49 Comparison of propeller thrust and thrust increment against advance ratio for propeller axis heights of 600mm and 900mm.

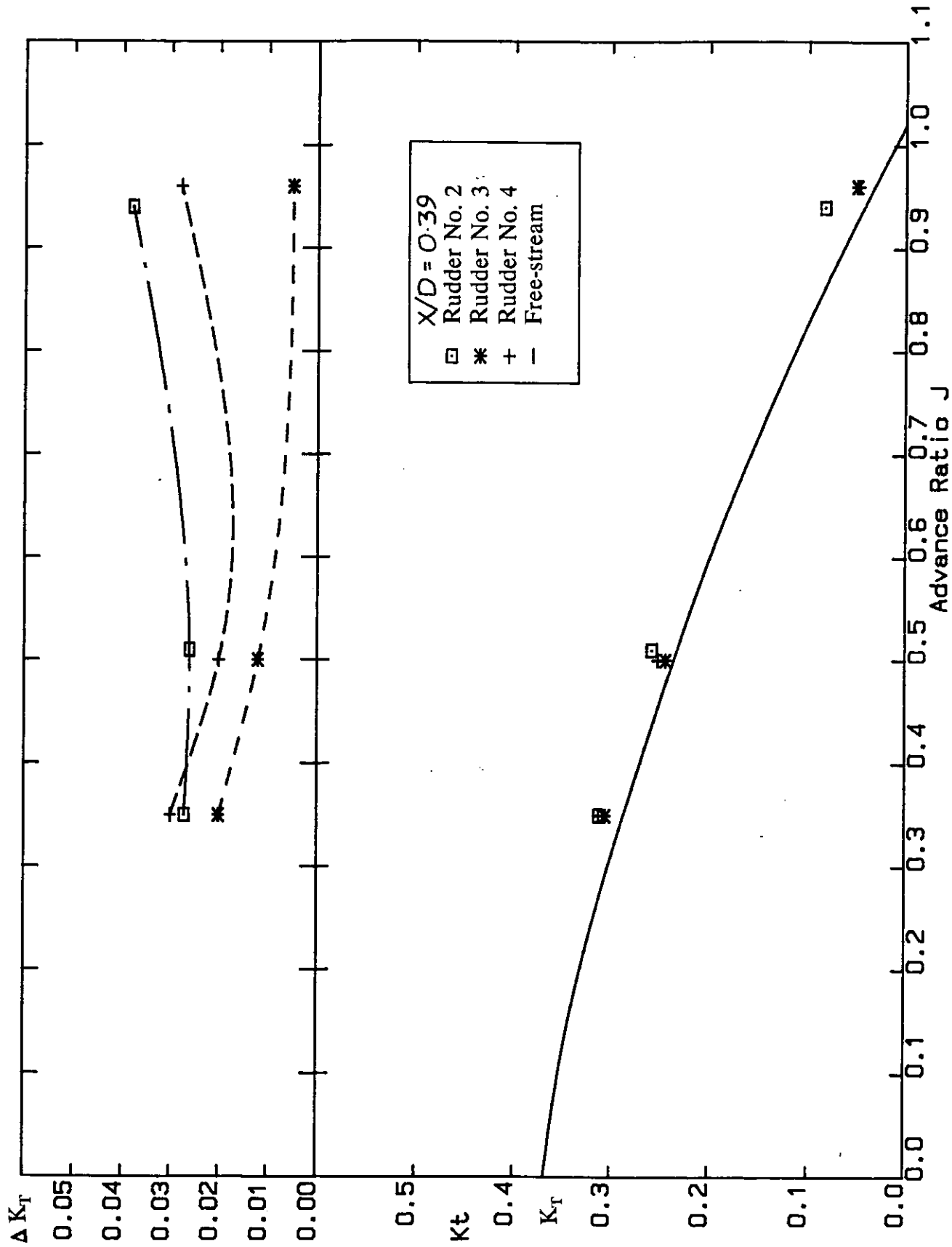

Figure 50 Comparison of propeller thrust and thrust increment against advance ratio for all-movable rudder no's 2, 3 and 4.

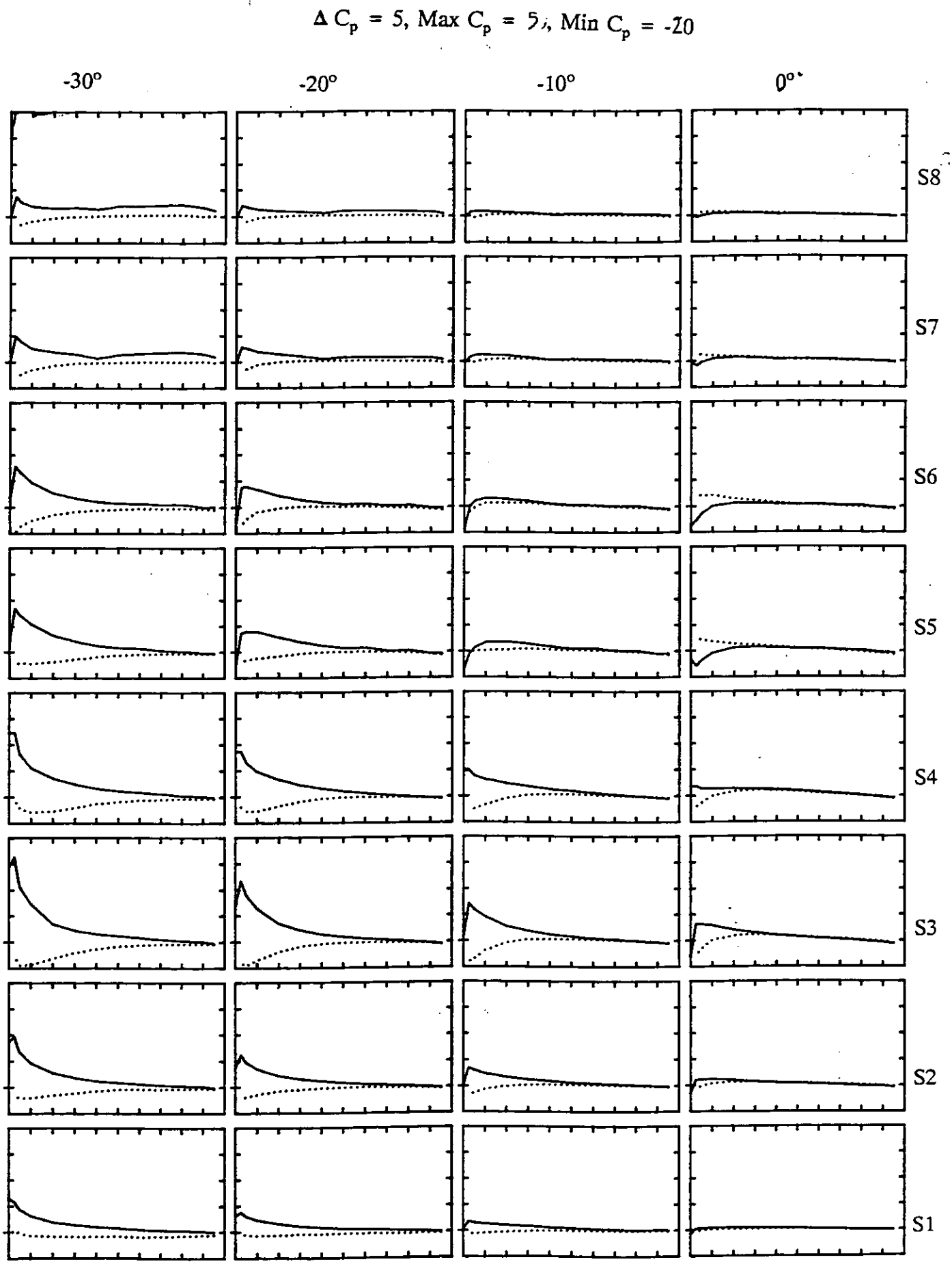

Figure 51 Chordwise pressure distributions at 8 spanwise positions for all-movable rudder no. 2 at J=0.42 and P/D=0.69 for rudder incidences of -30.4°, -20.4°, -10.4°, -0.4°, 9.6°, 19.6° and 29.6°.

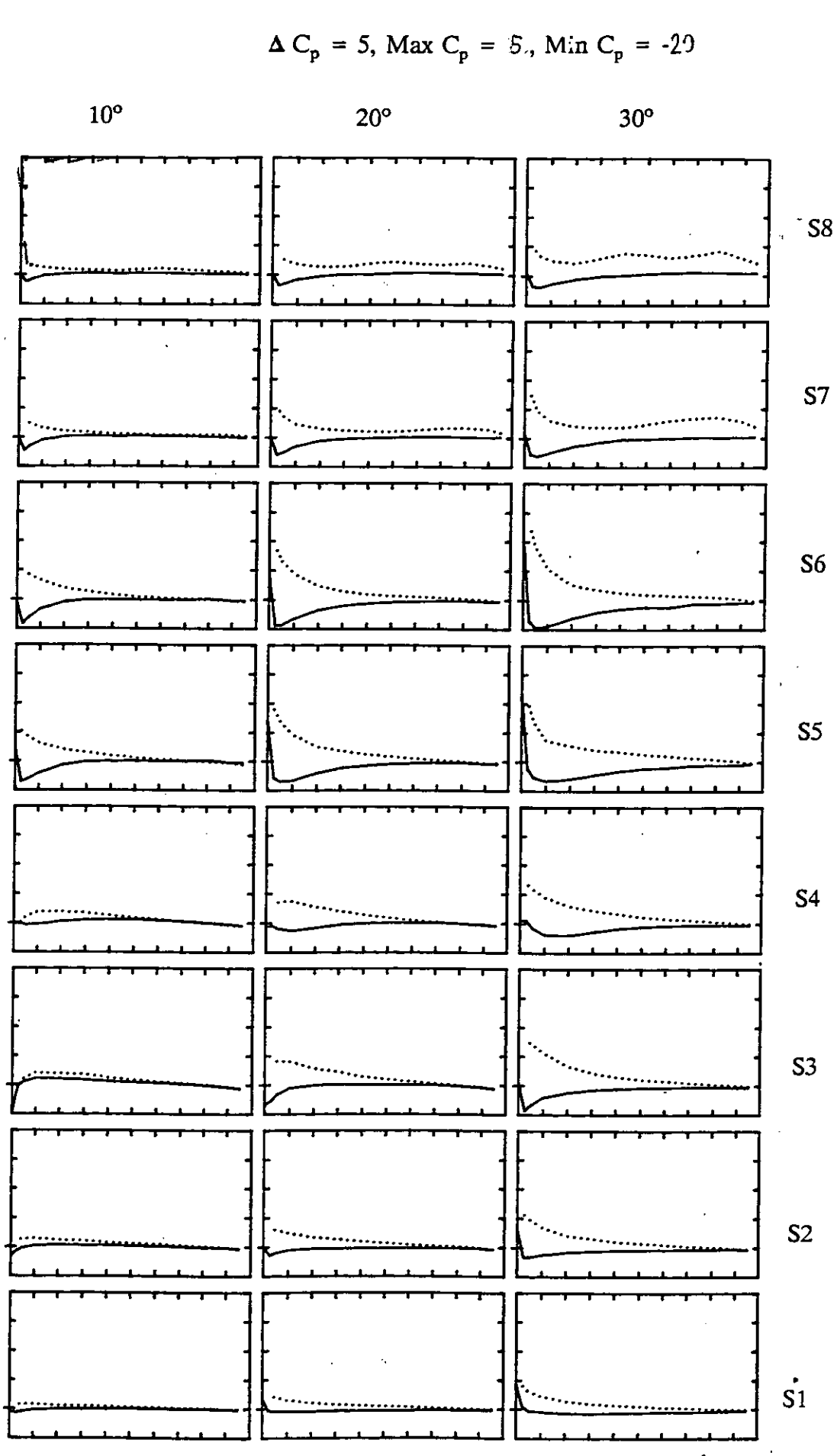

Figure 51 Chordwise pressure distributions at 8 spanwise positions for all-movable rudder no. 2 at J=0.42 and P/D=0.69 for rudder incidences of -30.4°, -20.4°, -10.4°, -0.4°, 9.6°, 19.6°, and 29.6°.

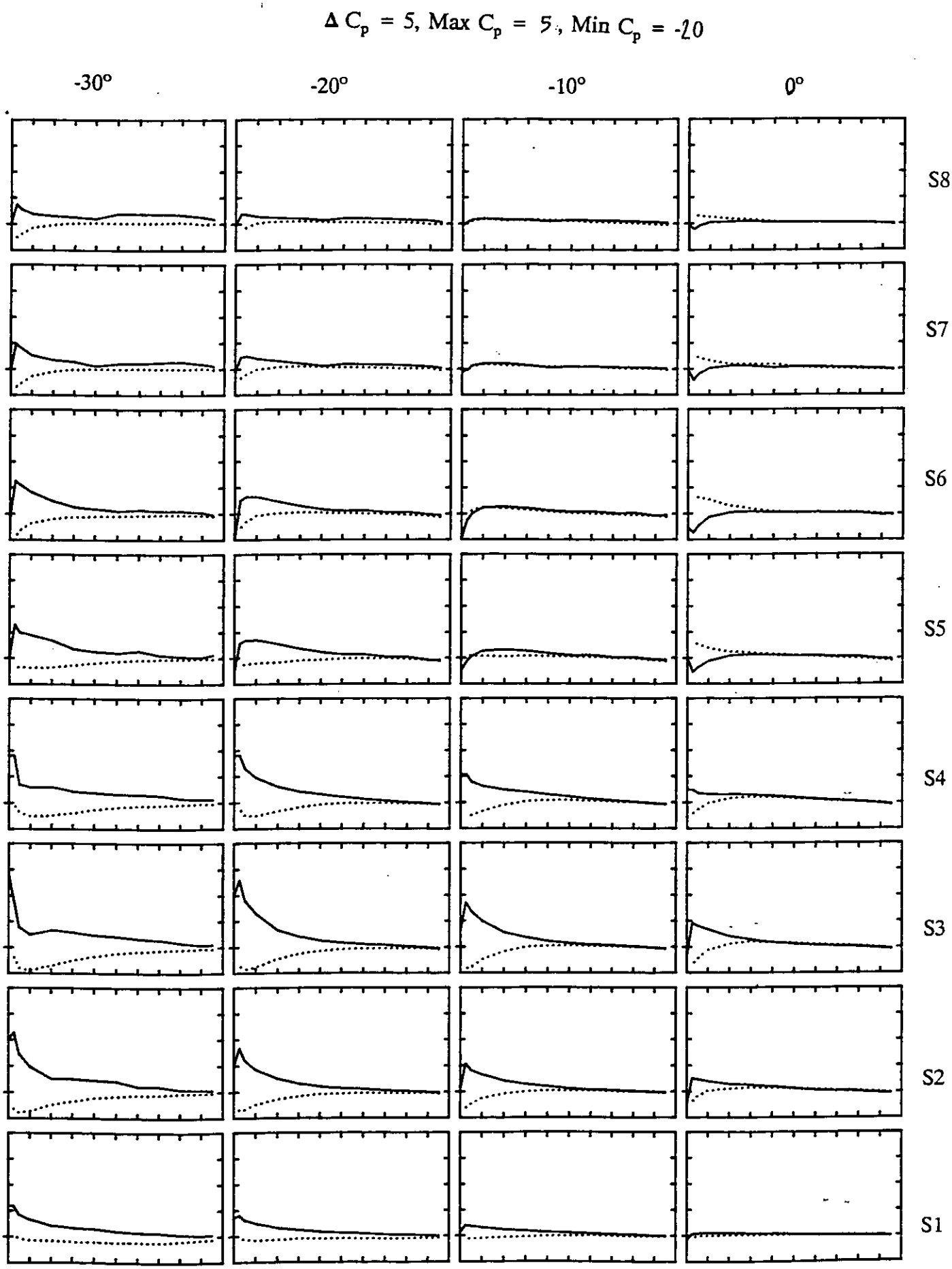

Figure 52 Chordwise pressure distributions at 8 spanwise positions for all-movable rudder no. 2 at J=0.61 and P/D=1.34 for rudder incidences of -30.4°, -20.4°, -10.4°, -0.4°, 9.6°, 19.6° and 29.6°.

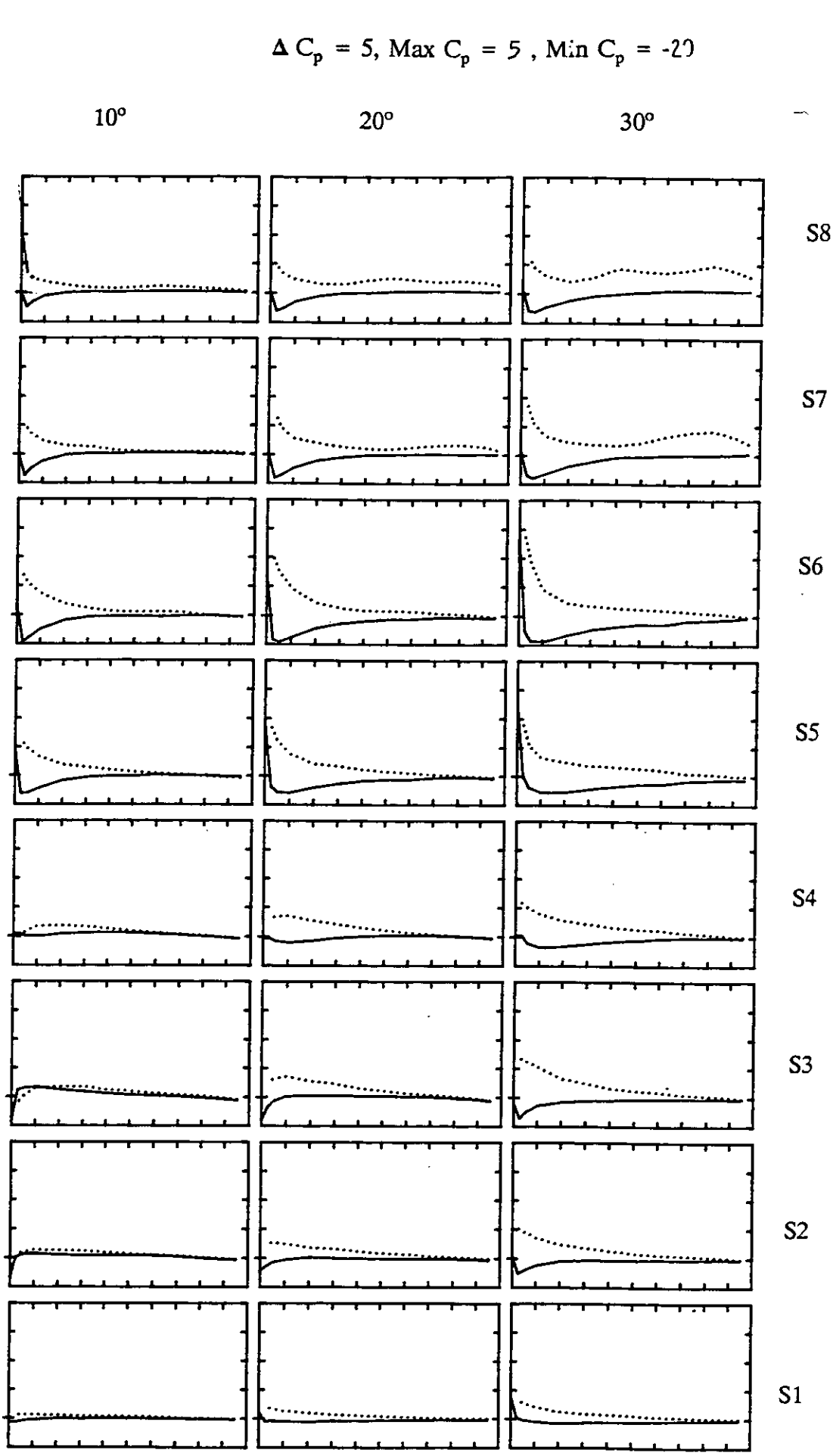

Figure 52 Chordwise pressure distributions at 8 spanwise positions for all-movable rudder no. 2 at J=0.61 and P/D=1.34 for rudder incidences of -30.4°, -20.4°, -10.4°, -0.4°, 9.6°, 19.6°, and 29.6°.

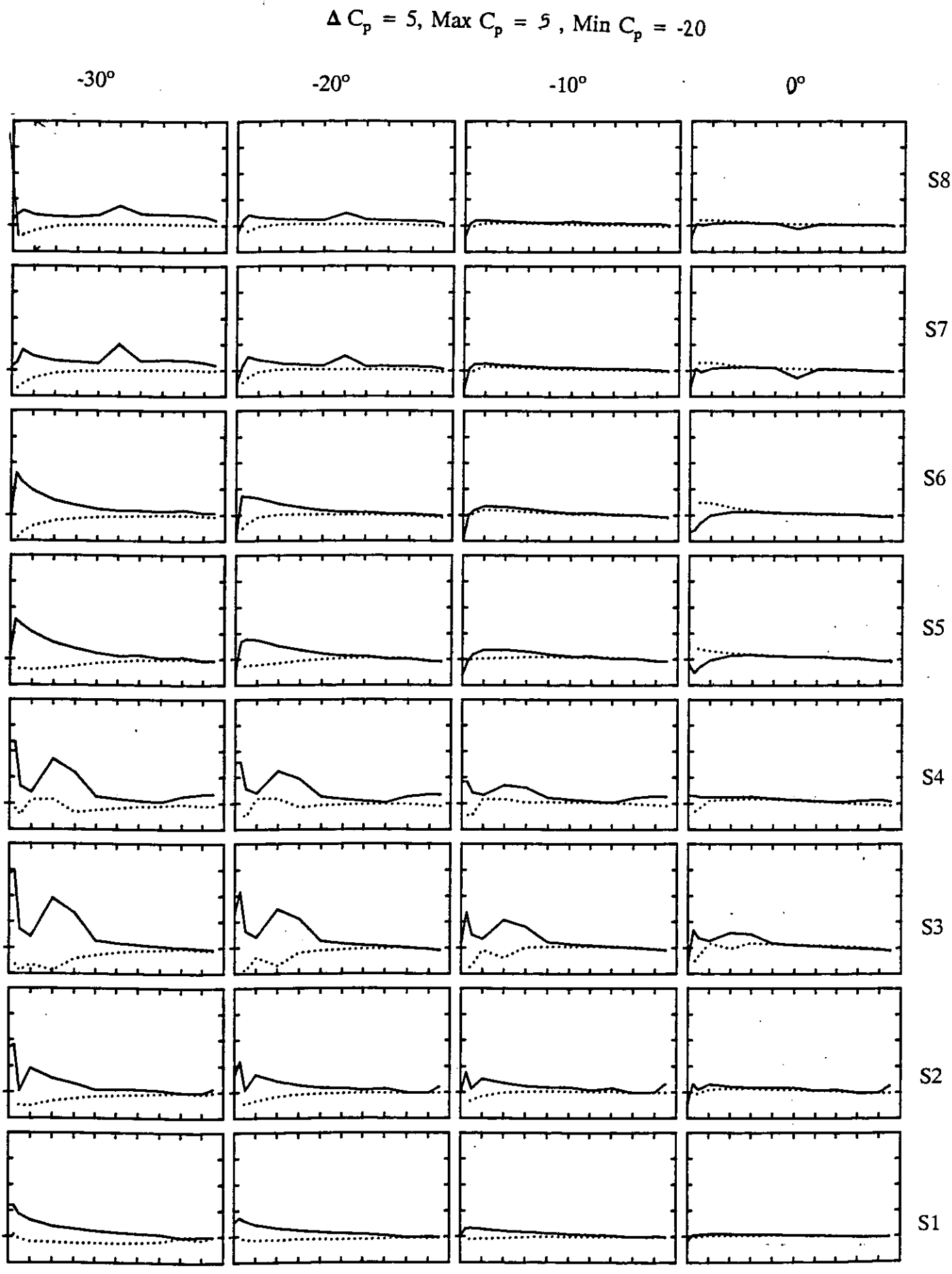

Figure 53 Chordwise pressure distributions at 8 spanwise positions for all-movable rudder no. 5 at J=0.51 for rudder incidences of -30.4°, -20.4°, -10.4°, -0.4°, 9.6°, 19.6°, and 29.6°.

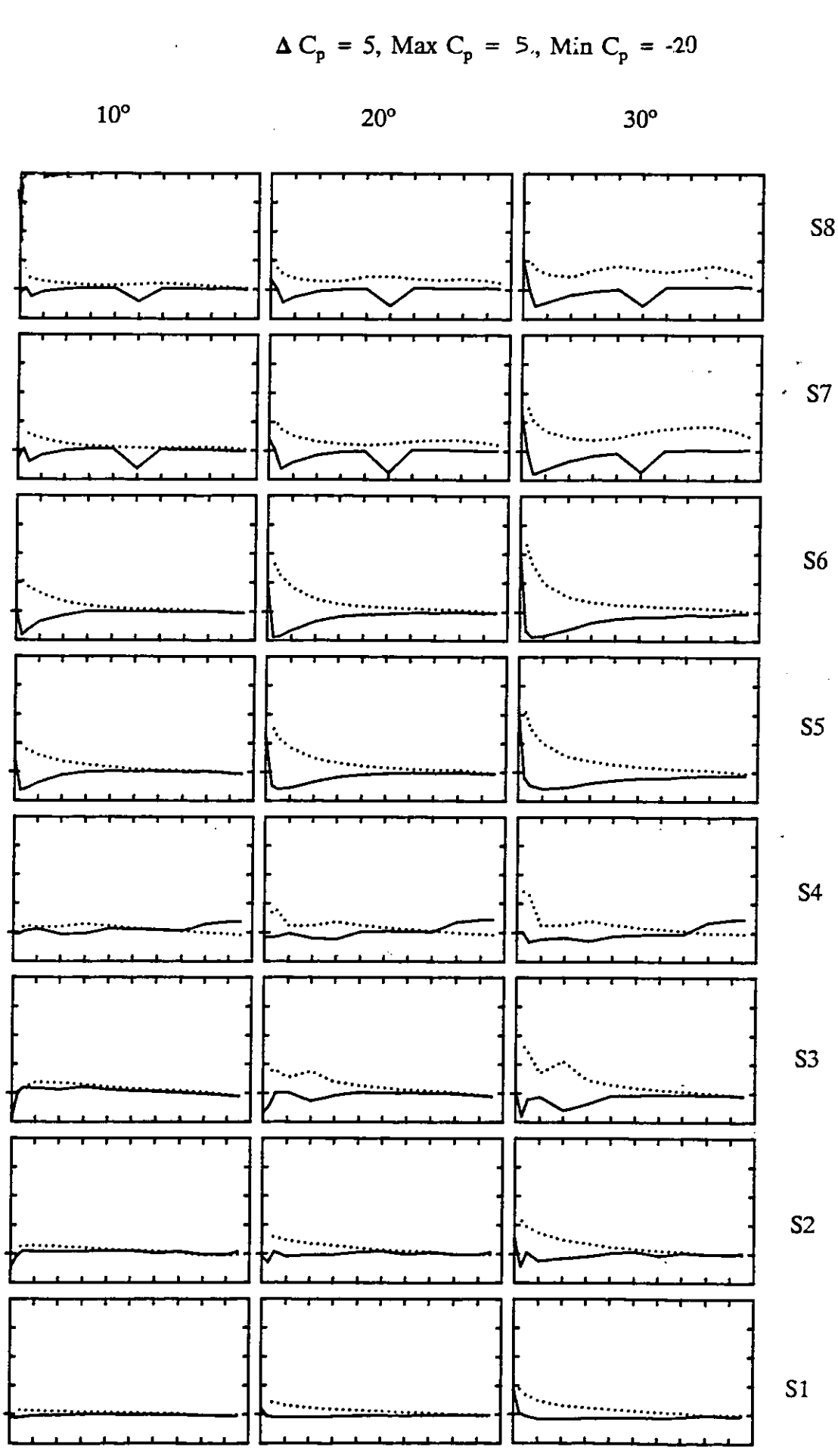

Figure 53 Chordwise pressure distributions at 8 spanwise positions for all-movable rudder no. 5 at J=0.51 for rudder incidences of -30.4°, -20.4°, -10.4°, -0.4°, 9.6°, 19.6°, and 29.6°.

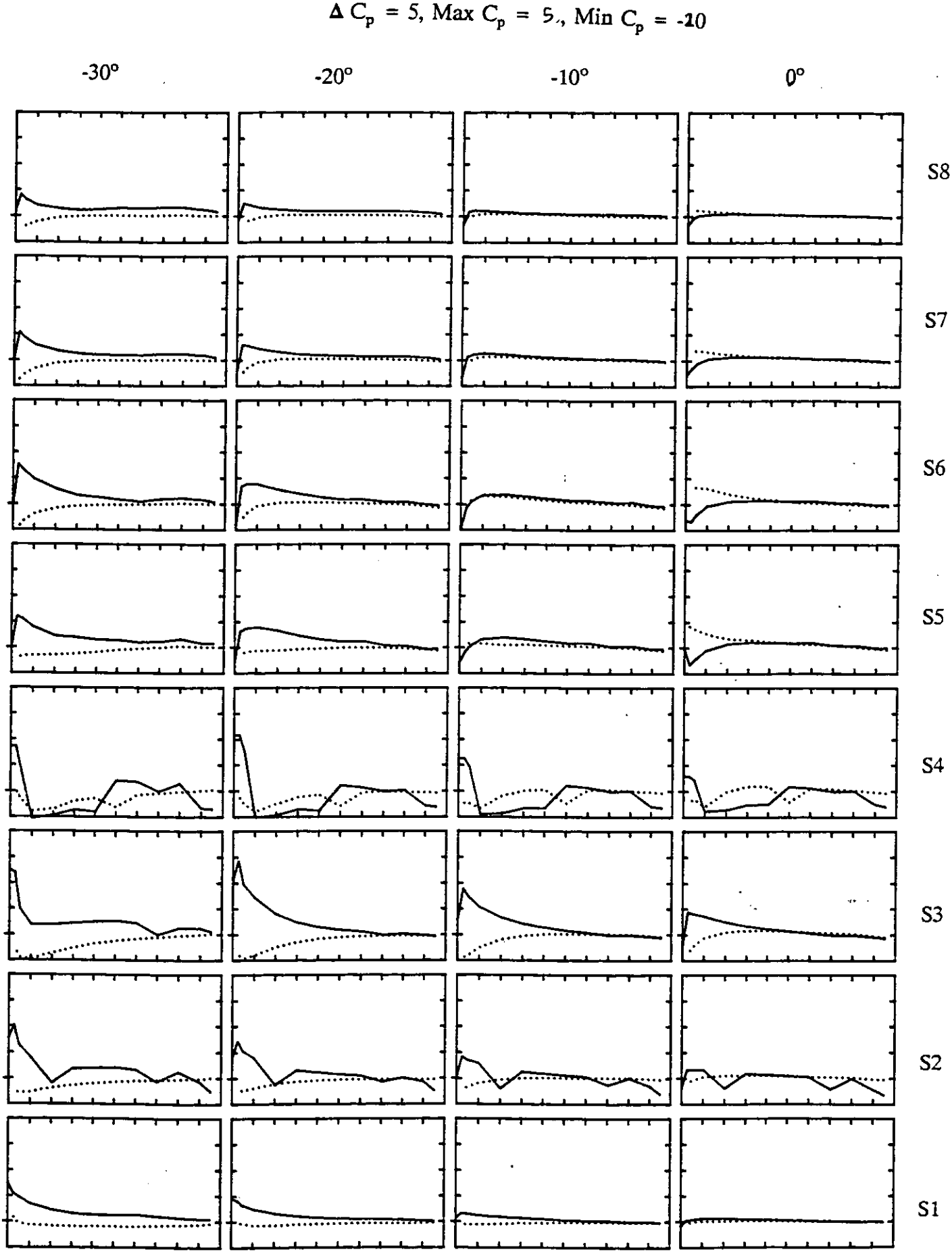

Figure 54 Chordwise pressure distributions at 8 spanwise positions for all-movable rudder no. 6 at J=0.51 for rudder incidences of -30.4°, -20.4°, -10.4°, -0.4°, 9.6°, 19.6°, and 29.6°.

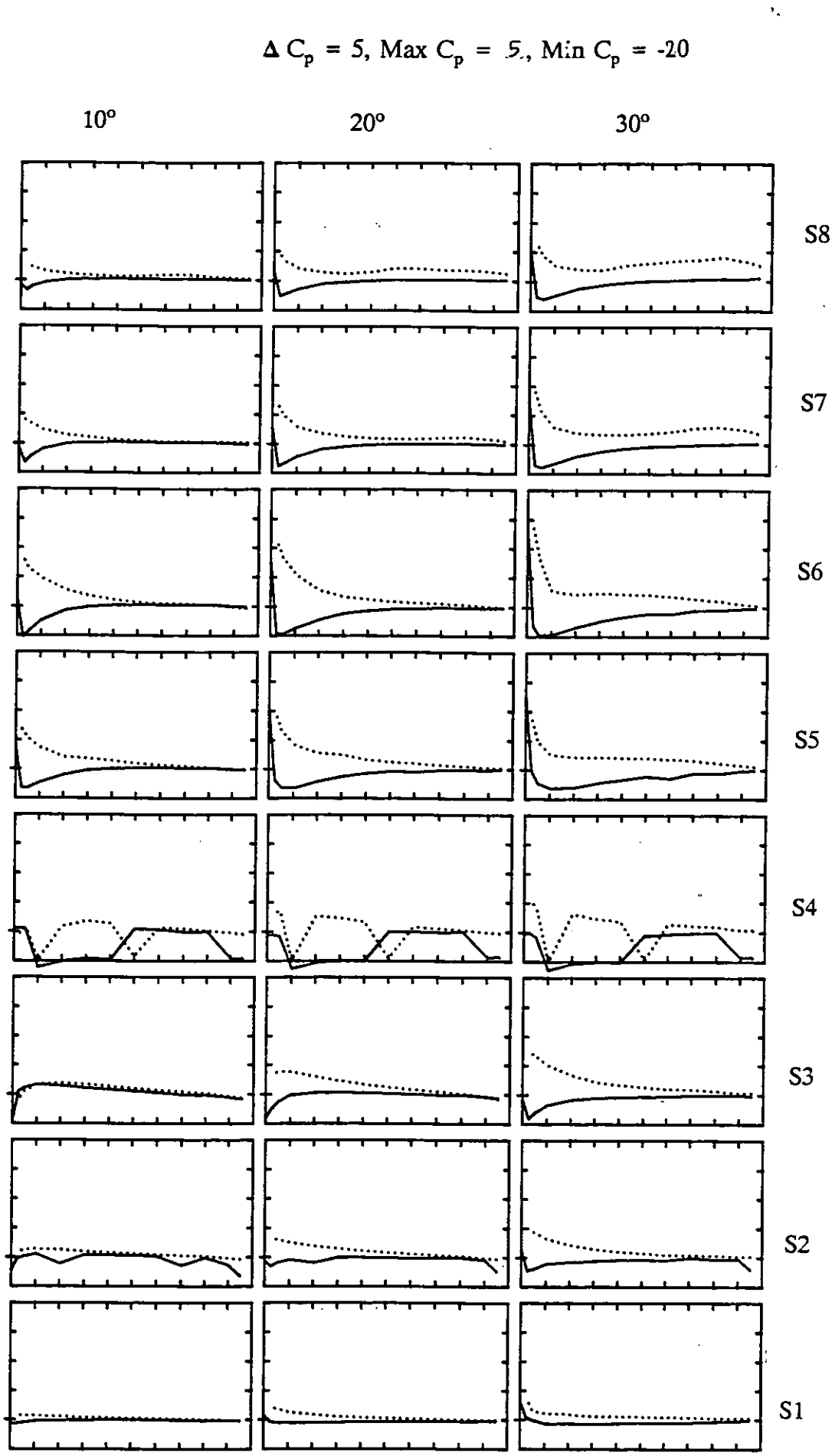

Figure 54 Chordwise pressure distributions at 8 spanwise positions for all-movable rudder no. 6 at J=0.51 for rudder incidences of -30.4°, -20.4°, -10.4°, -0.4°, 9.6°, 19.6°, and 29.6°.

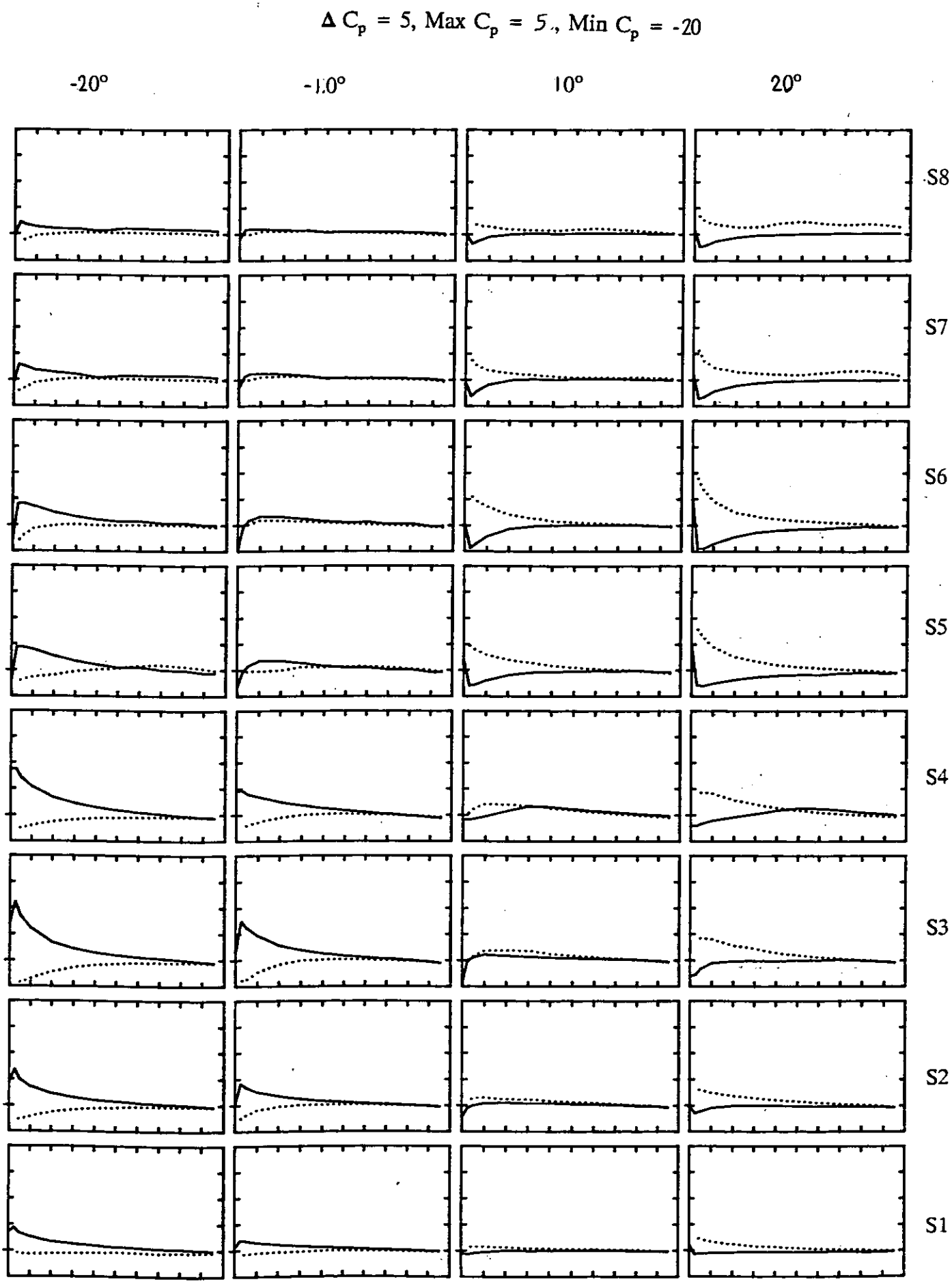

Figure 55 Chordwise pressure distributions at 8 spanwise positions for all-movable rudder no. 2 with the rudder stock at 54% chord and at J=0.51 for rudder incidences of , -20.4°, -10.4°, 9.6° ,19.6°.

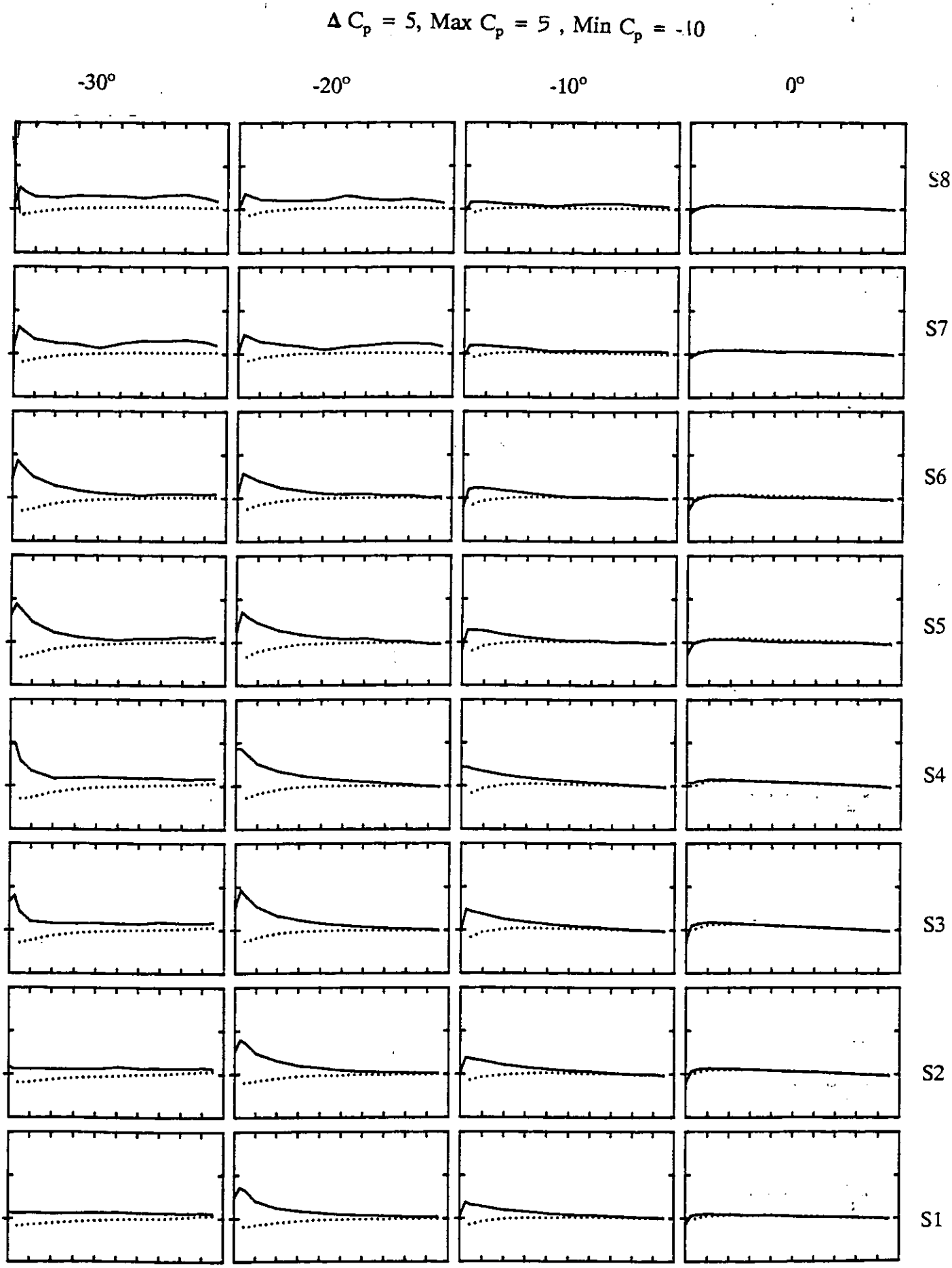

Figure 56 Chordwise pressure distributions at 8 spanwise positions for all-movable rudder no. 2 with a lateral separation Y/D=-0.25 and at J=0.94 for rudder incidences of -30.4°, -20.4°, -10.4°, -0.4°, 9.6°, 19.6°, and 29.6°.

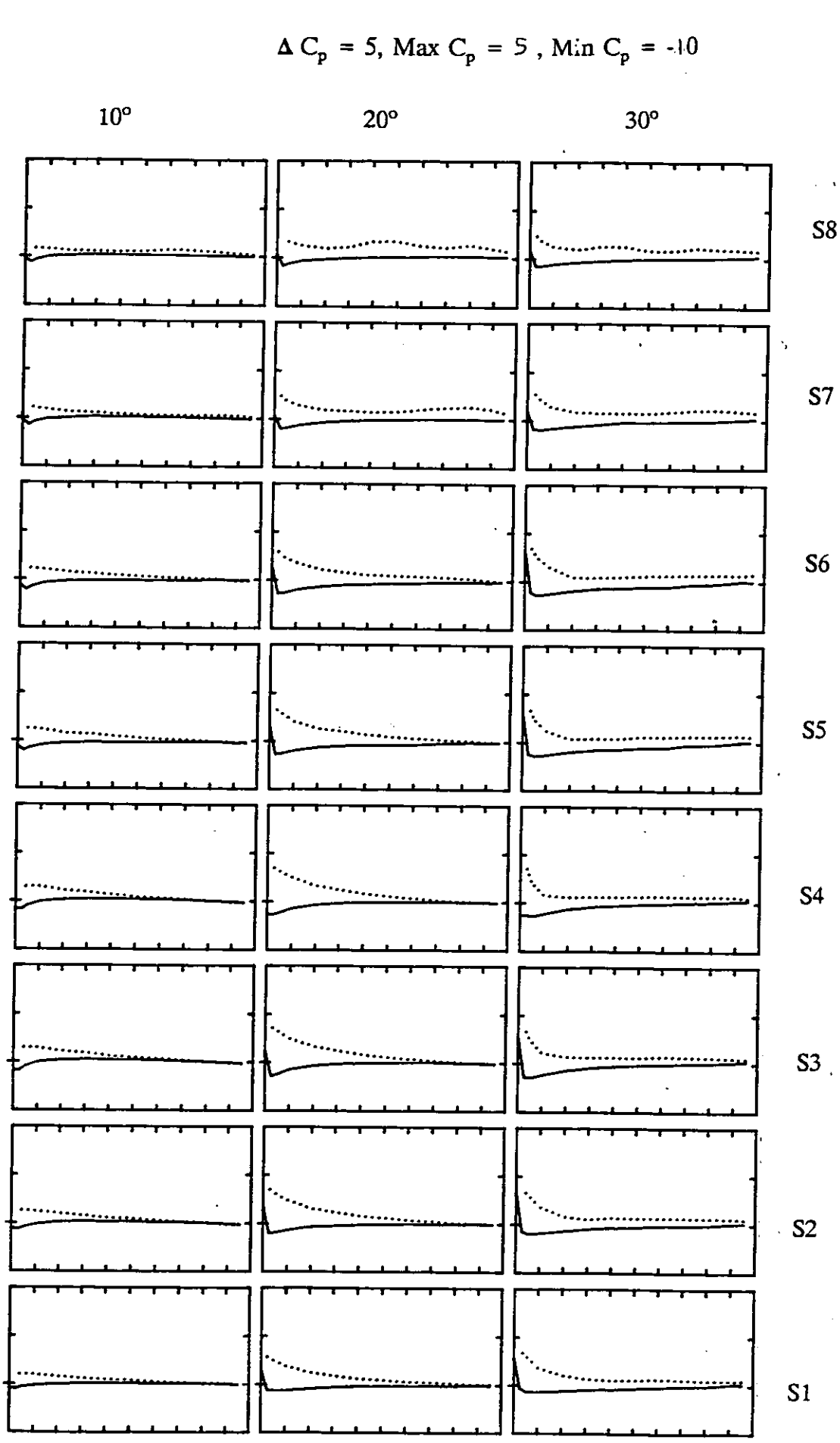

Figure 56 Chordwise pressure distributions at 8 spanwise positions for all-movable rudder no. 2 with a lateral separation Y/D=-0.25 and at J=0.94 for rudder incidences of -30.4°, -20.4°, -10.4°, -0.4°, 9.6°, 19.6°, and 29.6°.

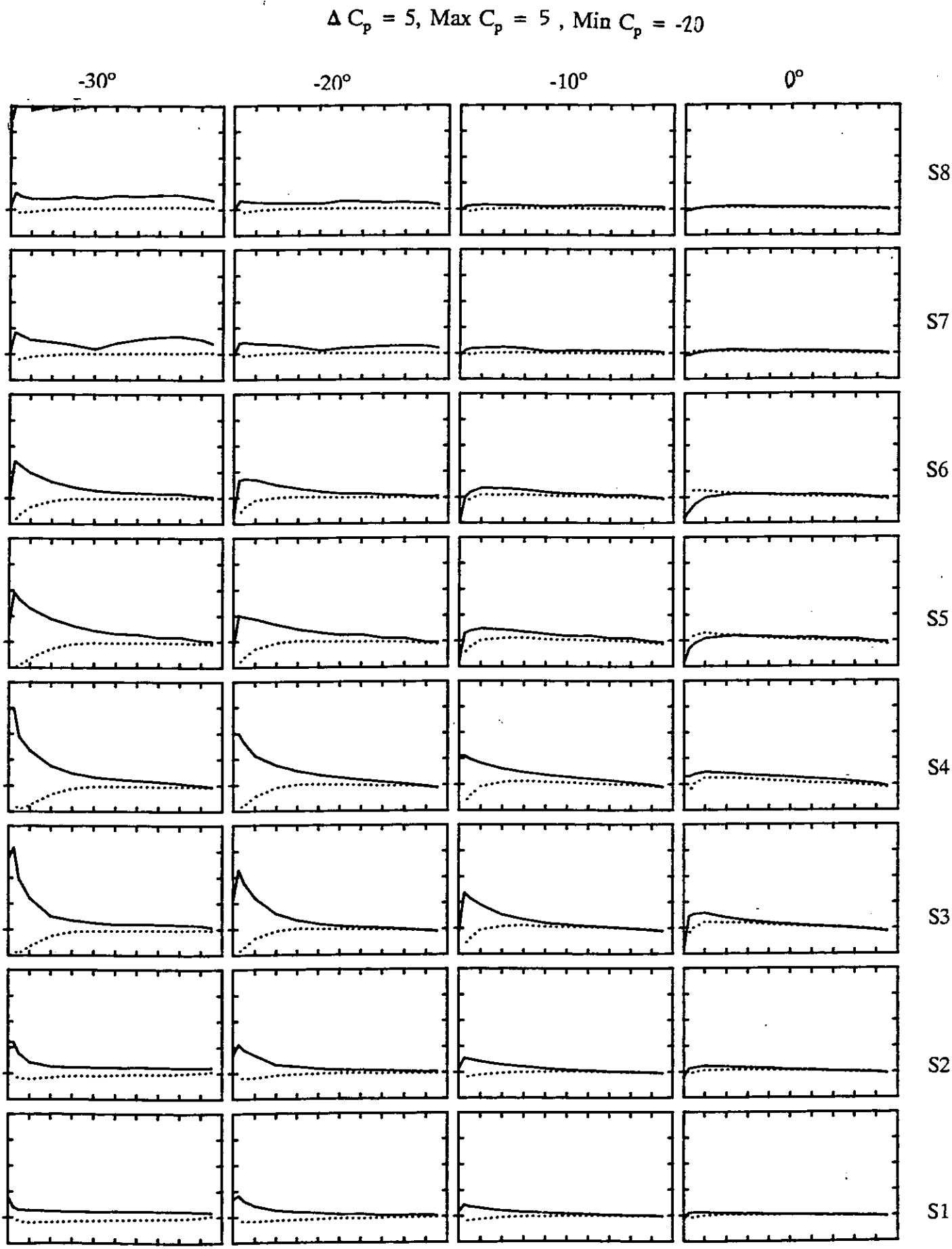

Figure 57 Chordwise pressure distributions at 8 spanwise positions for all-movable rudder no. 2 with a lateral separation Y/D=-0.25 and at J=0.51 for rudder incidences of -30.4°, -20.4°, -10.4°, -0.4°, 9.6°, 19.6°, and 29.6°.

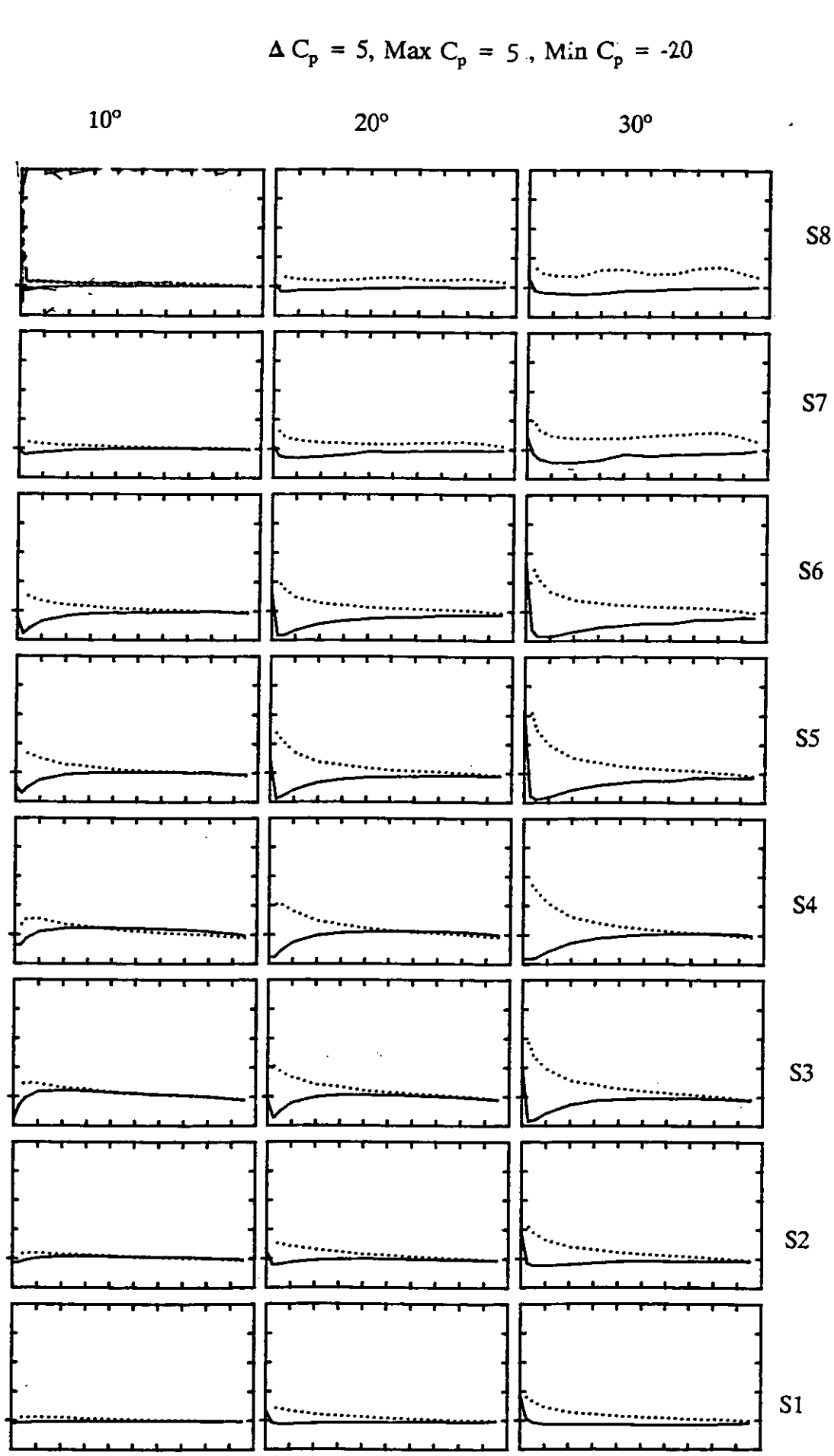

Figure 57 Chordwise pressure distributions at 8 spanwise positions for all-movable rudder no. 2 with a lateral separation Y/D=-0.25 and at J=0.51 for rudder incidences of -30.4°, -20.4°, -10.4°, -0.4°, 9.6°, 19.6°, and 29.6°.

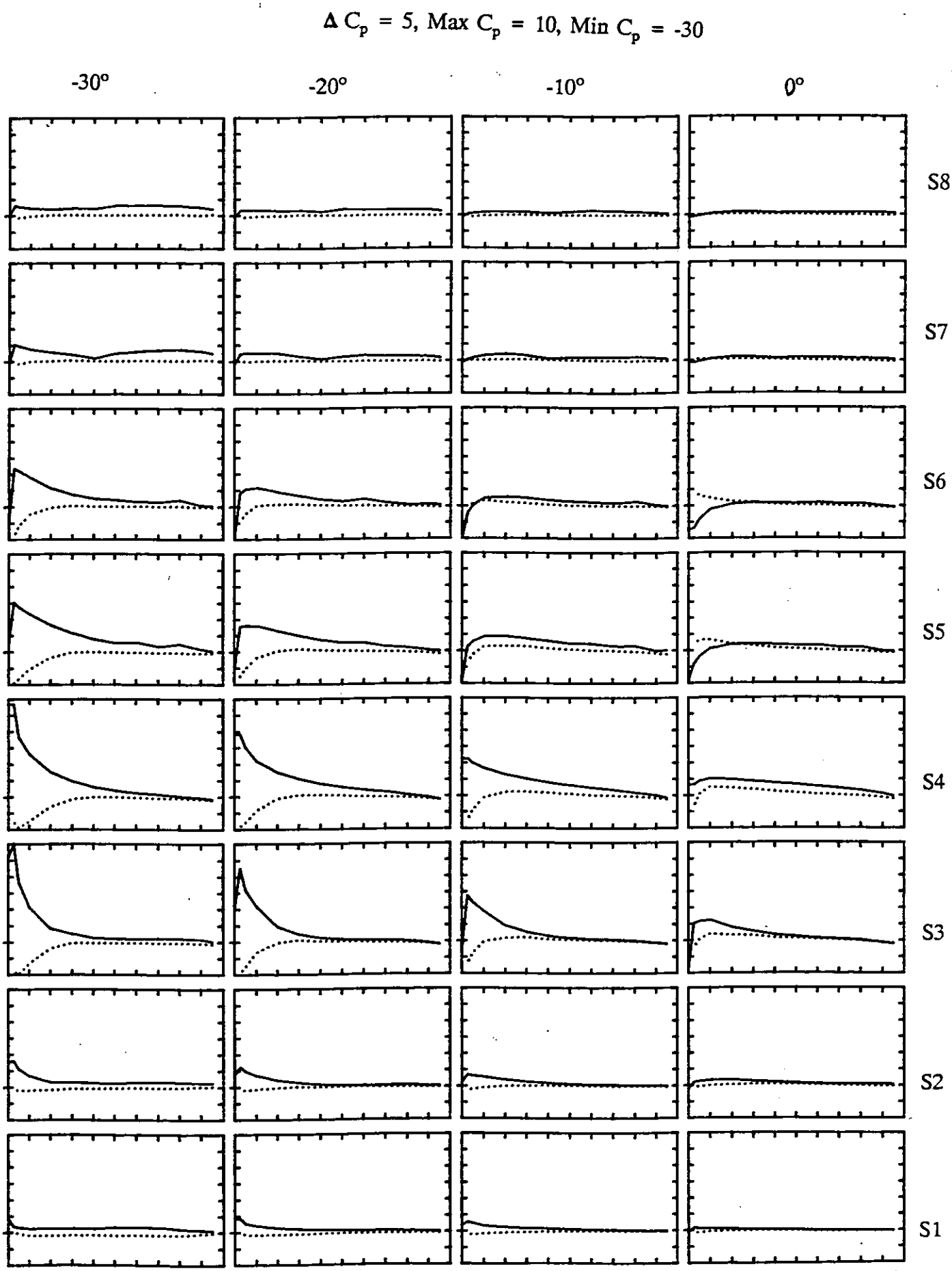

Figure 58 Chordwise pressure distributions at 8 spanwise positions for all-movable rudder no. 2 with a lateral separation Y/D = -0.25 and at J = 0.35 for rudder incidences of -30.4°, -20.4°, -10.4°, -0.4°, 9.6°, 19.6°, and 29.6°.

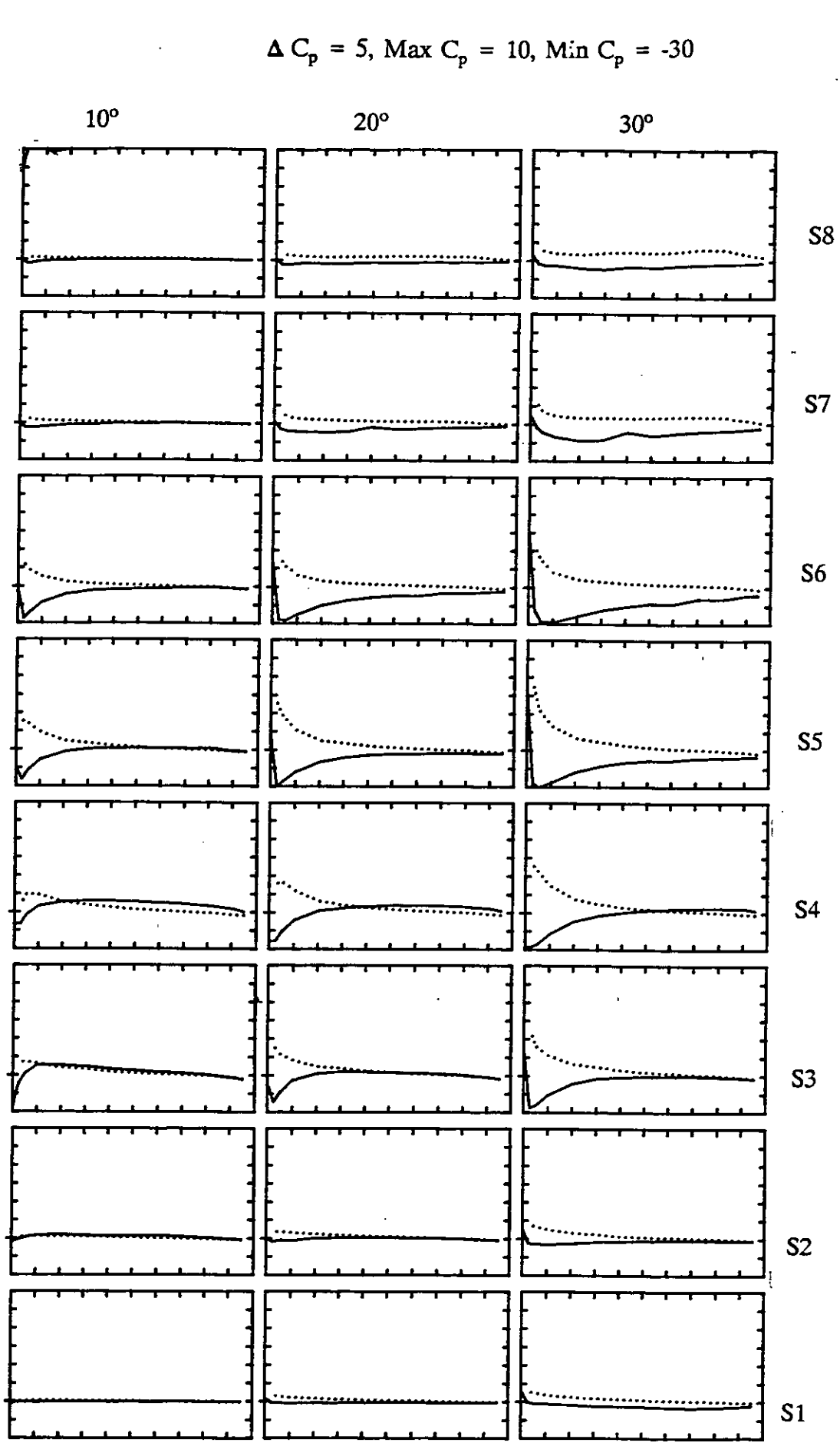

Figure 58 Chordwise pressure distributions at 8 spanwise positions for all-movable rudder no. 2 with a lateral separation Y/D = -0.25 and at J = 0.35 for rudder incidences of -30.4°, -20.4°, -10.4°, -0.4°, 9.6°, 19.6°, and 29.6°.

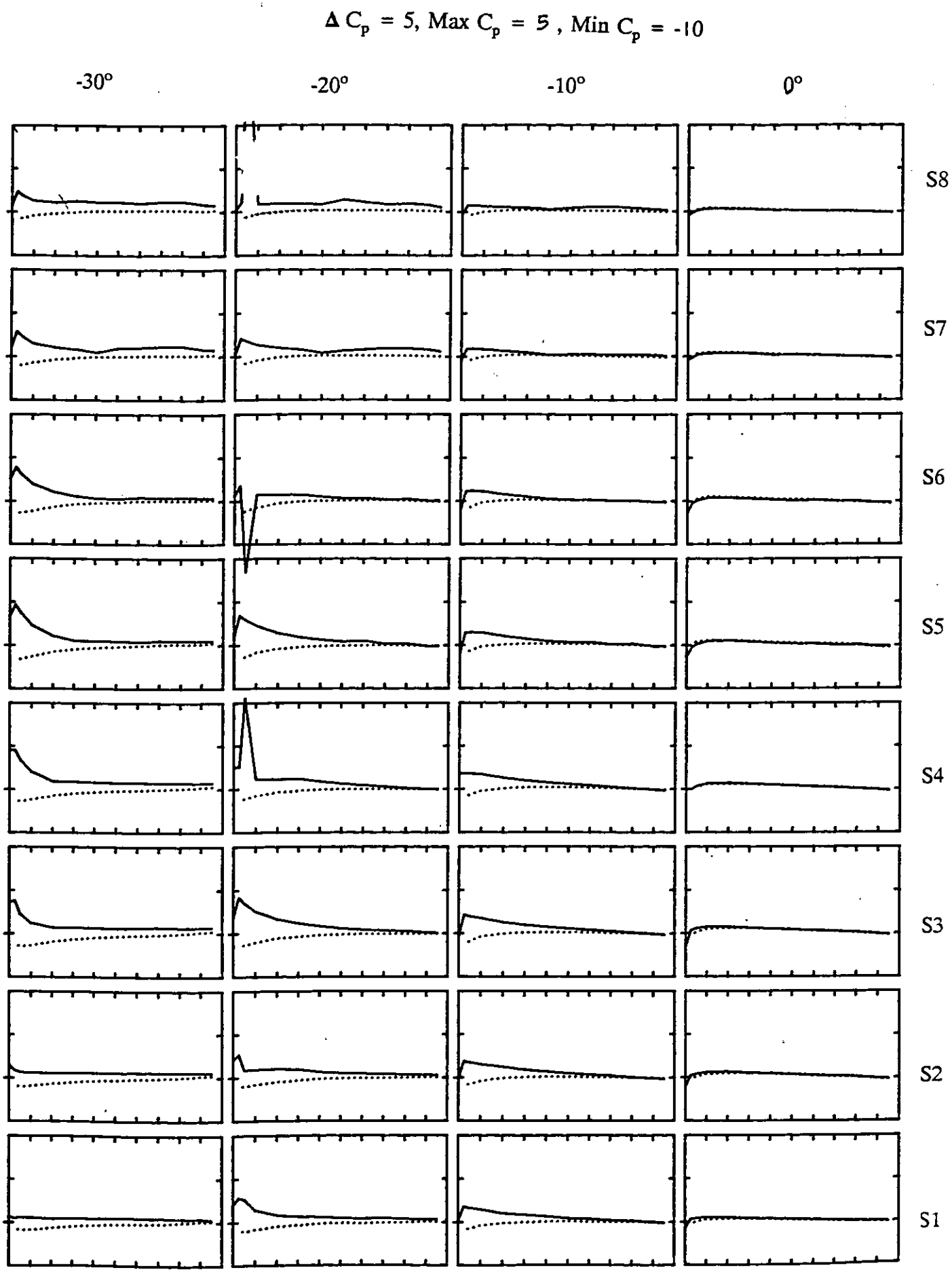

Figure 59 Chordwise pressure distributions at 8 spanwise positions for all-movable rudder no. 2 with a lateral separation Y/D=+0.25 and at J=0.94 for rudder incidences of -30.4°, -20.4°, -10.4°, -0.4°, 9.6°, 19.6°, and 29.6°.

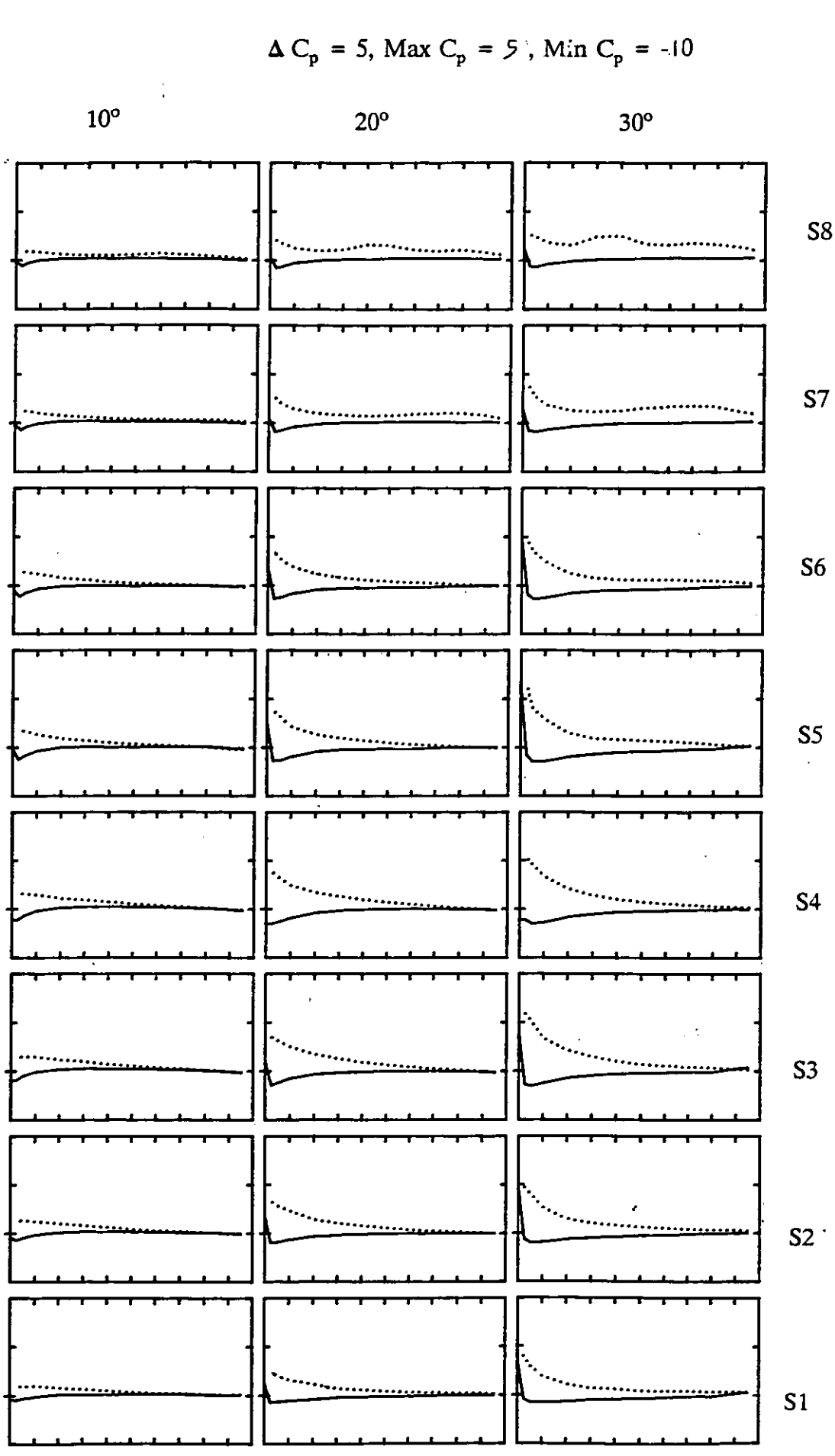

Figure 59 Chordwise pressure distributions at 8 spanwise positions for all-movable rudder no. 2 with a lateral separation Y/D = +0.25 and at J=0.94 for rudder incidences of -30.4°, -20.4°, -10.4°, -0.4°, 9.6°, 19.6°, and 29.6°.

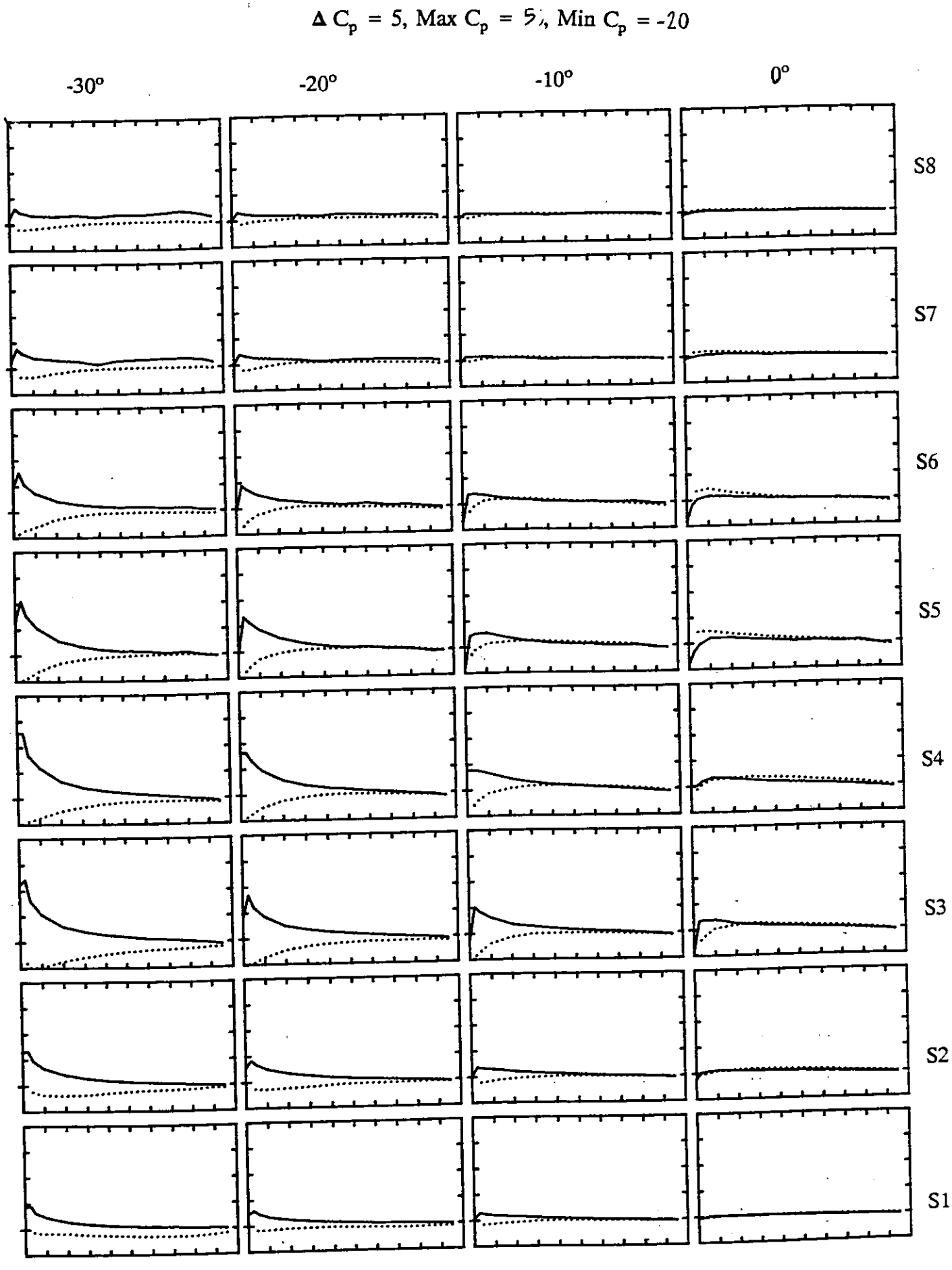

Figure 60 Chordwise pressure distributions at 8 spanwise positions for all-movable rudder no. 2 with a lateral separation Y/D = +0.25 and at J=0.51 for rudder incidences of -30.4°, -20.4°, -10.4°, -0.4°, 9.6°, 19.6°, and 29.6°.

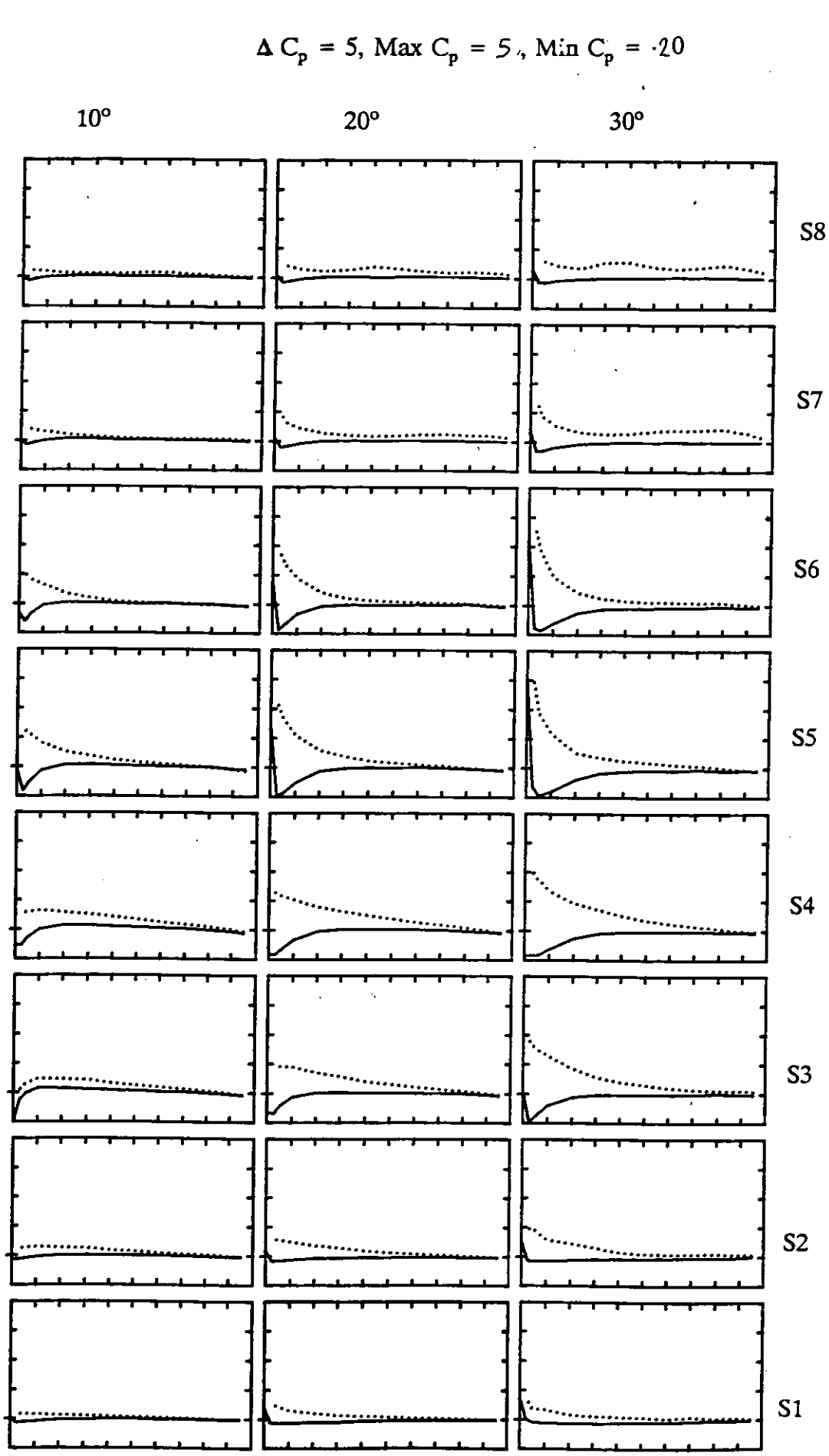

Figure 60 Chordwise pressure distributions at 8 spanwise positions for all-movable rudder no. 2 with a lateral separation Y/D=+0.25 and at J=0.51 for rudder incidences of -30.4°, -20.4°, -10.4°, -0.4°, 9.6°, 19.6°, and 29.6°.

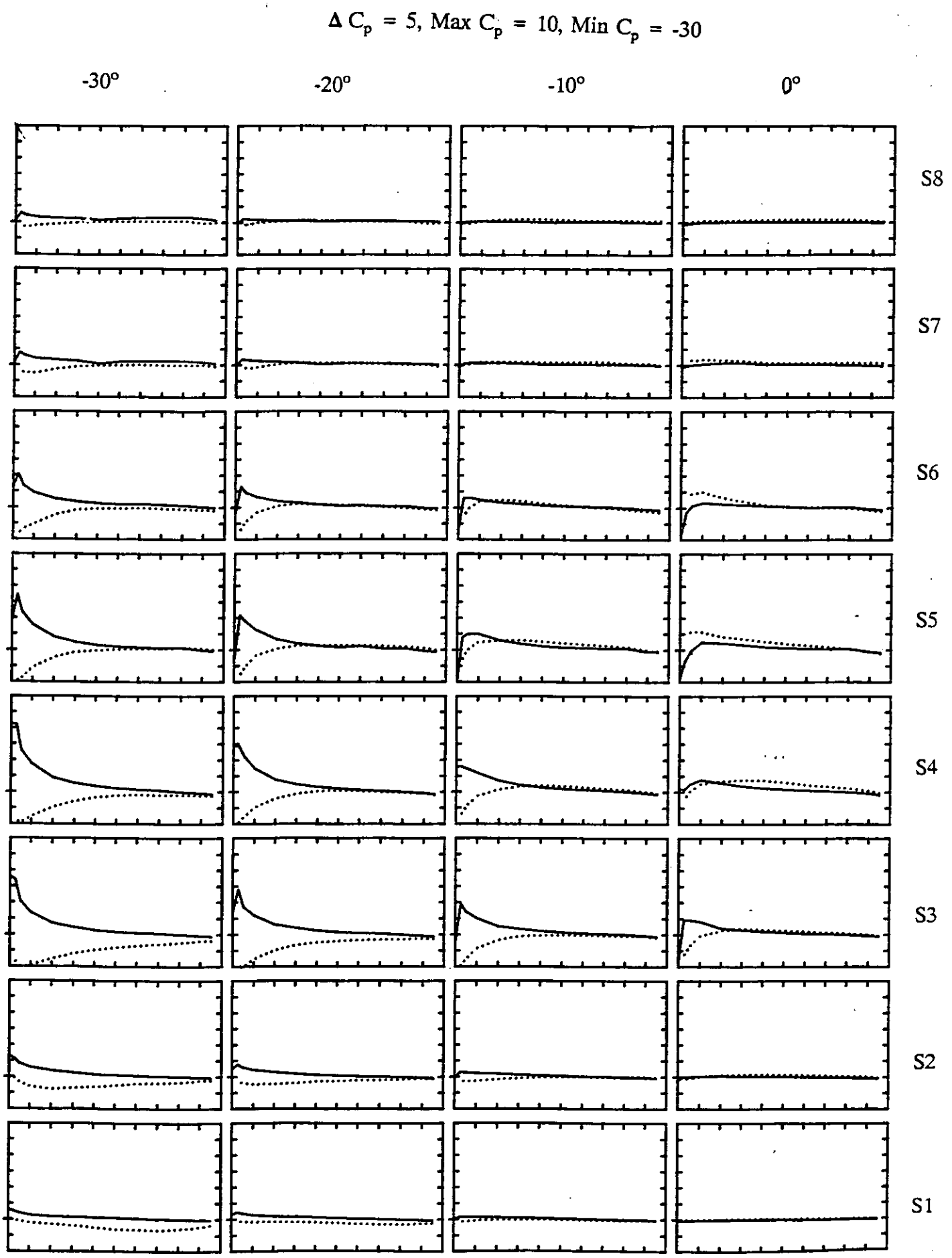

Figure 61 Chordwise pressure distributions at 8 spanwise positions for all-movable rudder no. 2 with a lateral separation Y/D = +0.25 and at J=0.35 for rudder incidences of -30.4°, -20.4°, -10.4°, -0.4°, 9.6°, 19.6°, and 29.6°.

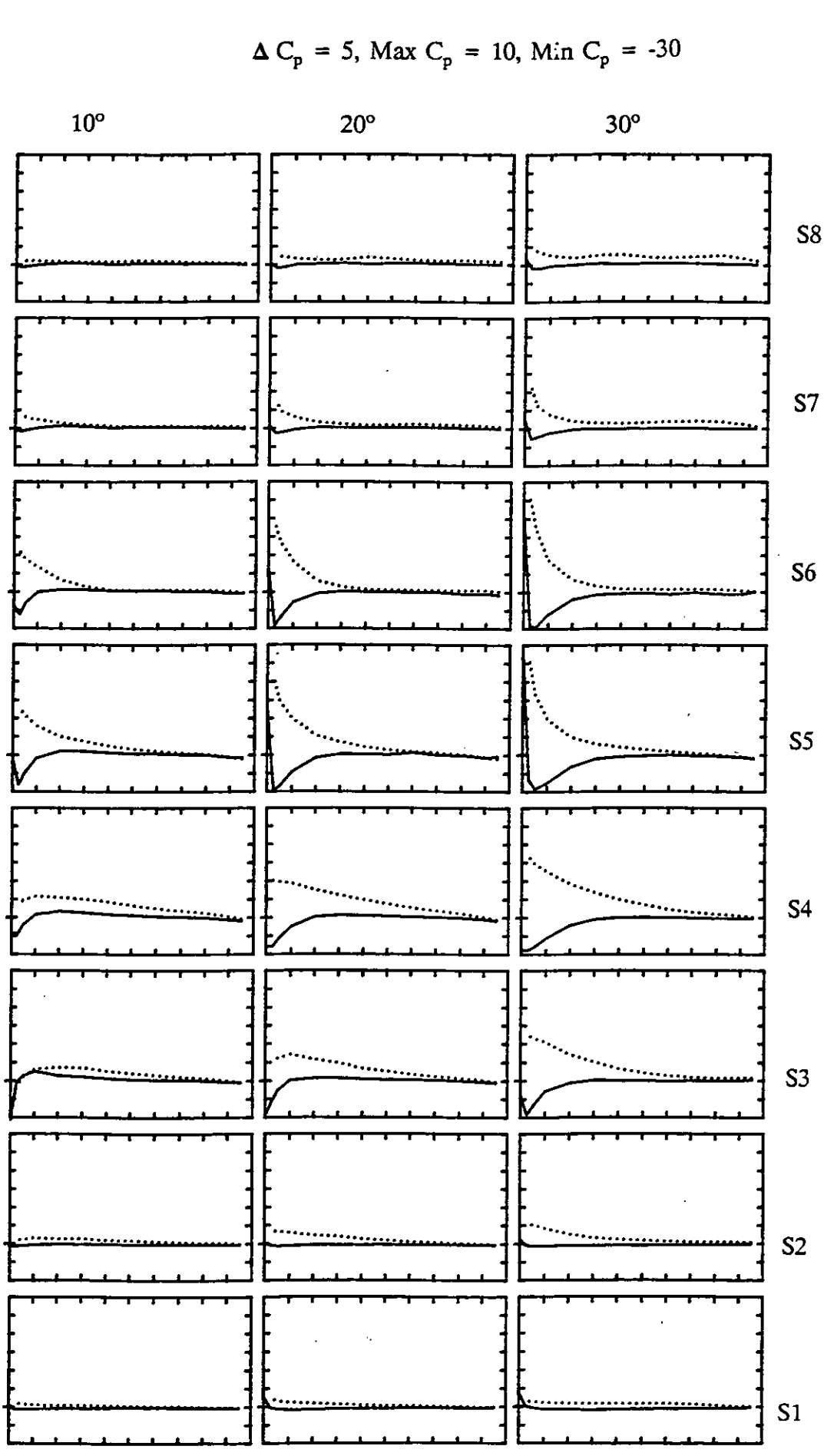

Figure 61 Chordwise pressure distributions at 8 spanwise positions for all-movable rudder no. 2 with a lateral separation Y/D=+0.25 and at J=0.35 for rudder incidences of -30.4°, -20.4°, -10.4°, -0.4°, 9.6°, 19.6°, and 29.6°.

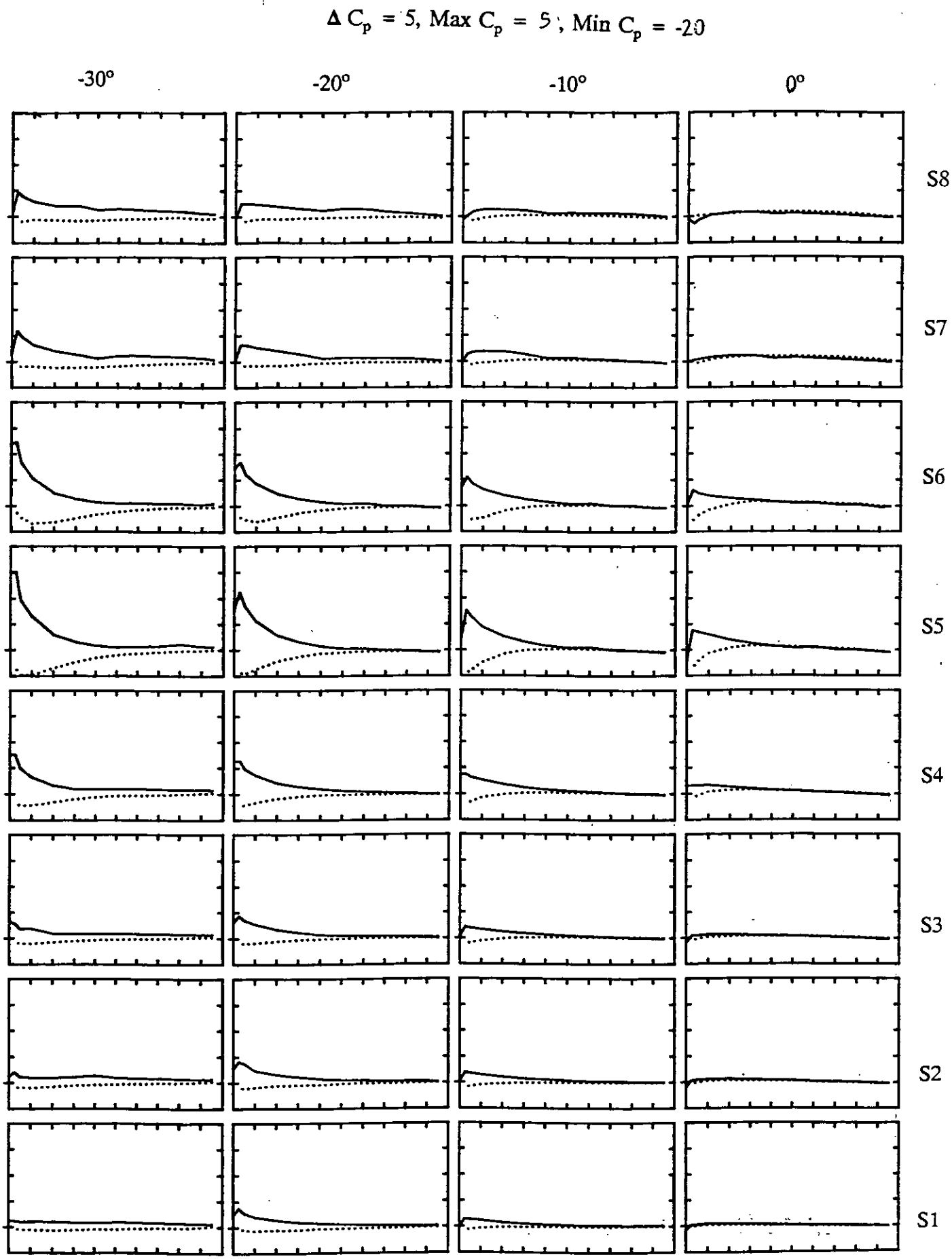

Figure 62 Chordwise pressure distributions at 8 spanwise positions for all-movable rudder no. 2 with a propeller axis height of 900mm and at J=0.51 for rudder incidences of -30.4°, -20.4°, -10.4°, -0.4°, 9.6°, 19.6°, and 29.6°.

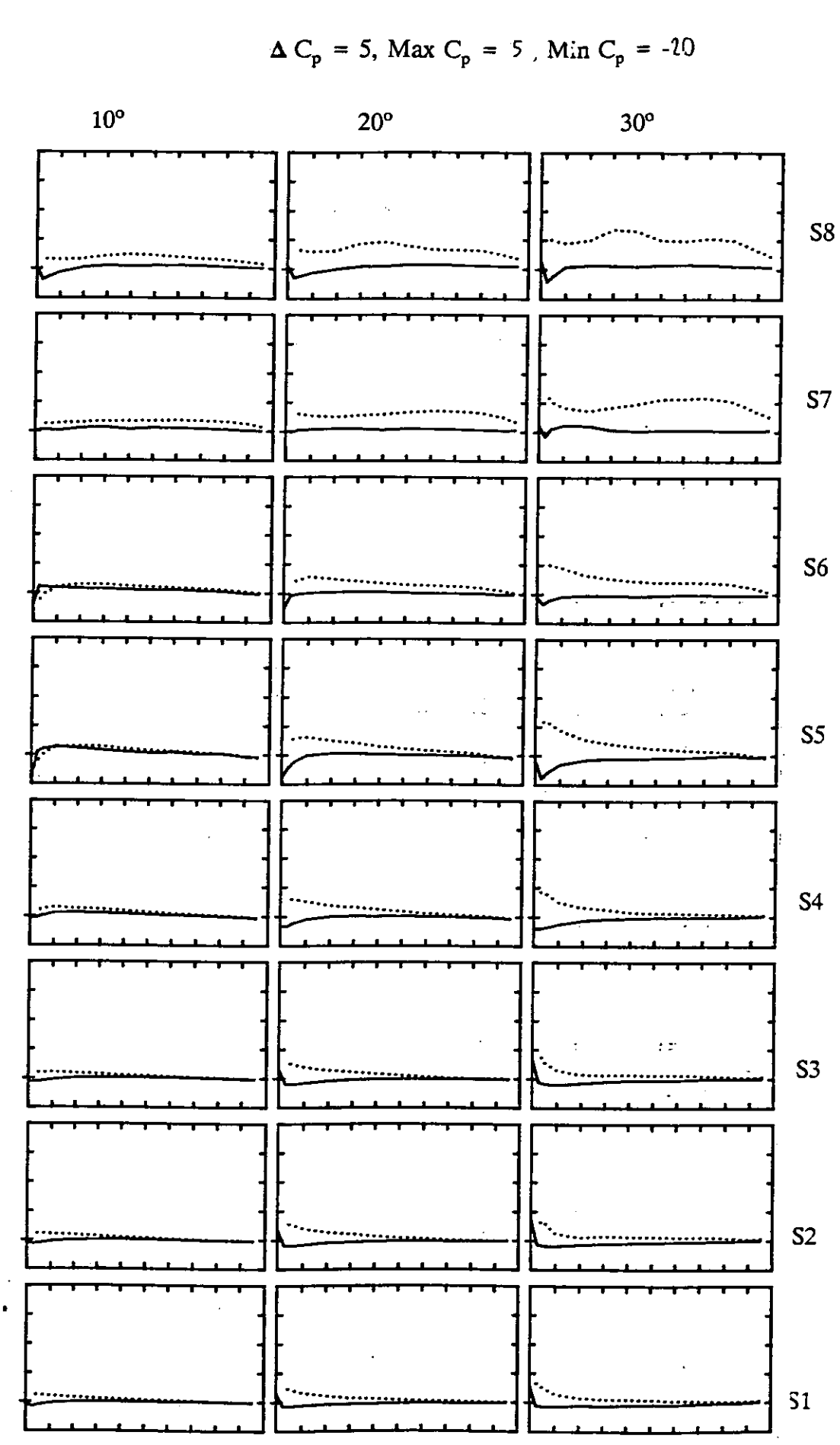

Figure 62 Chordwise pressure distributions at 8 spanwise positions for all-movable rudder no. 2 with a propeller axis height of 900mm and at J=0.51 for rudder incidences of -30.4°, -20.4°, -10.4°, -0.4°, 9.6°, 19.6°, and 29.6°.

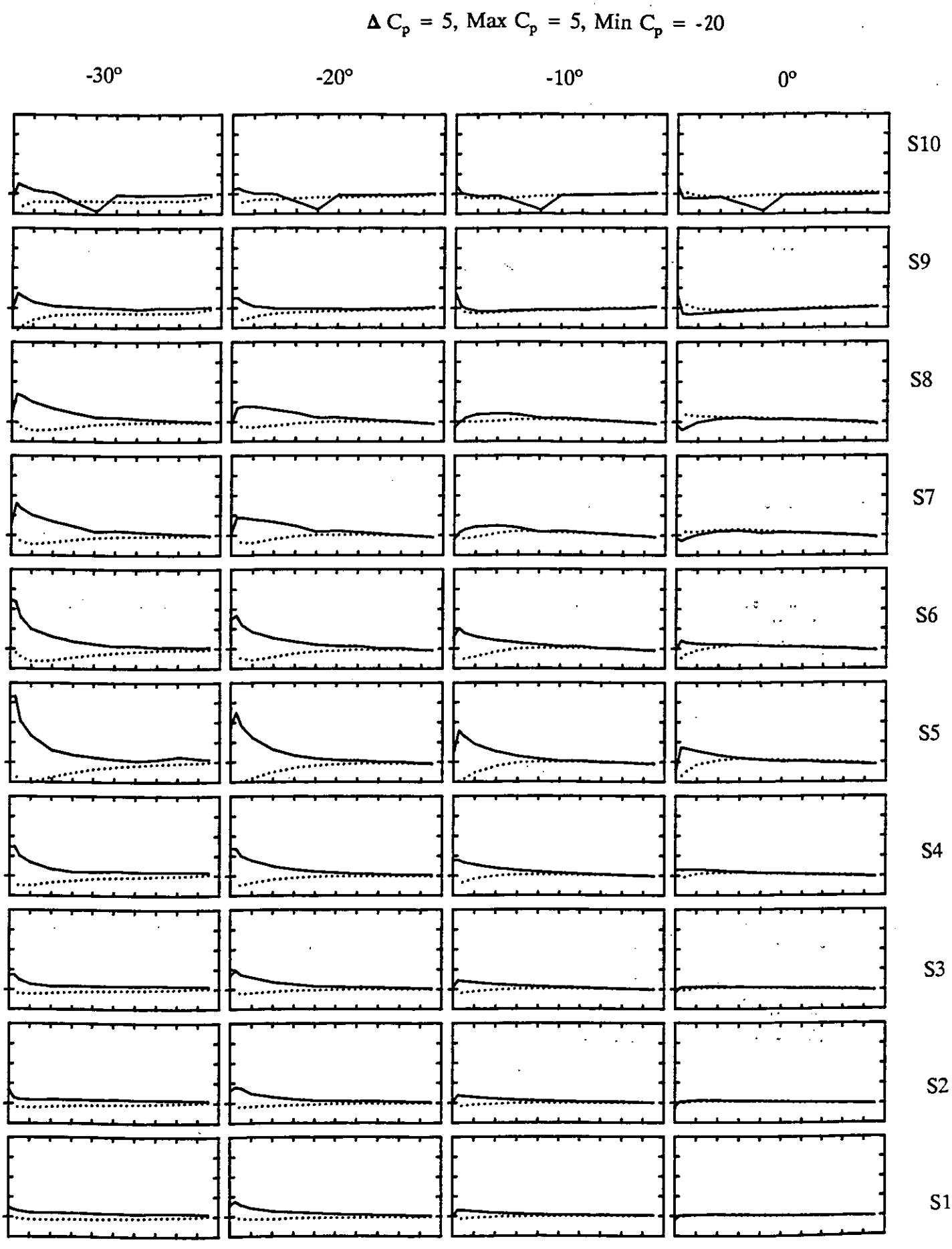

Figure 63 Chordwise pressure distributions at 10 spanwise positions for all-movable rudder no. 4 at J=0.51 for rudder incidences of -30.4°, -20.4°, -10.4°, -0.4°, 9.6°, 19.6°, and 29.6°.

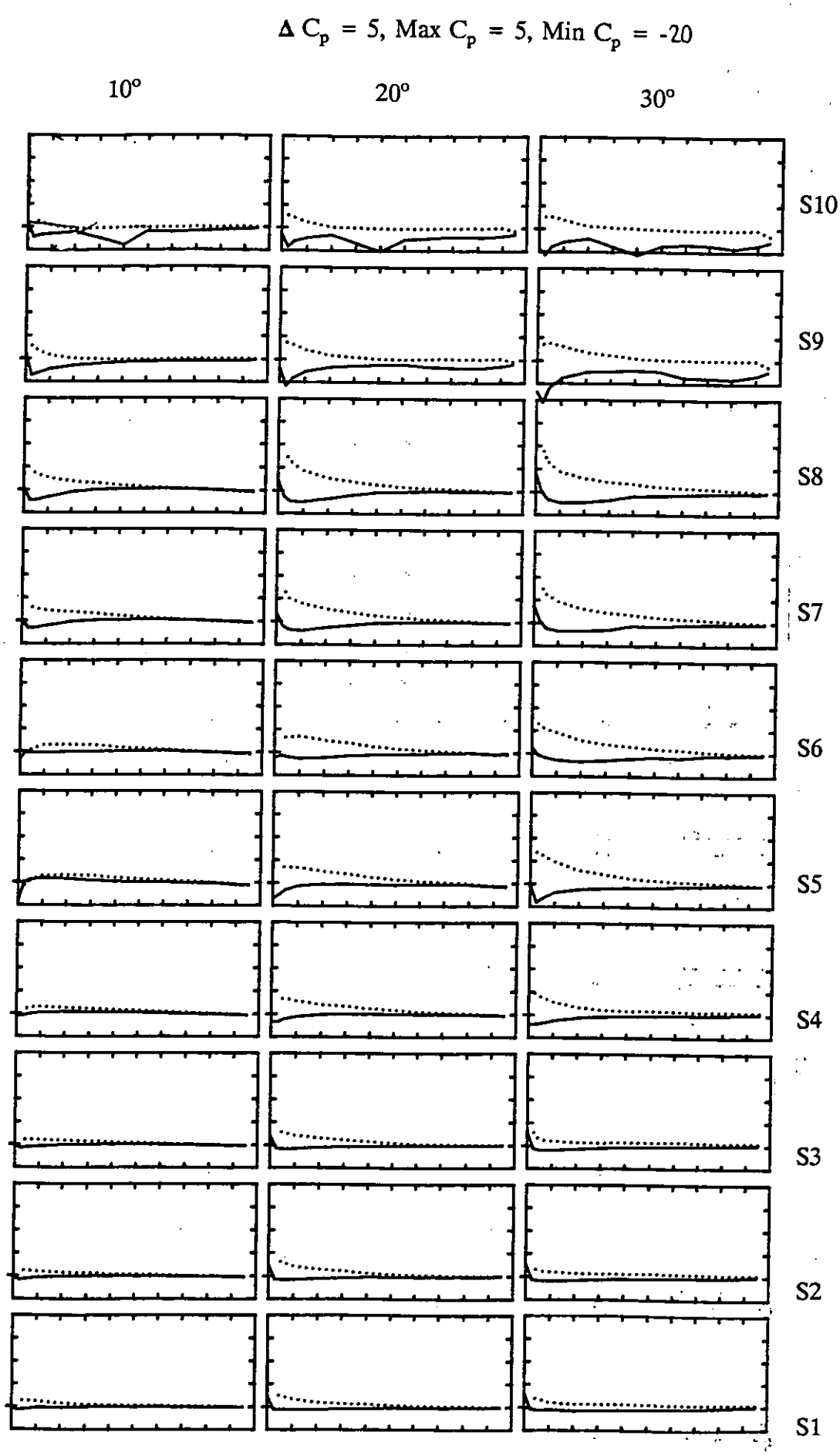

Figure 63 Chordwise pressure distributions at 10 spanwise positions for all-movable rudder no. 4 at J=0.51 for rudder incidences of -30.4°, -20.4°, -10.4°, -0.4°, 9.6°, 19.6°, and 29.6°.